**THE UNIVERSITY OF CALGARY**

# Developmental Changes in Potassium Currents in Mouse Heart

by

Li Wang

A DISSERTATION

SUBMITTED TO THE FACULTY OF GRADUATE STUDIES

IN PARTIAL FULFILMENT OF THE REQUIREMENTS FOR THE

DEGREE OF DOCTOR OF PHILOSOPHY

DEPARTMENT OF CARDIOVASCULAR/RESPIRATORY SCIENCES

CALGARY, ALBERTA

FEBRUARY, 1996

## APPROVAL PAGE

## THE UNIVERSITY OF CALGARY, FACULTY OF GRADUATE STUDIES

The Undersigned certify that they have read, and recommend to the Faculty of Graduate Studies for acceptance, a dissertation entitled "Developmental Changes in Potassium Currents in Mouse Heart" submitted by Li Wang in partial fulfillment of the requirements for the degree of Doctor of Philosophy.

Dr. Henry J. Duff (Supervisor), Department of Cardiovascular/Respiratory Sciences

Dr. Wayne R. Giles, Department of Cardiovascular/Respiratory Sciences

Dr. Gilbert A. Schultz, Department of Biochemistry and Molecular Biology

Dr. Robert J. French, Department of Neuroscience

Dr. Michael C. Sanguinetti (External Examiner), Division of Cardiology, Program in Human Molecular Biology and Genetics, University of Utah, UT, USA.

February 12, 1996

## ABSTRACT

Developmental changes in mouse cardiac $K^+$ channels have been assessed in this dissertation using three techniques: whole-cell patch clamp, conventional microelectrode and [$^3$H]-dofetilide binding assay. Patch-clamp studies showed that $I_{Kr}$ was the dominant outward $K^+$ current in fetal mouse ventricular myocytes (day 18 of gestation). One day after birth, both $I_{Kr}$ and $I_{Ks}$ were observed, and $I_{Ks}$ became the dominant component of $I_K$ in day 3 neonatal ventricular myocytes. In adult, neither $I_{Kr}$ nor $I_{Ks}$ was observed. In parallel, the extent of action potential prolongation ($APD_{95}$) by dofetilide (1 $\mu$M), a $I_{Kr}$ channel blocker, dramatically decreased from 137% $\pm$18% in fetal, to 75% $\pm$ 29% in day 1 neonatal, and 20% $\pm$ 15% in day 3 neonatal mouse ventricular endocardium ($p<0.01$). Dofetilide did not prolong $APD_{95}$ in adult ventricle. Correspondingly, a high affinity binding site of [$^3$H]-dofetilide was found in fetal mouse ventricle but was absent in adult. The complementary data demonstrate that expression of $I_{Kr}$ and $I_{Ks}$ in mouse heart is developmentally regulated.

The density of $I_{to}$ in mouse ventricular myocytes significantly increased during development. At +50 mV, the density of $I_{to}$ was 6.7 $\pm$ 0.4 pA/pF in day 1 neonate, 12.9 $\pm$ 1.2 pA/pF in day 3 neonate and 19.8 $\pm$ 2.3 pA/pF in adult. In parallel, action potential duration progressively and significantly decreased in mouse ventricle during normal development. 4-Aminopyridine (1 mM), a $I_{to}$ channel blocker, produced a greater prolongation of action potential duration in adult mouse ventricle than in neonate. These data suggest that developmental increase in the density of $I_{to}$ is associated with age-related

shortening of action potential duration in mouse ventricle.

Unlike $I_{Kr}$, $I_{Ks}$ and $I_{to}$, the density of $I_{K1}$ remained relatively constant from day 18 fetal to adult mouse ventricular myocytes and resting membrane potential did not significantly alter in mouse ventricle during the same developmental stages.

In conclusion, the findings in this dissertation illustrate that expression of $K^+$ currents in mouse heart is age-dependent. The pattern of developmental changes in $K^+$ currents in mouse heart is unique and different from previous reports of age-related changes in cardiac $K^+$ currents of other species.

## ACKNOWLEDGEMENTS

I have been a member of the Cardiovascular Research Group for seven years. During this period of time, I have been granted a Master's degree and I am currently finishing my Ph.D training program. All these achievements would never have been possible without great help from all my teachers, my friends and my colleagues.

First, I would like to say many thanks to my supervisor Dr. Henry Duff for his intellectual input, generous support, genuine kindness and constant encouragement throughout my studies.

I am also greatly indebted to each of my supervisory committee members: Dr. Wayne Giles, Dr. John Tyberg and Dr. Gilbert Schultz for their excellent guidance, kindness, invaluable advice and great help with their expertise.

I wish to thank both Dr. Robert French and Dr. Michael Sanguinetti for their critical input on my dissertation and for serving on my examination committee.

I am very grateful to Dr. Robert Clark for his enormous help with his knowledge and expertise. In addition, I appreciate Dr. Robert Sheldon for his advice and help.

It is also a pleasure and privilege to acknowledge the support, help and encouragement from many friends and colleagues: Zhong-Ping Feng, Xin-Qiang Han, Celine Fiset, Jim Lees-Miller, Colleen Kondo, Caroline Symonds, Nipavan Chiamvimonvat and Ela Thakore.

## DEDICATION

To my husband Zhao-Hua Han and my daughter Meng-Meng Han

and to my parents, Xiu-Lian Luo and Yu-Fu Wang

They are truly special to me

Their endless love, deep understanding and emotional support made this work possible

For them, no words can express my deepest appreciation

## TABLE OF CONTENTS

## LIST OF TABLES

## LIST OF FIGURES

# CHAPTER ONE: BACKGROUND

Potassium channels are membrane-spanning proteins that have fundamental importance in controlling repolarization of the action potential, regulating resting membrane potential, acting as substrates for neuromodulatory control of cardiac function, and are potential targets for Class III antiarrhythmic agents (33,59,140). During the last few years information about the structure, function, and pharmacological regulation of $K^+$ channels has rapidly expanded. The integration of this information is particularly important to cardiac electrophysiology, to the design of class III antiarrhythmic agents and to understanding of the genetic basis of certain disorders in the heart, such as long QT syndrome.

## 1.1 Potassium Channel Classification

Recent advances in whole-cell and single-channel patch clamp techniques have extended our understanding of the $K^+$ currents in heart. A variety of distinct types of $K^+$ currents with different time- and voltage-dependent properties and pharmacological sensitivities has been identified in mammalian heart (14,34,86,121,124,144,156,166). Based on their biophysical properties, these cardiac $K^+$ currents are broadly classified into two groups: the depolarization-activated $K^+$ currents and the inwardly rectifying $K^+$ currents.

In addition, advances in molecular cloning of $K^+$ channel subunits have led to the discovery of a wide variety of $K^+$ channels with different gating properties in the heart. Some of these cloned $K^+$ channels have been shown to closely match the properties of

some native $K^+$ currents. Currently used nomenclature for cloned $K^+$ channels is generally based on structural similarities, such as *Shaker*-related $K^+$ channel family, eag family, and inward rectifier family.

### 1.1a Classification of $K^+$ channels in the heart

***Depolarization-activated $K^+$ currents***

Two types of depolarization-activated $K^+$ channels are common to many myocardial tissues. They are the transient outward $K^+$ current ($I_{to}$) and delayed rectifier $K^+$ current ($I_K$). Other depolarization-activated $K^+$ currents, which are different from $I_{to}$ and $I_K$ in terms of their gating properties and pharmacological profiles, have also been reported. However, these $K^+$ currents are usually found and described in a particular tissue only. Examples of these depolarization-activated $K^+$ currents include: a rapidly activating and non-inactivating current, which is insensitive to $I_K$ channel blockers and named as plateau $K^+$ current ($I_{Kp}$) in guinea pig ventricular myocytes (10,188); a rapidly activating, slowly inactivating, 4-AP-sensitive $K^+$ current referred as $I_{Kslow}$ in rat atrial myocytes (17); a rapidly activating and non-inactivating $K^+$ current referred as $I_{ss}$ in rat atrial myocytes or $I_{sus}$ in human atrial myocytes (17,179).

***Inwardly rectifying $K^+$ currents in the heart***

To date, three inwardly rectifying $K^+$ channels have been identified in myocardial preparations. They are $I_{K1}$, $I_{KATP}$ and $I_{KAch}$, which denote a background $K^+$ channel; a cellular ATP-regulated $K^+$ channel and an acetylcholine (ACh)-regulated $K^+$ channel, respectively (22,63,123,124). Although the degree of rectification differs among these

inward rectifying $K^+$ channels, they all pass $K^+$ preferentially in the inward direction at membrane potentials negative to the equilibrium potential for $K^+$ ($E_K$) but show profoundly reduced conductance in the outward direction at membrane potentials positive to $E_K$. This property is referred to as inward rectification.

### 1.1b Classification of the cloned $K^+$ channels

Based on their different molecular structures, the cloned $K^+$ channels have been classified into: 1). the *Shaker*-related $K^+$ channel family (Kv family), which contains six transmembrane segments (80,140); 2). the *eag* $K^+$ channel family, which also contains six transmembrane segments, but has little amino acid sequence identity to that in the *Shaker*-related $K^+$ channels (140,180). 3). inward rectifies contain two transmembrane segments (16,96); 4). the minimal $K^+$ channel (minK) contains only one transmembrane segment (85). Figure 1 illustrates the proposed transmembrane topology of $K^+$ channel subunits from different $K^+$ channel families.

In addition, each of the cloned $K^+$ channel families also contains several subfamily members. For example, the *Shaker*-related $K^+$ channel family has been subdivided into subfamilies including *Shaker (Kv1), Shab (Kv2), Shaw (Kv3), Shal (Kv4)* (88,183). Furthermore, each of the *Shaker*-related $K^+$ channel subfamilies also contains many members (140). For example, Kv1.1, Kv1.2 and Kv1.5 in the *Shaker* subfamily have been identified in mammalian heart (40). The amino acid sequences of these $K^+$ channels are similar but their gating properties are different. Currently used nomenclature for the cloned cardiac $K^+$ channels is summarized in Table 1.

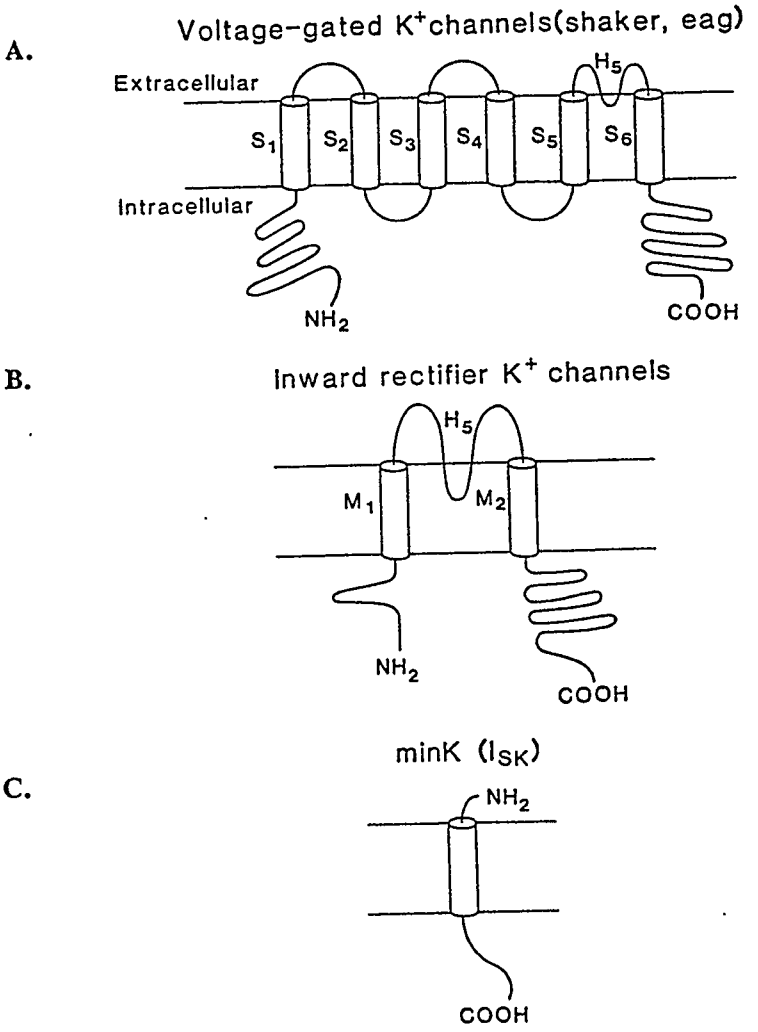


**Figure 1** **Proposed transmembrane topologies of $K^+$ channel subunits.** Three different types of $K^+$ channel subunits are displayed. Both the *Shaker*-related $K^+$ channel proteins and eag family $K^+$ channel proteins contain six transmembrane segments and a pore region (H5), both of which are voltage-gated $K^+$ channels (Panel A). The inward rectifier $K^+$ channel proteins contain two transmembrane segments and one H5-like pore region (Panel B). The minK protein contains only a single transmembrane domain and no corresponding H5 region (Panel C).

**Table 1** **Nomenclature of Cloned Cardiac $K^+$ Channels and Their Biophysical Properties.**

| $K^+$ Channel Families | | Names | Activation | Inactivation | Blocker |
|---|---|---|---|---|---|
| ***Shaker* family** | *Shaker* (Kv1) | Kv1.2 | Fast | Very slow | 4AP |
| | | Kv1.5 | Fast | Very slow | 4AP |
| | *Shab* (Kv2) | Kv2.1 | Slow | Very slow | TEA |
| | *Shaw* (Kv3) | ? | | | |
| | *Shal* (Kv4) | Kv4.2 | Fast | Fast | 4AP |
| ***eag* family** | | HERG | Slow | Very slow | Dofetilide |
| **minK family** | | minK | Very slow | None | Clofilium |
| **Inward Rectifier family** | | IRK1 | | | $BaCl_2$ |
| | | GIRK | | | |

## 1.2 Functional Roles of $K^+$ Currents in the Heart

It is obvious that $K^+$ channels are more diverse than other types of ion channels expressed in cardiac myocytes. The number of $K^+$ channel families will probably be increased as we learn more about the complex nature of $K^+$ channels. However, it is important to recognize that, despite their apparent complexity, $K^+$ channels serve to control the action potential duration in the cardiac myocytes via the same basic mechanism: providing a pathway for efflux of $K^+$ ions, resulting in repolarization.

Depolarization-activated $K^+$ channels in the heart are mainly involved in regulating the various phases of the cardiac action potential repolarization (especially phase 1 and phase 3 repolarization). The inwardly rectifying $K^+$ current, $I_{K1}$ is critical for the determination of resting membrane potential. In addition, $I_{K1}$ also contributes to the final phase of the action potential repolarization (142). A summary of the different $K^+$ currents responsible for the action potential repolarization in the heart is shown in Figure 2.

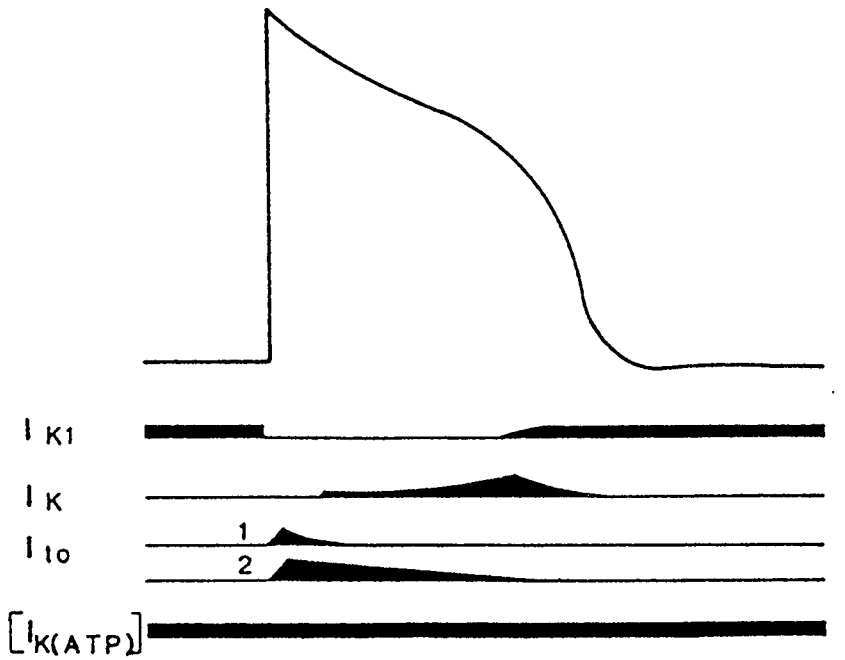


**Figure 2** **A cardiac action potential and underlying repolarizing $K^+$ currents.** A ventricular action potential is diagrammed, as are a subset of the outward currents contributing to its voltage-time course. $I_{K1}$ denotes the inward rectifying $K^+$ current; $I_K$ denotes the delayed rectifier $K^+$ current including $I_{Kr}$ and $I_{Ks}$; $I_{to}$ denotes the transient outward $K^+$ current including $I_{to1}$ and $I_{to2}$; $I_{KACh}$ represents acetylcholine (Ach)-dependent $K^+$ current; $I_{KATP}$ represents ATP-dependent $K^+$ current (modified from reference 141).

Because of differences in their kinetics, voltage-dependence, and responses to regulators, these $K^+$ currents serve distinct functions in normal and diseased hearts. In addition, it has been documented that the distribution of these $K^+$ currents in myocardial preparations is regional, species- and age-dependent (3,157). These differences contribute to the variability in action potential configurations recorded from different regions of the heart, different species and at different ages.

This dissertation focuses on developmental changes in $I_K$, $I_{to}$ and $I_{K1}$ in mouse ventricle. Therefore, the biophysical properties, the physiological functions and the structure-function relationships of these $K^+$ channels will be reviewed in detail in the following sections.

## 1.3 The Cardiac Delayed Rectifier $K^+$ Channels ($I_K$)

### 1.3a Biophysical properties and functional roles of $I_K$

The first detailed description of the cardiac delayed rectifier current was made in 1969 by Noble and Tsien (121). They found two components of $K^+$ sensitive currents in the sheep cardiac Purkinje fibers. Since the currents were not perfectly $K^+$ selective as judged by the equilibrium potentials, they named the currents $i_{x1}$ and $i_{x2}$. Because activation of $i_{x1}$ and $i_{x2}$ was very slow and delayed as compared with rapidly activating $Na^+$ and $Ca^{2+}$ currents, these conductances were referred to as delayed rectifier currents. After this pioneering work, other groups reported similar findings in a wide variety of cardiac preparations (111,122). In most of these studies, the activation and deactivation kinetics of the delayed rectifier $K^+$ current were found to be complex, supporting the original viewpoint of Noble and Tsien that the delayed rectifier $K^+$ current might consist of two individual components.

The idea of two components of $I_K$ was supported by the use of a selective $K^+$ channel blocker, E-4031 (a Class III antiarrhythmic drug). In guinea pig ventricular myocytes, Sanguinetti and Jurkiewicz found that the current activated during depolarization pulses is less sensitive to E-4031 than the tail current induced during repolarization pulses (146). By subtracting the drug-sensitive current, they showed that E-4031-sensitive current and E-4031-resistant current exhibited fundamentally different activation kinetics and rectification properties. Therefore, these authors concluded that the delayed rectifier $K^+$ current in guinea pig ventricular cells consists of two components: a rapidly activating and E-4031 sensitive current (named $I_{Kr}$) and a slowly

activating and E-4031 resistant current (named $I_{Ks}$). Both $I_{Kr}$ and $I_{Ks}$ are activated in response to a positive shift in membrane potential but exhibit different properties of rectification. During progressive depolarization, the whole-cell conductance either increased and displayed outward rectification ($I_{Ks}$) or decreased and displayed a region of negative slope conductance ($I_{Kr}$). Using selective $I_{Kr}$ channel blockers, $I_{Kr}$ and $I_{Ks}$ have been identified in nodal cells, Purkinje fibers, atrial and ventricular myocytes in many species (148). The existence of the two components of $I_K$ in human atrial myocytes and $I_{Kr}$ in human ventricular myocytes has also been reported (15,94,172,178).

The presence of $I_{Kr}$ and $I_{Ks}$ in the heart, and their relative magnitude are tissue- and species-dependent (2,79,146,147,151,171). Since $I_{Kr}$ and $I_{Ks}$ play an important role in phase 3 repolarization of cardiac action potentials (31,59,60,148), the different distribution of $I_{Kr}$ and $I_{Ks}$ can result in different action potential configurations as recorded from different regions of the heart and from different species. In addition, $I_{Kr}$ and $I_{Ks}$ channels are the major targets for Class III antiarrhythmic drugs. The investigation of the properties of $I_{Kr}$ and $I_{Ks}$ and their regulation have significant clinical implications.

### 1.3b Molecular basis of $I_{Kr}$

Recent studies have reported that the human ether-a-go-go related gene, *HERG* encodes a $K^+$ channel with biophysical properties almost identical to $I_{Kr}$ in cardiac myocytes (149). *HERG* was initially identified by screening a human hippocampal cDNA library with a mouse homolog of ether-a-go-go (*eag*), a *Drosophila* $K^+$ channel gene, which consists of six transmembrane segments but only shares amino acid sequence

similarity with the S4 transmembrane and the H5 pore region of the *Shaker* $K^+$ channels. *HERG* was localized to human chromosome 7 by polymerase chain reaction (PCR) analysis of a somatic cell hybrid panel by Warmke and Ganetzky (181). Recently, mutations in HERG have been found in patients with the chromosome 7-linked form of inherited long QT Syndrome (35). Northern blot analyses showed that *HERG* was strongly expressed in the human heart, suggesting that HERG current may play an important role in the repolarization of cardiac action potentials (35). To define the physiological role of HERG, Sanguinetti *et al* cloned the full-length cDNA of *HERG* and expressed the HERG channel in *Xenopus* oocytes (149). Voltage clamp analyses of the expressed channel currents have revealed that *HERG* encodes a $K^+$ channel with biophysical characteristics nearly identical to $I_{Kr}$ in cardiac myocytes. The unique feature of $I_{Kr}$ (i.e. the negative slope conductance of the current-voltage relationship at potentials $> 0$ mV) was observed in HERG current (149). In addition, HERG current was also $K^+$ selective, increased by an elevation of extracellular $K^+$ concentration, blocked by lanthanum and displayed voltage-dependent activation with a peak current near 0 mV. So far, no other cloned $K^+$ channels share all these characteristics with cardiac $I_{Kr}$.

### 1.3c Molecular basis of $I_{Ks}$

The biophysical properties of $I_{Ks}$ are not well correlated with the properties of any cloned $K^+$ channels from the *Shaker*-related family or the *eag* family. Instead, the properties of $I_{Ks}$ resemble those of *minK* encoded $K^+$ current. The minK channel was originally cloned from rat kidney and uterus (133,162). MinK has also been cloned in

human genomic DNA and neonatal rodent hearts (52,71,115). The minK protein predicted by the cDNA contains only 129-130 amino acids and only one transmembrane-spanning domain. Therefore, minK is a unique $K^+$ channel which is structurally different from the *Shaker*-type $K^+$ channels and has no amino acid sequence similarity with other cloned $K^+$ channels (85).

The physiological function of minK in the heart is still controversial. The arguments are focused on whether this small protein itself forms a functional $K^+$ channel in the heart or whether it is a regulatory protein which modifies the properties of other $K^+$ channels, such as $I_{Kr}$ (188). Evidence that the minK protein itself, may form a $K^+$ channel, has been obtained from functional studies of recombinant channel activity expressed and measured in *Xenopus* oocytes. Injection of *Xenopus* oocytes with RNA encoding minK resulted in expression of a time- and voltage-dependent, non-inactivating outward current which resembles $I_{Ks}$ in cardiac myocytes. Similar to cardiac $I_{Ks}$, the minK current was blocked by a Class III antiarrhythmic drug, clofilium and by high external concentrations of $Ba^{2+}$ and TEA (52,71). Furthermore, transfection of mammalian (HEK 293) cells with minK demonstrates that its electrophysiological characteristics are similar to those of $I_{Ks}$ recorded from guinea pig ventricular myocytes under similar experimental conditions (55). In addition, an antibody directed against the minK channel protein reacted with a surface antigen on adult guinea pig ventricular myocytes and sinoatrial nodal cells, where $I_{Ks}$ is the dominant outward $K^+$ current (55). These data indicate that a minK like protein may underlie $I_{Ks}$.

In summary, *HERG* likely encodes the $I_{Kr}$ channel and *minK* probably encodes the

$I_{Ks}$ channel. $I_{Kr}$ and $I_{Ks}$ are important repolarizing $K^+$ currents in the heart under physiological conditions. Mutations in *HERG* are associated with acquired long QT syndrome, an inherited disorder that can cause lethal ventricular arrhythmias in affected individuals.

## 1.4 The Cardiac Transient Outward $K^+$ Current ($I_{to}$)

The transient outward $K^+$ current ($I_{to}$) is thought to consist of two components: a voltage-dependent, $Ca^{2+}$-independent, and 4-AP sensitive component named $I_{to,1}$ and a $Ca^{2+}$-dependent, 4-AP-insensitive component named as $I_{to,2}$ (57,156). Since only the developmental changes in $I_{to,1}$ are studied in this dissertation. $I_{to,1}$ will be referred as to $I_{to}$ in the following sections for simplicity.

### 1.4a Biophysical properties and functional roles of $I_{to}$

$I_{to}$ has been characterized in many myocardial preparations including mouse, rat, cat, ferret, rabbit, canine and human ventricular myocytes as well as rat, rabbit, canine and human atrial myocytes (5,13,19,20,58,100,152). $I_{to}$ is absent or relatively scarce in guinea pig myocardial cells (146,147). In addition, the distribution of $I_{to}$ also varies in different regions of the heart (98,100,119). For example, the density of $I_{to}$ in sub-epicardial myocytes of human left ventricle was fourfold higher than the current density of $I_{to}$ in sub-endocardial myocytes isolated from non-failing myocardium (119). Although $I_{to}$ recorded from various cardiac myocytes displays similar $K^+$ selectivity and 4-AP sensitivity, the properties of $I_{to}$ activation and inactivation vary in different species and different regions of the heart. Activation thresholds of $I_{to}$ range from approximately -40 mV to 0 mV (20). Half-activation potentials range from -12 mV in rabbit atrium (29) to +22 mV in ferret ventricle (19). The characteristics of $I_{to}$ inactivation also vary from species to species (47,152). The inactivation time courses of $I_{to}$ were well described by a single exponential function in some species (20), while they were best fit by a double

exponential equation in other species (20). The kinetics of recovery from inactivation for $I_{to}$ have also been described with single or double exponential functions. The range of recovery time constants differs strikingly from species to species. In rabbit atrium, it was 5.4 sec, while in rat ventricle, it was 25.3 ms. Because of substantially different recovery kinetics, $I_{to}$ is proposed to have a more pronounced effect on the frequency-dependent modulation of the action potential configuration in rabbit atrium (slow kinetics) than that in rat ventricle, where recovery is very fast.

$I_{to}$ with rapid activation kinetics is able to produce the rapid phase 1 repolarization, which is responsible for the so-called "spike and dome" action potential configuration recorded in canine and human ventricular epicardium (20). Because of the regional differences in expression of $I_{to}$, the action potential configuration differs among various regions of the heart, such as in canine epicardium vs endocardium (100). Even though the amplitude of $I_{to}$ substantially declines due to inactivation during depolarization, some maintained current may still flow during the later phase of the action potential plateau. Thus, in addition to the contribution to phase 1 repolarization, $I_{to}$ may also play a role in the action potential plateau (phase 2) and early phase 3 of the action potential repolarization. Following repolarization, $I_{to}$ channels recover from inactivation. Since the recovery kinetics are region and species dependent, the contribution of $I_{to}$ to the frequency-dependent modulation of the action potential configuration in various myocardial cell types also varies in the different regions of the heart and in different species.

## 1.4b The structure of *Shaker*-related $K^+$ channels and molecular basis of cardiac $I_{to}$

***The Shaker-related $K^+$ channels*** The derived protein sequences of the *Shaker* $K^+$ channels were found to have similarities to previously cloned $Na^+$ and $Ca^{2+}$ channels except that each of the four subunits (I,II, III and IV) is not covalently linked as they are in $Na^+$ and $Ca^{2+}$ channels (69,82). Voltage-dependent $K^+$ channels are multimers composed of four separate protein subunits (80,132). The $NH_2$ and COOH termini of the individual subunits are both intracellular, whereas the middle core region contains six transmembrane-spanning hydrophobic segments designated S1 to S6, and a pore region (H5) between S5 and S6 as shown in Figure 1A.

**Inactivation** Inactivation is a characteristic of $I_{to}$. Two distinct mechanisms, termed N-type and C-type inactivation have been proposed for both *Shaker* $K^+$ channels and *Shaker*-related $K^+$ channels. Data from extensive mutagenesis of the N-terminal region of *Shaker* $K^+$ channels suggest that the first 20 amino acids in the N-terminal region are particularly important for the process of fast inactivation and are collectively termed as "inactivation ball" (73). Since there are positively charged residues in the inactivation ball, one might expect that the receptor for the presumed inactivation ball in the N-terminal region would carry some negative charges. Indeed, the sequence that connects the S4 sequence with the S5 sequence contains five negative residues and mutation of these amino acids remarkably changed inactivation properties (76). The S4-S5 loop is also near the cytoplasmic end of the pore. All these data suggest that the S4-S5 loop acts as a receptor for the fast inactivation "ball" after channel activation. Fast N-type

inactivation mechanism may also underlie cardiac $I_{to}$ inactivation.

However, the mechanism of C-type inactivation is unknown. C-type inactivation is usually slow, and sensitive to external TEA (18). It has been noted that inactivation kinetics were different in alternatively spliced *Shaker* $K^+$ channels that share common N termini but differ in their C termini (18,74). In these channels, inactivation has been shown to be sensitive to amino acid composition of the $K^+$ channel pore (78,104). A single amino acid at position 413 or 463 in S6 near the C terminus of the channel protein was found to be possibly responsible for the C-type inactivation (18). However, how this residue influences the properties of $K^+$ channel inactivation is unknown.

Recently, two $\beta$ subunits from the *Shaker* subfamily were cloned from rat brain (23,135). Co-expression of $\alpha$ and $\beta$ subunits revealed that the $\beta$ subunit modulates the inactivation kinetics of some $K^+$ channels in the *Shaker* subfamily. Therefore, an alteration in the accessory $\beta$ subunits associated with $\alpha$ subunits of the $K^+$ channel may also contribute to the different kinetics of $K^+$ channel inactivation. For example, co-expression of a $K^+$ channel $\beta$-subunit (Kv$\beta$3) with Kv1.4 $\alpha$-subunit accelerated Kv1.4 inactivation and slowed recovery from inactivation for Kv1.4 (23).

**Activation and Selectivity** The S4 sequence, referred to as the voltage sensor, appears to be specifically involved in voltage-dependent activation of $K^+$ channels (159). The H5 region is composed of approximately 20 amino acids and highly conserved among the $K^+$ channels. Numerous mutagenesis studies indicate that H5 is the $K^+$ channel pore, and may contain multiple $K^+$ binding sites. Therefore, the H5 region is considered to be responsible for the $K^+$ permeation and $K^+$ channel selectivity.

***Molecular basis for $I_{to}$*** Several transient outward $K^+$ channels have been cloned from rat and human heart (129,138,139,163) based on homology with the *Shaker* $K^+$ channels. The $K^+$ channels cloned from rat heart are Kv1.2, Kv1.4, Kv1.5 (*Shaker* subfamily), Kv2.1 (*Shab* subfamily) and Kv4.2 (*Shal* subfamily). Their expression in adult atrial and ventricular myocytes has been proven by Northern blots and quantitative RNase protection assays. In addition, the expression of these $K^+$ channels is tissue specific. RNase protection data reveal that mRNA levels of *Shaker* subfamily (Kv1.2, Kv1.4, and Kv1.5) are higher in rat atria than in rat ventricle, whereas mRNA levels of *Shal* subfamily (Kv4.2) are higher in ventricle (40).

What is the relation between these cloned $K^+$ channels and $I_{to}$ in native cardiac myocytes? It is generally believed that Kv1.4 and Kv4.2 channels are the most likely candidates for mammalian $K^+$ channels that conduct $I_{to}$ since expression of Kv1.4 or Kv4.2 in *Xenopus* oocytes reveals a transient outward $K^+$ current similar to that recorded in rat ventricular myocytes. However, Barry *et al* have shown that Kv1.4 is barely detectable in the membranes of adult rat ventricular myocytes by immunohistochemistry (antibodies) and Western blot analysis, suggesting that it is unlikely that Kv1.4 contributes to rat ventricular $I_{to}$ (11). On the other hand, Kv4.2 is abundant on the membrane of adult rat ventricular myocytes. These data suggest that Kv4.2 most likely underlies $I_{to}$ in adult rat ventricular myocytes.

## 1.5 The Cardiac Inwardly Rectifying $K^+$ Channel ($I_{K1}$)

### 1.5a Biophysical properties and functional roles of $I_{K1}$

Cardiac $I_{K1}$ is $K^+$ selective and is blocked by barium ($Ba^{2+}$) (170). Whole-cell $I_{K1}$ displays asymmetry in its $K^+$ conductance. The $I_{K1}$ channel preferentially passes $K^+$ in the inward direction at membrane potentials negative to the $K^+$ equilibrium potential ($E_K$), but provides high resistance to $K^+$ flow in the outward direction at membrane potentials positive to $E_K$, a property important for maintaining the cell resting membrane potential. The physiological membrane potentials are generally positive to $E_K$ (69). Therefore, little outward $I_{K1}$ flows during the action potential plateau, which permits a long action potential duration and minimizes both intracellular $K^+$ loss and extracellular $K^+$ accumulation. During the final phase of repolarization (from -60 mV to -70 mV), $I_{K1}$ conducts relatively large outward current. Therefore, $I_{K1}$ also plays a role in the final phase of the action potential repolarization.

In the heart, $I_{K1}$ is present in high abundance in the atrial and ventricular myocytes as well as Purkinje cells, but it appears to be absent in pacemaker cells (170). Selective blockade of $I_{K1}$ causes an increase in the action potential duration and changes the cell resting membrane potential to a more positive potential.

### 1.5b Mechanisms of inward rectification

The $K^+$ conductance of $I_{K1}$ channels is increased with hyperpolarization and decreased with depolarization. This rectification is the opposite of that expected from the $K^+$ gradient. Matsuda *et al* have shown that the physiological levels of intracellular

$Mg^{2+}$ produce voltage-dependent blockade of the $I_{K1}$ channel, resulting in inward rectification (110). The inward rectification disappears if intracellular $Mg^{2+}$ concentration is reduced (110). Evidence for a blocking particle ($Mg^{2+}$) model of inward rectification has also been provided by Vandenberg (169). She used single-channel recordings to implicate internal $Mg^{2+}$ ions as the endogenous blocking particles responsible for inward rectification. Addition of 17 $\mu$M or 1.2 mM $Mg^{2+}$ to the bath solution gave partial rectification or restored the normal extent of rectification, respectively. The steady-state block of the $I_{K1}$ channel was increased both by positive potential and by increasing the internal $Mg^{2+}$ concentration. $Mg^{2+}$ can not traverse through the pore, but it can be displaced by incoming $K^+$. Thus, $Mg^{2+}$ plugs the inner mouth of $I_{K1}$ channel, which leads to inward rectification. Although the intracellular $Mg^{2+}$ is not the only factor to contribute to the rectification of $I_{K1}$, $Mg^{2+}$ is likely to be physiologically important because of its high concentration in the cell (0.5 - 1.0 mM) (117). These concentrations of $Mg^{2+}$ are sufficient to cause a marked inward rectification of $I_{K1}$ under cell-attached patch conditions.

Recently, several lines of evidence indicate that intracellular polyamines such as spermine and spermidine also play an important role in the determination of the properties of inward rectification of $I_{K1}$ (45,50,102). Lopatin *et al* have shown that after patch excision, the intrinsic gating of the cloned IRK1 channels disappeared, however, application of spermine and spermidine to the inside-out patches restored all the essential features of intrinsic rectification (102). These polyamines are present in almost all known cells and are more potent blockers of IRK1 channels than $Mg^{2+}$. Therefore, these

data suggest that the polyamines may be important intrinsic rectifying factors for $I_{K1}$ channels.

### 1.5c Molecular basis of $I_{K1}$

Several inwardly rectifying $K^+$ channels have recently been cloned and expressed in *Xenopus* oocytes or mammalian cell lines. These include IRK1 (96), GIRK1 (36,97), ROMK1 (70). Another inward rectifier $K^+$ channel cloned from cardiac tissue was named as $rcK_{ATP}$ by Ashfold *et al* (8) or as CIR by Krapivinsky *et al* (95). Ashfold *et al* found that the biophysical properties of $rcK_{ATP}$ was similar to $K_{ATP}$ in native cardiac myocytes. This finding was not confirmed by Krapivinsky *et al*. They found that the expressed CIR channels were not inhibited by intracellular ATP or opened by pinacidil. However, they have shown that the CIR subunits co-assemble with GIRK1 to form the cardiac muscarinic receptor-activated $I_{KAch}$.

The molecules of the inward rectifier $K^+$ channels are predicted to have only two transmembrane segments, M1 and M2 separated by an H5 segment (96). Like the *Shaker*-related $K^+$ channels, the N- and C-termini of the inward rectifier $K^+$ channels are modelled to reside within the cell. In addition, the H5-like region exhibits amino acid sequence similarity with the H5 region of other cloned $K^+$ channels, except for minK. Therefore it appears that the cloned inward rectifier $K^+$ channels and the *Shaker*-related $K^+$ channels share the same basic pore design.

IRK1 (96) and GIRK1 (36,97) exhibit strong inward rectification, while ROMK1 (70) and CIR (8) display weak inward rectification. On the other hand, IRK1 and

ROMK1 are activated solely by membrane hyperpolarization (16), while GIRK1 requires the involvement of acetylcholine and G-protein. Among the hyperpolarization-activated, inwardly rectifying $K^+$ channels, the expression of ROMK mRNA was only found in the kidney, whereas, an abundance of IRK1 mRNA was expressed in the heart (77,96,182). Expression of cloned IRK1 channels in *Xenopus* oocytes yields inwardly rectifying $K^+$ currents with properties similar to those of $I_{K1}$ described in a number of different cell types. Therefore, IRK1 most likely underlies cardiac $I_{K1}$.

In summary, the $I_{K1}$ channel plays an important role not only in maintaining the cell resting membrane potential but also in controlling the shape of the action potential in the heart. Strong inward rectification of $I_{K1}$ at depolarized potentials is essential to achieve these functions. Strong inward rectification of $I_{K1}$ is mainly due to a open-channel block by intracellular $Mg^{2+}$ and polyamines. IRK1 may encode cardiac $I_{K1}$. Further studies on the cloned inward rectifying $K^+$ channels will pave the way for a molecular understanding of the structure and function of cardiac $I_{K1}$.

## 1.6 Developmental Changes in $I_K$, $I_{to}$ and $I_{K1}$

Recent studies have indicated that an age-related alteration of the cardiac action potential configuration is associated with developmental changes in $K^+$ channel expression in the heart. Therefore, determination of the characteristics of $K^+$ currents in immature cardiac myocytes is of importance for understanding the cellular physiology of the heart as it develops through the late fetal and postnatal periods. In addition, evaluation of the ionic channels expressed in the fetal and neonatal hearts is clinically relevant since certain pathological conditions (i.e. cardiac hypertrophy) can result in re-expression of fetal gene programs (168).

### 1.6a Developmental changes in $I_K$

$I_K$ plays an important role in the action potential repolarization in the heart. However, there is little information about the developmental changes in cardiac $I_K$ in the literature. A previous study by Abrahamsson *et al* compared the effects of Class III antiarrhythmic agents (dofetilide, almokalant, and d-sotalol), known to preferentially block $I_{Kr}$ channels, on the action potential duration recorded from fetal (13.5 days of gestation) and adult rat ventricular preparations (1). In fetal rat heart, all these agents produced a concentration-dependent prolongation of the action potential duration. In contrast, action potential prolongation was not observed in the adult heart (1), indicating that $I_{Kr}$ is not likely to be involved in the action potential repolarization in adult rat ventricle. However, a study with the whole-cell voltage clamp configuration revealed that both fetal and adult rat ventricular myocytes exhibited an almokalant-sensitive

current (presumably $I_{Kr}$) (1). In this cited study, neither the density nor the properties of $I_{Kr}$ in fetal and adult rat ventricular myocytes were assessed for developmental changes.

Thus, although cardiac $I_{to}$ and $I_{K1}$ have been reported to change remarkably during postnatal development (these will be discussed in the next two sections), there are no clear data on developmental changes in cardiac $I_K$. Therefore, in this dissertation my efforts have mainly focused on evaluating developmental changes in $I_K$ in mouse heart.

### 1.6b Developmental changes in $I_{to}$

In most species, the action potential configuration recorded from the heart of neonates is different from that recorded in the adult heart (3,81,90,127). For example, in neonatal rats, the action potential recorded from ventricular preparations has a distinct plateau phase and relatively long duration (90). During postnatal development, the plateau phase of the action potential disappears and the duration of the action potential rapidly decreases. By 21 days of age, the rat ventricular action potential has attained the adult configuration (90). Moreover, Kilborn and Fedida have shown that there is an approximately four-fold increase in the current density of $I_{to}$ in neonatal rat ventricular myocytes from day 1 to day 10 (90). Since $I_{to}$ plays an important role in the action potential repolarization in the heart (58), a marked increase in the density of $I_{to}$ in rat ventricular myocytes would explain the age-related shortening of the ventricular action potential in this species during postnatal development.

Age-related changes in the action potential configuration have also been found in

canine epicardium and Purkinje tissues (3,127). The spike and dome morphology of the action potential found in adult canine ventricular epicardium is totally absent in the action potentials recorded from neonatal heart, and gradually appears over the first few months of life. The progressive development of the spike and dome morphology parallels a gradual increase in the density of $I_{to}$ recorded from canine ventricular myocytes (3,81).

Age-related changes in the manifestation of the spike and dome morphology have also been described in human atrial tissue (43). In parallel, the density of $I_{to}$ in human atrial myocardium also increases during the same developmental period (43). For example, Clarkson *et al* have shown that $I_{to}$ was absent in neonatal human atrial myocytes (3-7 days old) but present in adults (28-72 years old) (30). This absence of $I_{to}$ may explain the action potential morphology (no spike and dome) recorded from human neonatal atrium.

Although developmental changes in cardiac $I_{to}$ have been observed in many species, it has not been systematically assessed in mouse heart. Since the distribution and expression of $I_{to}$ in myocardial tissues are species dependent, it is important to evaluate $I_{to}$ evolution in mouse heart.

### 1.6c Developmental changes in $I_{K1}$

Previous studies have shown that the resting membrane potential becomes more negative during development (92,157). Kojima *et al* found that the resting membrane potential in rat ventricular muscle increased significantly from -55 mV to -80 mV between fetal days 12 and 18, and reached the adult level at neonatal day 1 (92). $I_{K1}$ is

essential in controlling resting membrane potential of cardiac myocytes (75). However, quantitative investigations of $I_{K1}$ in immature myocardium have revealed a close relationship between the developmental changes in the resting membrane potential and the developmental increase in cardiac $I_{K1}$. These studies have focused on comparisons of the differences in the properties of $I_{K1}$ among the adult, neonatal and fetal hearts from rats (90,108,173), rabbits (26,75), and embryonic chicks (83). Most of these studies demonstrated that the density of cardiac $I_{K1}$ increased developmentally. For example, the whole-cell $I_{K1}$ in rabbit ventricular myocytes increased between fetal day 21 and 28 (full term: 31 days). The current density remained constant throughout the neonatal period. Thereafter, $I_{K1}$ slightly increased until adulthood (75). In rat ventricular myocytes, whole cell $I_{K1}$ also increased substantially during postnatal development (173). It has been suggested that this increase in the density of $I_{K1}$ channels not only contributes to the developmental changes in the resting membrane potential, but also may be associated with the postnatal shortening of the rat ventricular action potential (173). Further support for the developmental increase in $I_{K1}$ comes from a study using single channel analysis (108). In contrast to all those findings, Kilborn and Fedida reported that $I_{K1}$ in rat ventricular myocytes decreased profoundly between neonatal day 1 and day 10 (90).

Although the developmental changes in cardiac $I_{K1}$ have been reported in many species, a detailed analysis of $I_{K1}$ in the developing mouse heart has not been reported. This consideration leads to the assessment of the developmental changes of $I_{K1}$ in mouse ventricles in this dissertation.

## 1.7 Expression of $K^+$ Channels in the Heart During Development

Although many cloned $K^+$ channels have been identified in the heart, only a few studies have assessed developmental changes in expression of *Shaker*-related $K^+$ channels in the rat heart, and only one study has evaluated developmental changes in minK mRNA expression in the mouse heart. To date, developmental changes in *HERG*- or *IRK1*-encoded $K^+$ channel have not been investigated in the heart.

### 1.7a Developmental changes in expression of the *Shaker*-related cardiac $K^+$ channels

***At the mRNA level:*** Roberds and Tamkun have examined the pattern of expression of six *Shaker*-related $K^+$ channel mRNAs: Kv1.1 to Kv1.5 and Kv2.1 over time from fetal to adult rat heart (139). Each of the $K^+$ channel mRNA examined in rat heart was expressed at its highest level at 20 days after birth. An exception was Kv1.5, which was expressed at a relatively constant level at all time points by Northern blot analysis. Roberds and Tamkun suggest that Kv1.5 may play an important role in the basic function of the rat heart and that other $K^+$ channels might take on various regulatory roles as the heart matures. However, Swanson *et al* reported that Kv1.5 in rat cardiac tissue significantly increased during development (160). In the later study, the amount of Kv1.5 mRNA increased abruptly in the first two weeks after birth and thereafter remained relatively constant (160).

***At the protein level:*** By Western blot analysis, Xu *et al* have demonstrated that Kv4.2,

the potential candidate for $I_{to}$ in rat ventricle increased 2 fold between postnatal day 5 and day 30 (185). In parallel, the density of $I_{to}$ in rat ventricular myocytes also significantly increased during the same period of postnatal development. This result further supports that Kv4.2 likely underlies $I_{to}$ in rat ventricular myocytes. These authors also examined the developmental expression of sarcoplasmic $K^+$ channel proteins encoded by Kv1.2, Kv1.5 and Kv2.1. In parallel they also measured the delayed rectifier $K^+$ current in the rat neonatal and adult ventricular myocytes. The rat delayed rectifier is distinctly different from cardiac $I_{Kr}$ and $I_{Ks}$ in other species in terms of the activation kinetics, rectification properties and pharmacological sensitivity. Xu *et al* found that the density of this rat delayed rectifier $K^+$ current decreased slightly between 15 day and 25 day old neonates. Similarly, Western blot analysis revealed a decrease in expression of the Kv2.1 encoded channel proteins, suggesting that Kv2.1 may be related to the rat delayed rectifier in ventricular myocytes (185). Further, Xu *et al* have shown that during postnatal development, Kv1.2 was also increased, but Kv1.5 in rat ventricle was unchanged. The physiologic functions of Kv1.2 and Kv1.5 in rat ventricle are still unknown.

### 1.7b Developmental changes in expression of the minK mRNA in mouse heart

It has been reported that expression of *minK* mRNA in mouse heart was significantly altered during development. The amount of *minK* mRNA expression in mouse heart started to increase at fetal day 19 (term: day 20), and reached a peak level between neonatal day 2 and day 7. Thereafter, the level of *minK* mRNA expression

dramatically diminished and was almost undetectable in adult mouse heart (49). However, the corresponding developmental changes in $I_{Ks}$ current in the mouse heart have not been examined. I believe that a measurement of $I_{Ks}$ in mouse ventricular myocytes over the same time period as those used in the examination of minK mRNA expression in the mouse heart should facilitate our understanding of the relationship between the native $I_{Ks}$ channels and the cloned minK channels.

## 1.8 Rationale for Studying Mouse Heart

The developmental changes in cardiac $K^+$ currents have been widely investigated in chick, rat, rabbit, canine and human. However, the assessment of the age-related changes of the $K^+$ currents in mouse heart has not been performed, and little is known information about the $K^+$ currents present in fetal mouse heart.

Transgenic animal experiments have provided unique insights into a variety of physiological and pathological processes in the cardiovascular system (28,42,51,137). It has recently been revealed that at least one form of the inherited cardiac arrhythmia, the long-QT syndrome is due to mutation of the *HERG*-encoded $K^+$ channels in human heart (149,181). Therefore, it will be very interesting to use transgenic animal models to explore the ionic basis for the altered cardiac electrophysiology. Currently, the techniques for developing transgenic animal model are limited primarily to mice (51). Despite availability of transgenic mice for molecular studies of the cardiovascular system and requirements for investigation of the ionic currents in wild-type mouse heart, currently there are only limited data regarding electrophysiological characteristics of the ion currents in adult (13), neonatal mouse cardiac myocytes (71) and cardiomyocytes differentiated from pluripotent mouse embryonic stem cells (10). The developmental change in the expression of $K^+$ channels has not been assessed. Therefore, investigation of the $K^+$ currents in mouse heart during different developmental stages is one of the necessary steps towards future studies of ionic currents in transgenic mouse models.

# CHAPTER TWO: HYPOTHESES

2.1 Developmental changes in $K^+$ currents such as $I_K$ ($I_{Kr}$ and/or $I_{Ks}$), $I_{to}$ and $I_{K1}$ occur in mouse heart. These changes may result from:

a. alterations in corresponding channel densities during development.

b. differential expression of the different types of $K^+$ channels during development.

c. combinations of "a" and "b".

2.2 Developmental changes in the action potential configuration occur in mouse heart. These changes are at least partially due to the age-related alterations in expression of the $K^+$ currents in mouse heart.

# CHAPTER THREE: MATERIALS AND METHODS

All experiments were performed in accordance with our institutional guidelines for animal use in research. All mice used in this dissertation were CD-1 mice purchased from Charles River, and then housed and maintained in compliance with the Guide to the Care and Use of Experimental Animals of the Canadian Council on Animal Care.

Since the goal of this dissertation was to study the $K^+$ currents and the action potential in mouse heart during normal development, the following age groups were chosen:

- Fetal mice, used at day 18 of gestation (full term at 19-20 days);
- Neonatal mice used at 1 day after birth;
- Neonatal mice used at 3 days after birth;
- Adult mice (2 months).

Measurements of the $K^+$ currents, the action potential and $^3$H-dofetilide binding assay were all performed in each of these age groups.

## 3.1 Whole-Cell Patch-Clamp Technique

### 3.1a Single cell isolation

***Fetal and neonatal ventricular myocytes*** Single ventricular myocytes were isolated from fetal and neonatal mice by a modified method of collagenase dispersion, previously described for the isolation of the neonatal rat ventricular myocytes (27,90). Pregnant mice were anaesthetized with ether and the fetuses were removed under sterile conditions. The fetuses and neonates were sacrificed by decapitation and hearts were excised into a filter sterilized (0.2 $\mu$m), nominally $Ca^{2+}$-free Minimum Essential Medium, (MEM, Gibco, New York, USA) plus (mM) $NaHCO_3$, 24; $MgSO_4$, 1.2; dl-carnitine, 1.0, pH 7.4 adjusted with NaOH. Atrial and great vessel tissues were carefully removed. The ventricles were washed twice with MEM solution and then minced in the same $Ca^{2+}$ free solution containing: collagenase 0.23 mg/ml (Yakult, Tokyo, Japan); bovine serum albumin 10 mg/ml (Sigma A-2153, Sigma, Missouri, USA); taurine 20 mM. The ventricular preparations were then incubated with 2 ml of the collagenase containing solution and stirred continuously at 37°C in a dry bath heater (Fisher Scientific, Ontario, Canada). The collagenase solution was replaced at 5-minute intervals. The supernatant obtained from the first 15 minutes was discarded. Thereafter, the supernatant was collected and diluted 1:1 in M-199 culture medium (Sigma) plus (mM) $NaHCO_3$, 26; HEPES, 10; fetal calf serum, 15% (HyClone Laboratories, Inc, Utah, USA); penicillin G (sodium), 100 units/ml; gentamicin, 100 $\mu$g/ml; regular insulin, 5 mg/ml; pH 7.40 adjusted with NaOH. After digestion, the cells were centrifuged at 800 r.p.m. for 3 minutes and re-suspended in M-199 culture medium. The viability of

the ventricular myocytes isolated by this method was ≥ 90% as assessed by the Trypan Blue dye exclusion test. The cells were plated onto tissue culture dishes and maintained at 37°C in a 5% $CO_2$ incubator for 20 minutes to remove the endothelial cells. Then the cells were re-plated at a density of 1.0-2.0 X $10^5$ cells/ml in the new tissue culture dishes containing glass coverslips. Finally, the ventricular myocytes were maintained in a 5% $CO_2$ incubator at 37°C until use (within 48 hours). No differences in the properties of the $K^+$ currents were observed during this short period of cell culture.

Freshly isolated fetal and neonatal mouse ventricular myocytes were spherical in appearance without visible striations after isolation. During the short term cell culture, the cells flattened, spread and showed spontaneous beating.

***Adult ventricular myocytes*** Adult mouse ventricular myocytes were isolated using a modified Langendorff procedure described by Benndorf *et al* (12). After the mouse was anaesthetized by ether and killed by cervical dislocation, the heart was rapidly excised. The aorta was then cannulated and the heart was retrogradely perfused with $Ca^{2+}$ free Tyrode solution at a rate of 2 ml/min for 5 minutes. The solution contained (mM): NaCl, 137; KCl, 5.4; $MgCl_2$, 0.5; $NaH_2PO_4$, 0.3; HEPES, 5; glucose, 10; pH 7.4 adjusted with NaOH. Afterward, the heart was continuously perfused with this solution containing collagenase (0.125 mg/ml, Yakult, Tokyo, Japan) for 10 minutes, followed by a 5 min perfusion with KB solution containing (mM): Taurine, 20; l-glutamic acid, 70; KCl, 25; $KH_2PO_4$, 10; $MgCl_2$, 3; EGTA(K), 0.5; HEPES, 10; Glucose, 10; pH 7.4 adjusted with KOH. During the whole procedure, the perfusion bath was maintained at

37 ± 0.2°C and the solutions were equilibrated with 100% $O_2$. At the end of the perfusion the ventricles were isolated, cut into 8-10 pieces and then put into a beaker containing 10 ml of the KB solution. The ventricular myocytes were dispersed by gently shaking the beaker for 3 minutes. The undigested tissues were removed by filtration through a nylon mesh. The ventricular myocytes were kept in KB solution at 4°C for at least 1 hour before they were used for the patch clamp study.

The adult mouse ventricular myocytes were $Ca^{2+}$ tolerant, and had typical rod-shaped appearance and clear striations. The viability of cells isolated by this method varied from 55% to 75%.

### 3.1b Whole-cell patch-clamp recording

Since the major aim of this dissertation was to identify and characterize the $K^+$ currents in mouse ventricular myocytes during different developmental stages, the fast inward $Na^+$ current ($I_{Na}$) was inhibited by holding the cell membrane at -40 mV and -50 mV during measurements of $I_K$ and $I_{K1}$. $I_{Na}$ was also inhibited by TTX (25 $\mu$M) in some experiments when $I_{to}$ was examined. The L-type $Ca^{2+}$ current was blocked by nisoldipine (0.4 $\mu$M) (87). For recordings of normal action potentials, the cells were perfused with normal Tyrode solution in the absence of $Na^+$ and $Ca^{2+}$ channel blockers.

Whole-cell patch clamp techniques (64) were used to record $K^+$ currents and action potentials. For the recordings in fetal or neonatal ventricular myocytes, the glass coverslip with the cultured ventricular myocytes was transferred to the recording chamber. For the recordings in adult cells, a few drops of the cell-containing solution

were put into the recording chamber and 5 minutes were allowed for the myocytes to attach to the substrate. Then the cells were superfused at 2 ml/min at room temperature (22°C) with the HEPES-buffered Tyrode solution containing (mM): NaCl, 140; KCl, 4; $MgCl_2$, 1; $CaCl_2$, 1; glucose, 5.5; HEPES, 10; pH 7.4 adjusted with NaOH.

An Axopatch 200 amplifier (Axon Instruments, California, USA) was used in all patch-clamp measurements. The amplifier was interfaced with a 386/33 MHz IBM compatible computer by a 125 kHz Labmaster board for data acquisition (Scientific Solutions Inc, Ohio, USA). The patch electrodes (thin-walled borosilicate tubing with 1.5 mm OD, World Precision Instruments, Inc, Florida, USA) were made with a horizontal pipette puller (Sutter Instruments, California, USA). The electrodes had resistances of 3.5-5 MΩ for fetal and neonatal cell recording, and 1-2 MΩ for adult cell recording when filled with an internal solution containing (mM): potassium aspartate, 110; $MgCl_2$, 6.4; $K_2ATP$, 4.2; $CaCl_2$, 2.7; NaCl, 8; HEPES, 5; EGTA, 5; pH 7.2 adjusted with KOH. The internal pipette solution was passed through a 0.22 $\mu$m filter prior to use. A liquid junction potential of approximately 10 mV (pipette negative) was corrected electrically. The $K^+$ currents measured in the present study were filtered at 1 kHz using a 4-pole Bessel filter and digitized at a sampling frequency of 2 kHz. The cell capacitance and series resistance were measured in whole-cell voltage clamp experiments from the capacitive transient elicited by a 20 mV depolarizing step from a holding potential of -100 mV. The capacitive transients were filtered at 10 kHz using a 4-pole Bessel filter and digitized at a sampling frequency of 50 kHz. The series resistance was electrically compensated in the range of 40% to 75% to minimize the

duration of the capacitive surge and to correct the voltage drop produced across the clamped cell membrane. The voltage command generation and data collection were controlled by pCLAMP software (Axon Instruments).

Although there was a variability in the size of the individual cells at a given age, it was noted that the cell sizes fundamentally increased during development. The average capacitance of mouse ventricular myocytes was 23.7 $\pm$ 2.3 pF for fetus, 24.3 $\pm$ 2.4 pF for day 1 neonates, 35.4 $\pm$ 5.9 pF for day 3 neonates and 166.4 $\pm$ 10.1 pF for adults ($p<0.01$).

## 3.2 Conventional Microelectrode Techniques

The myocardial tissues used for microelectrode recordings were not digested by collagenase and action potentials were recorded at a physiological temperature (37°C). The aims of these experiments were: 1) to assess whether developmental change in action potential configuration occurs in mouse ventricle; and 2) to evaluate functional roles of $K^+$ currents in action potential repolarization in mouse heart during normal development.

### 3.2a Preparations and recordings

This procedure has been previously described in detail (177). Briefly, right ventricular tissue was rapidly isolated from fetal, neonatal and adult mouse hearts and pinned to the bottom of a Sylgard coated Lucite muscle chamber with endocardium facing up. Thus, the intracellular recordings of the action potentials were obtained in the right ventricular endocardium for all age groups. The myocardial preparations were superfused at 37 $\pm$ 0.2°C with oxygenated HEPES-buffered Tyrode solution containing (mM): NaCl, 128; KCl, 5; $CaCl_2$, 1.1; $MgCl_2$, 1; sodium acetate, 2.8; glucose, 10; HEPES 10; pH 7.4 adjusted with NaOH. Stimulating frequency was 2 Hz. The recording electrodes were filled with 3M KCl and had tip resistances of 10-20 MΩ. An IBM AT computer with a custom made software routine (Bascom Consultants, Montreal, Quebec, Canada) was used to measure the resting membrane potential, action potential duration at 50% and 95% repolarization ($APD_{50}$ and $APD_{95}$) and the maximal upstroke velocity of phase 0 of the action potential ($\dot{V}_{max}$). The action potential configuration was stored and analyzed using CELLSOFT program (University of Calgary, AB, Canada).

## 3.3 [$^3$H]-Dofetilide Equilibrium Binding Assay

Dofetilide is a selective $I_{Kr}$ channel blocker (21,84). Recently, Chadwick *et al* and Duff *et al* have used [$^3$H]-dofetilide as a specific radioligand for $I_{Kr}$ channels and studied the drug and $I_{Kr}$ channel interaction at the molecular level (25,41). These studies have shown that [$^3$H]-dofetilide specifically binds to sites associated with $I_{Kr}$ channels in guinea pig ventricular myocytes. Therefore, [$^3$H]-dofetilide binding assay was used in this dissertation to evaluate whether there is an age-related change in $I_{Kr}$ channels in mouse ventricles at the molecular level.

### 3.3a Preparations

A crude membrane homogenate of mouse ventricles was used in [$^3$H]-dofetilide binding assay. The reasons for using this preparation were as follows: 1). Adult mouse heart is very small and one binding experiment may require pooling the ventricular myocytes isolated from at least 4 adult mouse hearts, thus limiting the feasibility of using mouse ventricular myocytes to carry out the [$^3$H]-dofetilide binding assay; 2). The procedure for purification of cardiac sarcolemma can result in loss or denaturation of $I_{Kr}$ channels or [$^3$H]-dofetilide binding sites (25); 3). Preliminary experiments from our laboratory have compared the results of [$^3$H]-dofetilide binding in the ventricular myocytes and ventricular homogenate from adult guinea pig, as well as the results in the ventricular myocytes and the ventricular homogenate from neonatal mouse. The ventricular myocytes and ventricular homogenate obtained from both species exhibited very similar isotherms of [$^3$H]-dofetilide binding. Thus, use of the mouse ventricular

homogenate in this dissertation to assess the developmental changes in $I_{Kr}$ channels or [$^3$H]-dofetilide binding sites in mouse heart is justified.

The mouse ventricular homogenate was prepared as follow. Briefly, hearts from fetal, neonatal and adult mice were rapidly excised and placed in nominally $Ca^{2+}$-free Minimum Essential Medium (Gibco, New York). The ventricles were isolated, washed and then immediately homogenized with a Brinkmann Polytron homogenizer for 20 seconds in ice-cold, $Ca^{2+}$-free incubation solution containing (mM): NaCl, 135; KCl, 5; $MgCl_2$, 1; HEPES, 10; glucose, 10; EGTA, 1; and pH 7.4 adjusted by NaOH. The homogenate was then filtered through a 200 $\mu$m silkscreen mesh. The protein concentrations were determined by the Lowry assay using bovine serum albumin as the standard.

### 3.3b [$^3$H]-dofetilide equilibrium binding

The ventricular crude membrane homogenate ($\approx$ 400 $\mu$g protein/assay) was incubated for 30 minutes at 37°C with [$^3$H]-dofetilide (10 nM) in the absence or presence of unlabelled dofetilide ranging from 0.3 nM to 10 $\mu$M. Reactions were terminated by adding 3 ml Tris buffer solution into the assay. The Tris buffer solution contained (mM): Tris HCl, 25; NaCl, 130; KCl, 5.5; $MgSO_4$, 0.8; glucose, 10; $CaCl_2$, 50 $\mu$M; BSA, 0.01% pH 7.4 adjusted with Tris base. Then, the reaction solution was filtered through pre-soaked Whatman GF/C glass filter with Tris buffer supplemented with 1% BSA, followed by 2 rinses with 3 ml Tris buffer using a 24 well Brandel Cell Harvester (Model M-24R). The filters were dried and counted in Beckman Ready Safe scintillation

fluid with 60% efficiency. The retained radioactivity represents [$^3$H]-dofetilide bound to the ventricular crude membrane homogenate. The rationale for the incubation and filtration conditions have been described previously (41). These conditions provide minimal background (nonspecific binding) and scatter with maximal specific binding. Total binding was determined in the absence of unlabelled dofetilide and nonspecific binding was determined in the presence of an excess amount of unlabelled dofetilide (10 $\mu$M). Specific [$^3$H]-dofetilide binding was determined by subtracting the nonspecific binding from total binding.

### 3.4 Chemicals

[$^3$H]-dofetilide and unlabelled dofetilide (N-[4-2-{2-[4-(methanesulfonamide) phenoxy]-N-methylethylamino}ethyl phenyl]) were kindly provided by Pfizer Research Central (Sandwich UK). To prepare the stock solution, dofetilide was dissolved in acidified distilled water (pH=4 adjusted with HCl) at a concentration of 10 mM (21). The stock solution was stored at 4°C and diluted to the final concentration during experiments. Nisoldipine (a gift from Bayer, Leverkusen, Germany) was prepared as a 2 mM stock solution in 100% ethanol. Collagenase was purchased from Yakult, Tokyo, Japan. Nominally $Ca^{2+}$ free Minimum Essential Medium was purchased from Gibco, New York, USA. Fetal calf serum was purchased from HyClone Laboratories, Inc, Utah, USA. All other chemicals were purchased from Sigma Chemical Co. St. Louis, MO, USA.

### 3.5 Data Analyses

Whole-cell patch clamp data were analyzed using pCLAMP software and plotted using graphic software, Fig.P. The time constants of activation, inactivation and deactivation of the $K^+$ currents were determined from the fitting procedure in Clampfit (pClamp 6) program. The action potential configuration recorded from microelectrode experiments was stored, processed and analyzed using CELLSOFT (University of Calgary, Calgary, Alberta, Canada). The affinity and density of [$^3$H]-dofetilide bindings were determined by Scatchard analysis using the nonlinear least squares curve fitting program LIGAND (Elsevier Biosoft, Cambridge, United Kingdom). All averaged and normalized data were presented as mean $\pm$ standard error (SE) unless otherwise indicated. Statistical significance among groups were determined using the one way Analysis of Variance (ANOVA). To define the difference between the subgroups compared within the ANOVA, such as fetal group vs adult group, the Dunnetts multiple range test was used. In addition, to evaluate the differences between paired observations, such as control vs drug treatment in the same cell, the Student *t*-test was used and p value less than 0.05 was considered significantly different.

# CHAPTER FOUR: RESULTS

## 4.1 Developmental Changes in $I_K$ in Mouse Ventricle

### 4.1a Characterization of $I_K$ in fetal mouse ventricular myocytes

To my knowledge, there are no previous data describing the presence of $I_K$ in fetal mouse ventricle. Therefore, the first question addressed was whether $I_K$ exists in fetal mouse ventricular myocytes. If $I_K$ does exist in fetal mouse ventricle, then the next question was whether both $I_{Kr}$ and $I_{Ks}$ co-exist in fetal mouse ventricular myocytes? Since $I_{Kr}$ and $I_{Ks}$ exhibit different biophysical properties and pharmacological sensitivity to several blockers, $I_{Kr}$ and $I_{Ks}$ were distinguished by studying their rectification properties, their activation kinetics, and their responses to selective $I_{Kr}$ and $I_{Ks}$ channel blockers. Finally, whether $I_K$ plays any role in action potential repolarization in fetal mouse ventricular myocytes was assessed.

*General properties of $I_K$ in fetal mouse ventricular myocytes*

To examine whether $I_{Kr}$ is present, fetal mouse ventricular myocytes were depolarized from -40 to +40 mV in 10 mV increments for 500 ms and then returned to the holding potential -40 mV as shown in the inset of Figure 3. The time-dependent outward $I_K$ elicited by depolarization pulses is defined as activating currents and $I_K$ assessed after repolarization pulses is defined as deactivating tail currents in this dissertation. An example of $I_K$ elicited by this protocol is shown in Figure 3A. The separate current traces elicited by each voltage step are shown in Figure 3B. The

activation of the currents was delayed, resulting in a sigmoidal time course. As shown in Figure 3A and 3B, the activating currents progressively increased from -30 mV and reached a maximum amplitude at 0 mV. The amplitude of currents gradually declined with further depolarization. Deactivating tail currents were measured after repolarization of the cell to the holding potential of -40 mV. The amplitude of deactivating tail currents also progressively increased with depolarization and peaked at 0 mV. Thereafter, the amplitude of the tail currents did not change significantly with further depolarization. Current-voltage relationships of activating currents and tail currents were plotted in Figure 3C. The currents activated during depolarization were measured at the end of the 500 ms depolarization pulse and the deactivating tail currents were measured at the maximum amplitude of the tail current. Note that a negative slope conductance of the current-voltage relationship for the activating currents was observed at potentials positive to 0 mV. Panel D shows the voltage-dependent activation plotted by normalizing amplitude of the peak tail current as a function of test potential. The curve through the data in Figure 3D is the best-fit Boltzmann function, given by equation 1:

$$I_{tail} = I_{max}/[1+\exp(V_h - V_m)/k]$$

where $I_{max}$, $V_h$, $V_m$ and $k$ denote the peak tail current amplitude, half-activation voltage, test potential and slope factor, respectively. The half-activation voltage was -16.3 mV and the slope factor was 6.3 mV. All the features of this current shown in Figure 3 are similar to $I_{Kr}$ described in guinea pig ventricular myocytes (146). Therefore, these results demonstrate that $I_{Kr}$ also exists in fetal mouse ventricular myocytes.

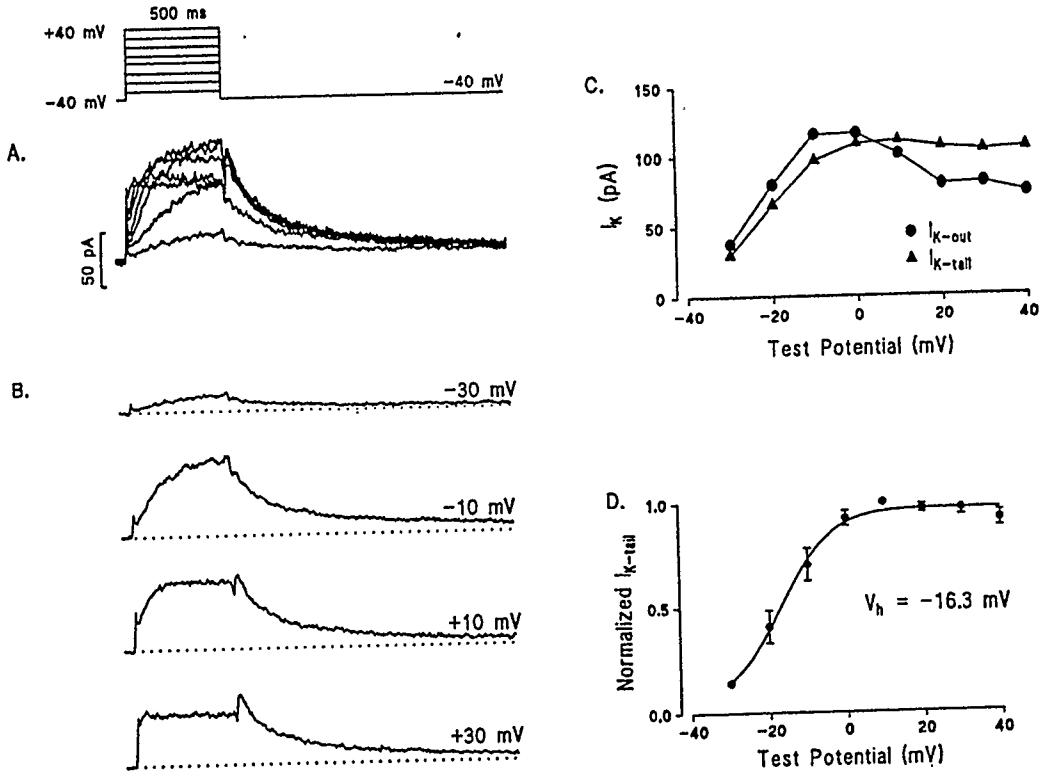


**Figure 3** **General properties of $I_K$ in fetal mouse ventricular myocytes**
Panel A: An example of the superimposed outward current elicited by the depolarizing protocol shown in the inset. Panel B: Single current traces elicited by each of the individual depolarizing steps from Panel A. Panel C: The current-voltage relationship for the activating currents ($I_{K\text{-}out}$) and the deactivating tail current ($I_{K\text{-}tail}$). The $I_{K\text{-}out}$ displays a negative slope conductance when test potentials were more positive than 0 mV. Panel D: Voltage-dependent activation curve of $I_K$ plotted by normalizing the tail currents as a function of test potentials. The continuous curve through the data points represents the best fit to the Boltzmann function (Eq. 1), n=7.

Does $I_{Ks}$ also exist in fetal mouse ventricular myocytes? To answer this question, a different protocol was used to elicit $I_{Ks}$. Since $I_{Kr}$ and $I_{Ks}$ exhibit different properties of voltage and time-dependent activation, one component, either $I_{Kr}$ or $I_{Ks}$, would dominate at a given membrane potential and depolarizing duration. For example, at +50 mV, the amplitude of $I_{Kr}$ is noticeably reduced due to strong rectification. However, the amplitude of $I_{Ks}$ is continuously increased with large depolarization. On the other hand, during the short duration of the depolarization pulse at 0 mV, the dominant current activated is $I_{Kr}$, since its activation kinetics are much faster than $I_{Ks}$.

The protocol used to examine $I_{Ks}$ is as follows. Depolarization from -30 mV to +60 mV in 10 mV increments for 2 sec were applied to the cell from a holding potential of -40 mV. An example of the single current traces elicited by this protocol is shown in Figure 4. The current activated during depolarization showed rapid activation and strong rectification at more positive test potentials. This feature is not consistent with the kinetics of the slowly activating and outwardly rectifying $I_{Ks}$. In addition, the properties of the tail currents also resemble those seen in Figure 3. A similar result was observed in 7 of 7 fetal mouse ventricular myocytes. Thus, the $I_K$ current in fetal mouse ventricular myocytes either does not contain an $I_{Ks}$ component, or the amplitude of $I_{Ks}$ is very small. Further pharmacological and envelope tests of the $I_K$ tail are required to prove the absence of $I_{Ks}$ in fetal mouse ventricular myocytes.

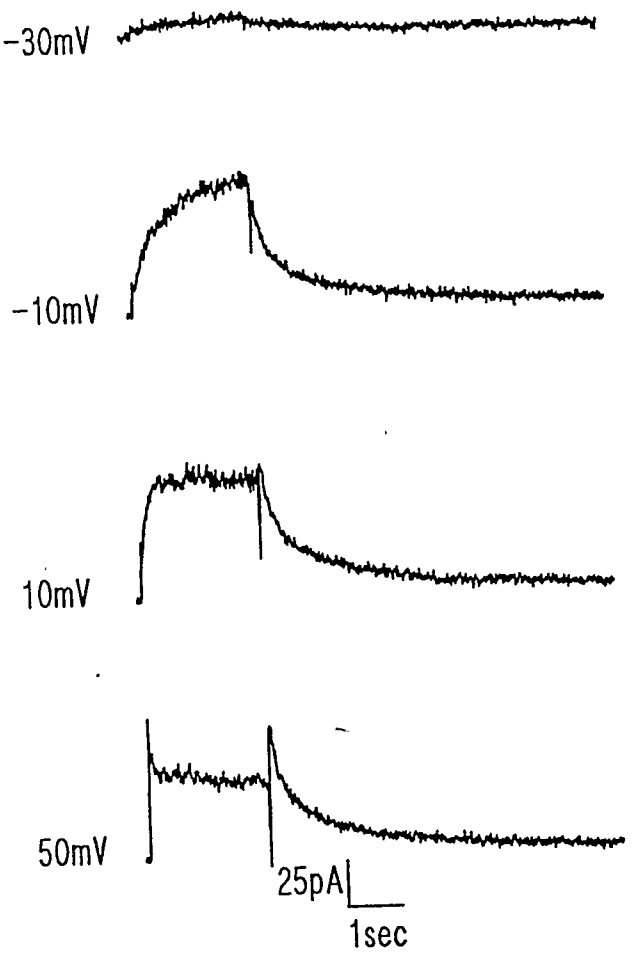


**Figure 4** **Effects of pulse duration and membrane potential on $I_K$ in fetal mouse ventricular myocyte.** The cell was depolarized from a holding potential of -40 mV to +60 mV for 2000 ms and then returned to the holding potential of -40 mV. Selected current traces evoked by depolarizing the cell to -30 mV, -10 mV +10 mV and +50 mV are shown. The current activated rapidly and full activation was seen at +10 mV. Thereafter, the amplitude of the activating currents decreased with further depolarization.

***Reversal potential of $I_K$ in fetal mouse ventricular myocytes***

To examine the ion selectivity of $I_K$ in fetal mouse ventricular myocytes, the reversal potential of the deactivating tail current was evaluated using a standard two pulse protocol. The constant first pulse ($P_I$) was from the holding potential of -40 mV to a test potential of +10 mV for 500 ms. $P_I$ was used to fully activate $I_{Kr}$. $P_I$ was followed by the second pulse ($P_{II}$), which repolarized the cells to various test potentials in the range from -100 mV to -10 mV for 1000 ms. Figure 5A illustrates a representative recording of the reversal potential in fetal mouse ventricular myocytes measured at 4 mM $[K^+]_o$. At this concentration, the deactivating tail currents in fetal mouse ventricular myocytes reversed around -80 mV. This value is close to the equilibrium potential predicted by the Nernst equation for $K^+$, thereby suggesting a high selectivity for $K^+$. In addition, the reversal potential was also measured at three different $[K^+]_o$ levels: 4, 8 and 16 mM. The mean reversal potentials in each of these $[K^+]_o$ levels were plotted in Figure 5B. The regression line for the $E_{rev}$ - $\log[K^+]_o$ relation had a slope of 59.8 mV per decade, close to the theoretical value of 58.2 mV as predicted by the Nernst equation for a $K^+$ selective current. These data demonstrate that the $I_K$ channel in fetal mouse ventricular myocytes is highly selective for $K^+$.

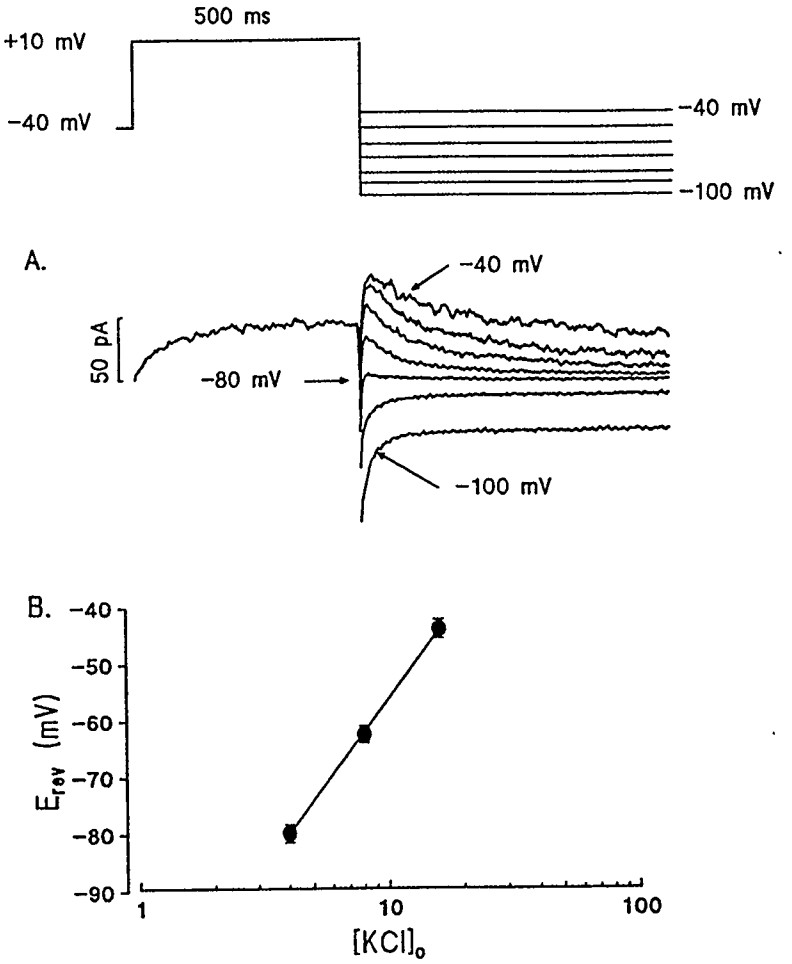


**Figure 5** **Measurements of the reversal potential for $I_K$ in fetal mouse ventricular myocytes.** Panel A: A representative recording of reversal potential elicited by a two-pulse protocol as shown in the inset. $P_I$ depolarized the cell from a holding potential of -40 mV to a test potential of +10 mV for 500 ms and followed by the $P_{II}$ ranging from -100 mV to -40 mV. Panel B: A plot of the reversal potentials obtained at three different $[K^+]_o$. The regression line had slope of 59.8 mV per 10-fold change in $[K^+]_o$ (n=5).

***Envelope of $I_K$ tails test in fetal mouse ventricular myocytes***

To further distinguish whether $I_K$ in fetal mouse ventricular myocytes is conducted through a single or multiple population of channels, an envelope of $I_K$ tails test was performed. Theoretically, if there is only one current component, the ratio of the deactivating tail currents to the activating currents will be constant and independent of the pulse duration. In contrast, if the ratio varies significantly as a function of test duration, it suggests that there is more than one component of $I_K$. Figure 6A shows a representative envelope of the $I_K$ tails test in fetal mouse ventricular myocytes. The cell was depolarized from a holding potential -40 mV to a test potential of 0 mV for various durations and then returned to the holding potential. Clearly, during the test pulse durations, the increase in the amplitude of the activating $I_K$ ($I_{K\text{-}out}$) was proportional to the increase in the deactivating $I_K$ tail current ($I_{K\text{-}tail}$). The ratio of $I_{K\text{-}tail}$ and $I_{K\text{-}out}$ was plotted as a function of the pulse duration shown in Figure 6B. In contrast to guinea pig ventricular myocytes (146), the ratio of $I_{K\text{-}tail}$ to $I_{K\text{-}out}$ in fetal mouse myocytes was constant and independent of pulse duration, indicating the presence of only one rectifying component of $I_K$.

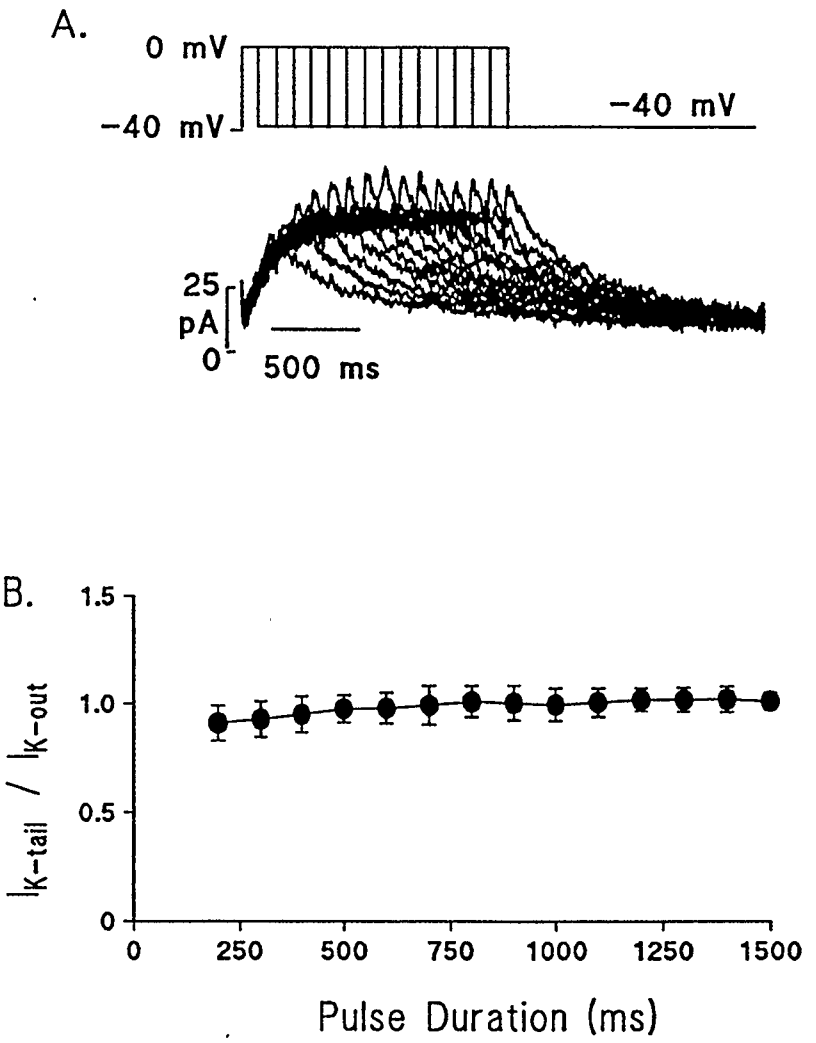


**Figure 6** **Envelope of $I_{K\text{-}tail}$ test in fetal mouse ventricular myocytes**
Panel A: A representative recording of the envelope of $I_{K\text{-}tail}$ tests elicited from a holding potential of -40 mV to a test potential of 0 mV for various pulse duration from 200 ms to 1500 ms. Panel B: The averaged ratio of $I_{K\text{-}tail}$ to $I_{K\text{-}out}$ as a function of the pulse duration (n=6). The envelope of $I_K$ tails test for one component of $I_K$ is satisfied .

Furthermore, if there is only one component of $I_K$, deactivation time constant of the tail current should be independent of test potentials. To test this hypothesis, the cells were depolarized from a holding potential of -40 mV to test potentials of -10 mV, 0 mV and +20 mV and then returned to the holding potential. The representative examples are shown in Figure 7A (-10 mV), 7B (0 mV) and 7C (+20 mV). The deactivation time constants for the tail currents evoked by each step of the test potentials were determined by bi-exponential fitting and plotted as a function of the pulse duration (Figure 7D). As shown in Figure 7D, both fast and slow deactivation time constants were independent of test duration and voltage. These results further support the findings that there is only one current component of $I_K$ ($I_{Kr}$) in fetal mouse ventricular myocytes.

An example of the activation kinetics of $I_K$ tail currents determined by the envelope of tail test is shown in Figure 8. The amplitude of tail currents was measured and plotted as a function of the pulse duration. The solid curve through the data points represents the least-squares one-exponential fit according to equation 2:

$$I_{Ktail} = I_{max} \times [1-\exp(-t/\tau)]$$

where $\tau$ and t denote the activation time constant and pulse duration, respectively. The time constant for the envelope of $I_K$ tail current was 158 ms at a test potential of 0 mV. The data were well described by a mono-exponential function. All these results, the envelope of the $I_K$ tails test and the plots of the $I_K$ tail current activation and deactivation kinetics, further support that $I_K$ in fetal mouse ventricular myocytes only consists of the rapidly activating component, $I_{Kr}$.

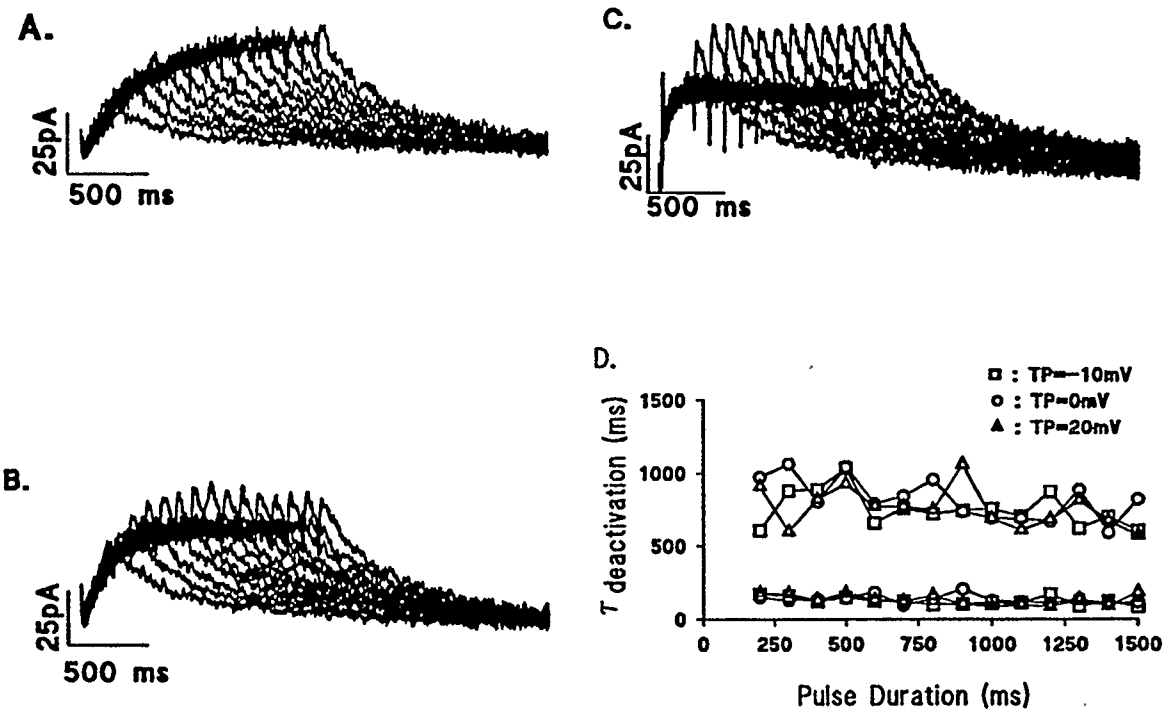


**Figure 7** **Representative recordings of the envelope of the $I_K$ tail tests recorded from different test potentials.** The cell was depolarized from a holding potential of -40 mV to test potentials of -10 mV (Panel A), 0 mV (Panel B) and +20 mV (Panel C) for various pulse duration from 200 ms to 1500 ms. Panel D shows the plots of deactivation time constants for each tail current as a function of the pulse duration at test voltages of -10 mV, 0 mV and +10 mV, respectively.

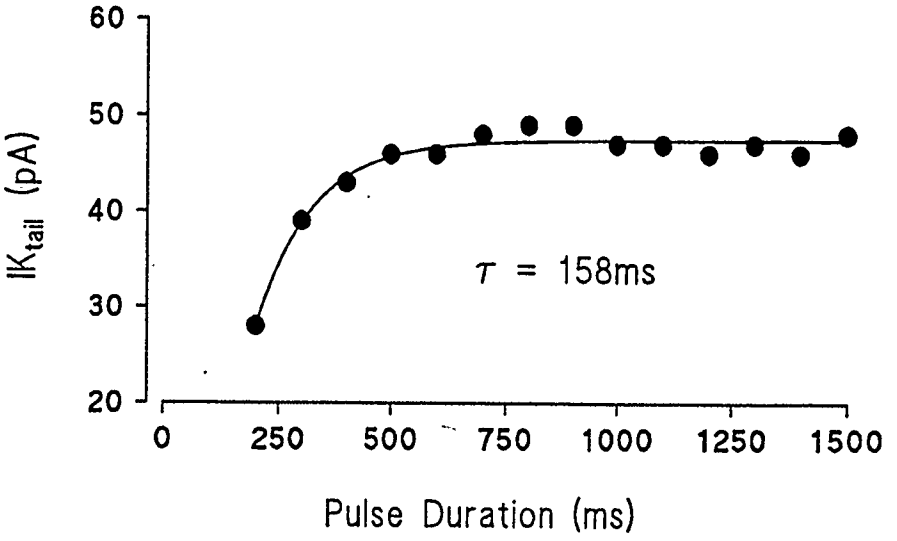


**Figure 8** **A plot of $I_K$ activation kinetics determined from the envelope of tail currents.** The amplitude of the $I_K$ tail currents elicited from repolarizing the cell from 0 mV to the holding potential of -40 mV was measured and plotted as a function of the pulse duration. The curve through the data points was the best fit to the least-squares single exponential function (Eq. 2). The activation time constant of the tail currents at 0 mV was 158 ms.

***The activation and deactivation kinetics of $I_K$ in fetal mouse ventricular myocytes***

The time constants of $I_K$ activation and deactivation were voltage-dependent. To assess the activation kinetics of $I_K$, the cell was depolarized to various membrane potentials ranging from -40 mV to +40 mV and then returned to the holding potential of -40 mV. To assess the deactivation kinetics of the $I_K$ tail currents, a double-pulse protocol was used. The cell was first depolarized to a fixed test of +10 mV. The second pulse was varied and repolarized to various membrane potentials ranging from -100 mV to -30 mV. The activation and deactivation time constants were determined by the exponential fitting of the currents evoked by each voltage step. The time constant for activation was best fit with a single exponential function. The rate of activation increased with incremental changes in the test potential (from 511 $\pm$ 71 ms at -20 mV to 54 $\pm$ 14 ms at +20 mV). The rapid activation kinetics further support that this current in the fetal mouse ventricular myocytes is $I_{Kr}$. The deactivation process of $I_K$ was voltage-dependent and well fit with a bi-exponential function. Rates of both fast and slow deactivation were faster at more negative potentials. The mean data of the activation and deactivation time constants of $I_K$ plotted as a function of the test potential are shown in Figure 9.

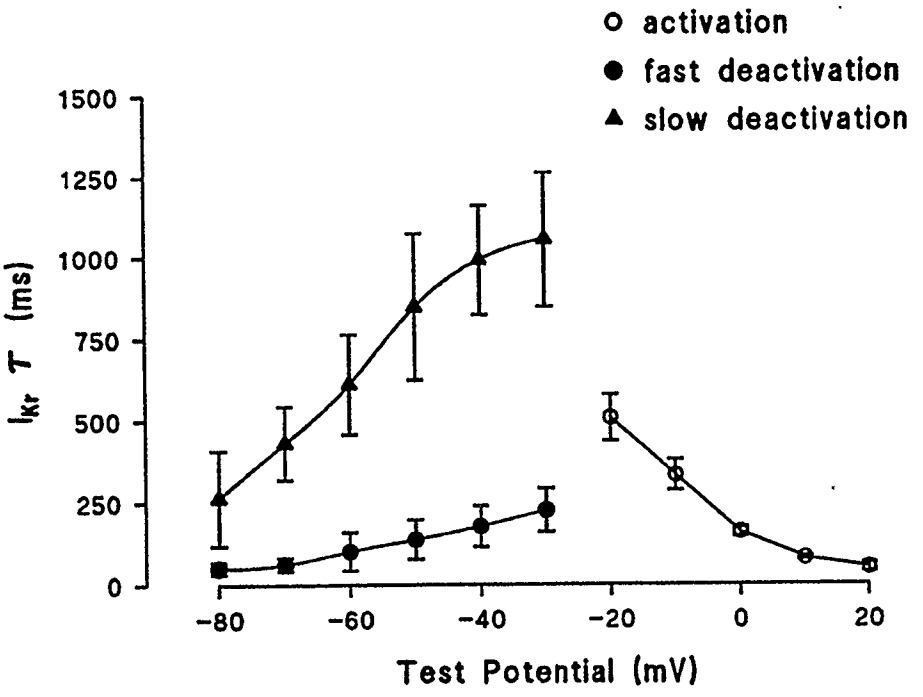


**Figure 9** **Time course of $I_K$ activation and deactivation in fetal mouse ventricular myocytes.** The graph shows voltage-dependent kinetics of $I_K$ activation and deactivation time constants (n=12).

***Effects of dofetilide on $I_K$ in fetal mouse ventricular myocytes***

It has been reported that dofetilide selectively blocks $I_{Kr}$ with an $IC_{50}$ of 32 nM, and completely abolishes $I_{Kr}$ at a concentration of 1 $\mu$M but had no effect on $I_{Ks}$ even at a concentration of 10 $\mu$M (84). Figure 10 displays the $I_K$ recordings before (Panel A) and after dofetilide application (Panel B). As shown in Panel B, dofetilide at a concentration of 1 $\mu$M completely abolished the $I_K$ tail currents, indicating that a dofetilide-sensitive component of $I_K$ is the major contributor to the repolarization-induced $I_K$ tail current in fetal mouse ventricular myocytes. Panel C shows the dofetilide-sensitive current which was obtained by subtracting the dofetilide-resistant current (Panel B) from drug-free current (Panel A). The current-voltage relationships for the control current and the dofetilide-sensitive current are shown in Panels D and E, respectively. The similarities in the amplitude of the currents during depolarizing pulses and the strong rectification for $I_{K\text{-}out}$ (Panels D and E) further suggest that fetal mouse ventricular myocytes express a single component of $I_K$, the $I_{Kr}$. A comparison of the biophysical and pharmacological properties of $I_{Kr}$ among fetal mouse ventricular myocytes, guinea pig ventricular myocytes (146), mouse AT-1 cell line (186) and *HERG* expressed in oocytes (149) is provided in Table 2.

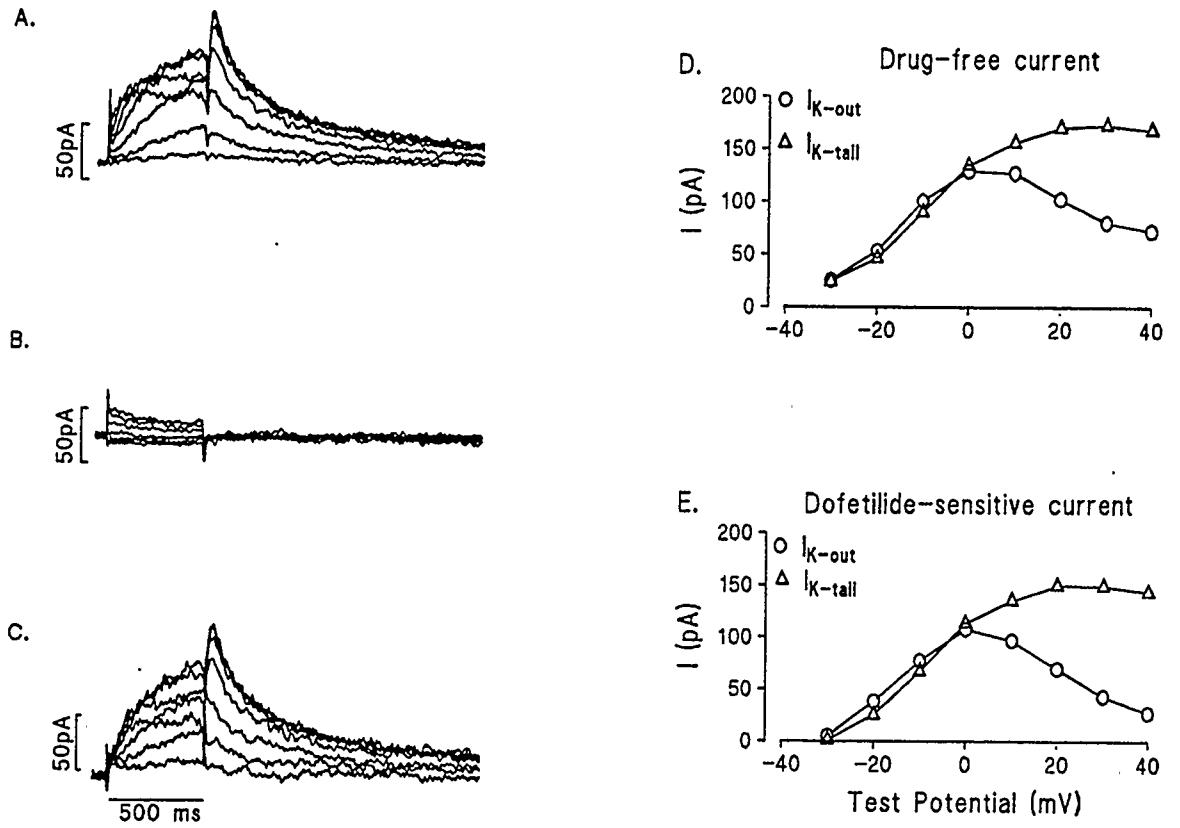


**Figure 10** **Effects of dofetilide on $I_K$ in fetal mouse ventricular myocytes.** The superimposed outward $K^+$ currents were recorded before (Panel A) and after (Panel B) application of 1 $\mu$M dofetilide. The currents were elicited from a holding potential of -40 mV to test potentials ranging from -30 mV to +40 mV by 10 mV step increment for 500 ms. The dofetilide-sensitive current is shown in Panel C. The current-voltage relationships for the control current and dofetilide-sensitive current are displayed in Panel D and E. $I_{K\text{-out}}$ and $I_{K\text{-tail}}$ denote the activating current and the deactivating tail current of $I_K$, respectively.

**Table 2 Comparison of the Characteristics of $I_{Kr}$ in Different Cardiac Preparations**

| $I_{Kr}$ in various preparations | $I_{(peak)}$ (mV) | Negative slope conductance | Activation | | Dofetilide ($IC_{50}$) (nM) | Reference |
|---|---|---|---|---|---|---|
| | | | $V_h$ (mV) | Slope (mV) | | |
| Fetal Mouse VM[a] | 0 | + | -16 | 6.7 | 13 | |
| Guinea Pig VM | 0 | + | -22 | 7.5 | 32 | 146 |
| Mouse AT-1 cells[b] | +10 | + | +0.9 | NA | 12 | 186 |
| Oocytes injected with *HERG*[c] | 0 | + | -15 | 7.9 | NA[d] | 149 |

[a] VM denotes ventricular myocytes; [b] AT-1 denotes atrial tumor cell line, [c] *HERG* represents human *eag*-related gene and [d] denotes not available in that study.

***Functional role of $I_{Kr}$ in fetal mouse ventricular myocytes***

To evaluate whether $I_{Kr}$ plays a physiological role in action potential repolarization, the effects of dofetilide (1 $\mu$M) on action potential duration were assessed in fetal mouse ventricular myocytes (Figure 11). $I_{Kr}$ and the action potentials were recorded in the same cell before and after application of dofetilide. $I_{Kr}$ was first recorded in the absence of the drug (Panel A●). Then the circuit of the patch amplifier was switched to the current-clamp mode, and the spontaneous action potentials were recorded under drug-free conditions and after application of dofetilide (1 $\mu$M) (Panel B). Thereafter, the circuit was switched back to the voltage-clamp mode to record the effects of dofetilide on $I_{Kr}$ (Panel A■). As shown in Figure 11A, dofetilide at 1 $\mu$M completely abolished the deactivating tail current. Blockade of $I_{Kr}$ by dofetilide caused a dramatic prolongation of the action potential duration (Panel B). In some fetal mouse ventricular cells, after-depolarization (ADs) were observed after dofetilide treatment (Panel C). These data suggest that $I_{Kr}$ plays an important role in action potential repolarization in fetal mouse ventricles.

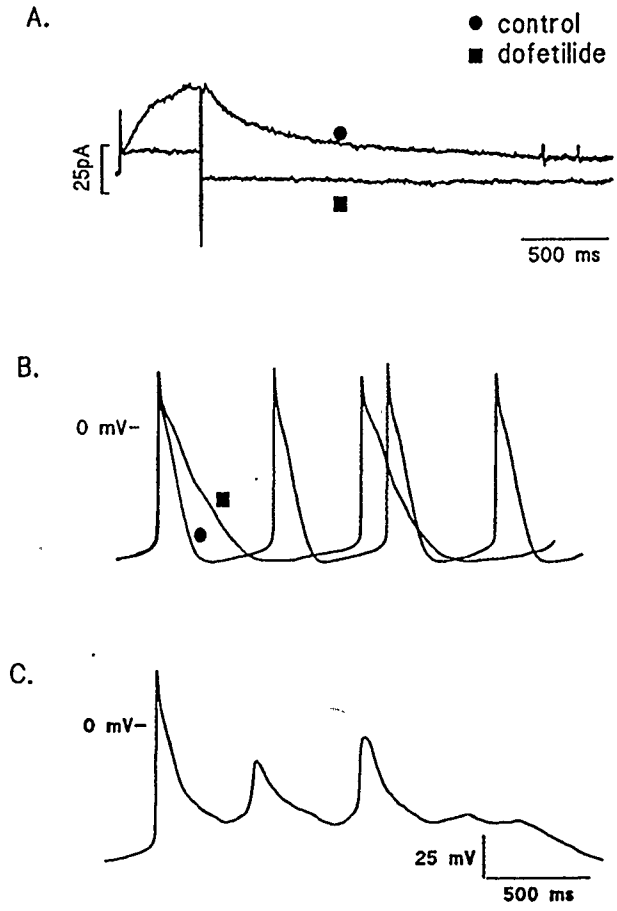


**Figure 11** **Effects of dofetilide on $I_{Kr}$ and the spontaneous action potentials in fetal mouse ventricular myocytes.** The currents were evoked from the holding potential of -40 mV to the test potential of 0 mV for 500 ms. In the same cell, $I_{Kr}$ (Panel A) and the action potentials (Panel B) were recorded both before and after 1 $\mu$M dofetilide was applied. ADs were observed in some cells after dofetilide was applied (Panel C).

## 4.1b Developmental changes in the delayed rectifier $K^+$ channels ($I_K$) in mouse ventricle

***Age-related changes in $I_K$ in mouse ventricular myocytes assessed by whole-cell voltage-clamp technique***

As mentioned previously, $I_{Kr}$ and $I_{Ks}$ differ in their activation kinetics, rectification properties and pharmacological sensitivity (146). Accordingly, to assess whether $I_{Kr}$ and $I_{Ks}$ are developmentally regulated, the properties of $I_K$ in ventricular myocytes from neonatal and adult mice were evaluated and compared with the parameters obtained from fetal mouse ventricular myocytes.

As shown in Figure 12, the properties of $I_K$ in day 1 neonatal ventricular myocytes varied from cell to cell. An example of currents obtained from a day 1 neonatal mouse ventricular myocyte which expressed dominantly $I_{Kr}$ is shown in Panel A. In contrast, Panel B shows that a different ventricular cell isolated from a day 1 neonate expressed a current with characteristics of $I_{Ks}$, such as slow activation and outward rectification. Approximately 60% of cells from day 1 neonatal hearts expressed a dominant $I_{Kr}$ pattern.

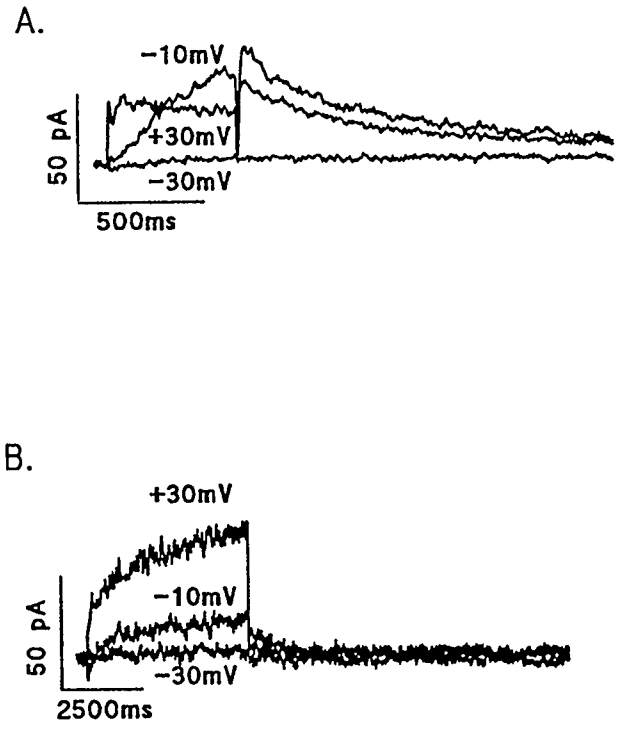


**Figure 12** **Variation of $I_K$ in day 1 neonatal mouse ventricular myocytes.** As shown in this Figure, both $I_{Kr}$ and $I_{Ks}$ are present in day 1 neonatal cells. Panel A shows an example of a cell which expressed dominant $I_{Kr}$ and Panel B shows an example of a cell which expressed dominant $I_{Ks}$. The currents were evoked from a holding potential of -40 mV to test potentials of -30 mV, -10 mV and +30 mV for 500 ms ($I_{Kr}$) and 5 s ($I_{Ks}$), respectively.

The $I_K$ recorded in day 3 neonatal mouse ventricular myocytes resembled $I_{Ks}$ in cardiac myocytes of other species. The current activated slowly and did not reach a steady state even during a 5 seconds depolarization pulse. The amplitude of the activating currents increased continuously with membrane depolarization. As a result, the current-voltage relationship of the activating current displayed a positive slope conductance throughout the voltage range examined. The properties of the slow activation and linear current-voltage relationship suggest that this current is largely $I_{Ks}$. Cells which expressed a dominant $I_{Kr}$ were not identified in day 3 neonatal mouse ventricular myocytes. Figure 13 illustrates the differences between the $I_{Kr}$ traces and the plot of its current-voltage relationship obtained from fetal mouse ventricular cells (Panel A and B), and $I_{Ks}$ traces and the plot of its current-voltage plot obtained from day 3 neonatal mouse ventricular cells (Panel C and D).

In adult mouse ventricular myocytes, neither $I_{Kr}$ nor $I_{Ks}$ type currents were observed when using the same depolarization protocols applied to fetal and neonatal mouse ventricular myocytes.

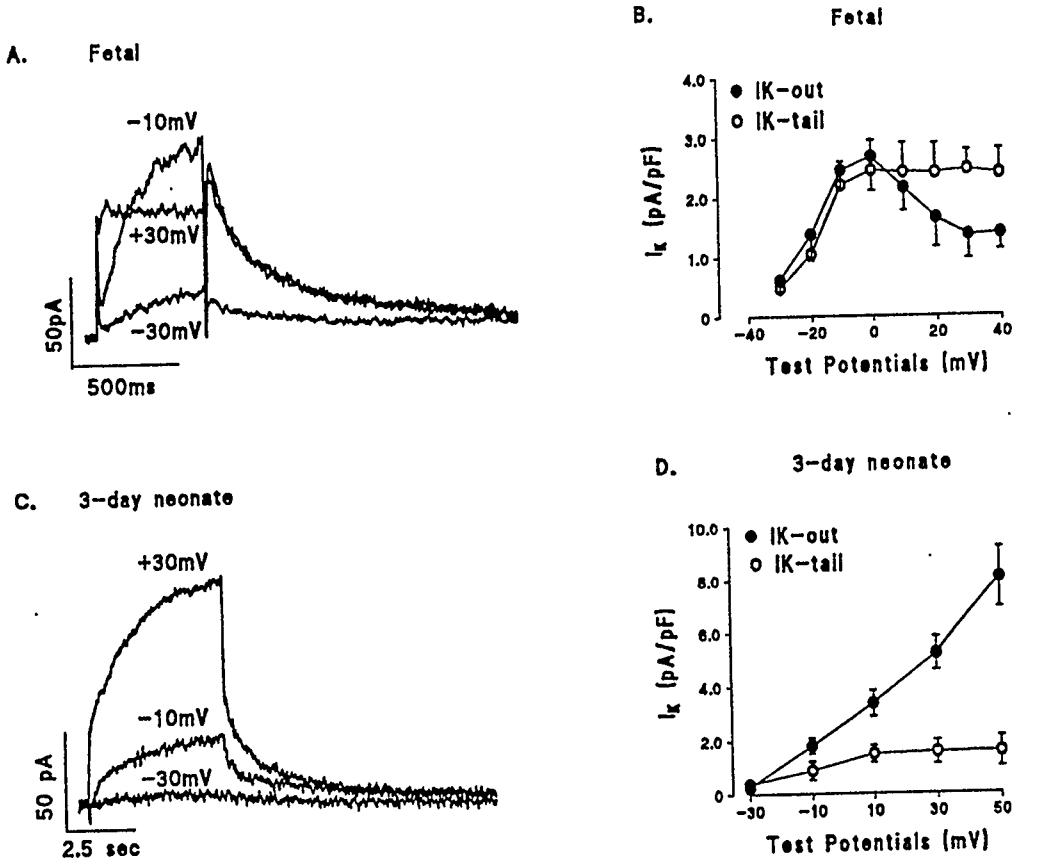


**Figure 13** **Comparison of the properties of $I_{Kr}$ in fetal and $I_{Ks}$ in day 3 neonatal mouse ventricular myocytes.** The holding potential was -40 mV in both preparations, but the duration of depolarization pulses applied in the day 3 cell was 10 fold longer than that in the fetal cell (5 s vs 500 ms). The activation kinetics and rectification properties are fundamentally different as compared $I_{Kr}$ in fetal mouse ventricular myocytes (Panel A and B), n=7 with $I_{Ks}$ in day 3 neonatal mouse ventricular myocytes (Panel C and D), n=5.

The representative activation fittings for $I_K$ in fetal, day 1 and day 3 neonatal mouse ventricular myocytes are shown in Figure 14. The currents were elicited from a holding potential of -40 mV to a test potential of +10 mV for 500 ms ($I_{Kr}$) or +50 mV for 5000 ms ($I_{Ks}$), respectively. Depolarizing the cell to +10 mV, $I_{Kr}$ reached a steady state during a 500 ms pulse in fetal (Panel A) and day 1 neonatal mouse ventricular myocytes (Panel B). The activation time constants at +10 mV were 82 $\pm$ 7 ms for fetal mouse ventricular myocytes (n=6) and 83 $\pm$ 7 ms for day 1 neonatal mouse ventricular myocytes in which $I_{Kr}$ was expressed dominantly (n=5). Activation of $I_{Ks}$, however, did not reach a steady state during a 5000 ms step to +50 mV (Panel C and D). At +50 mV, activation time constant of $I_{Ks}$ in day 1 neonatal mouse ventricular myocyte, which expressed dominantly $I_{Ks}$, was 1734 $\pm$ 438 ms (n=3); and activation time constant of $I_{Ks}$ in day 3 neonatal mouse ventricular myocytes was 1850 $\pm$ 300 ms (n=4).

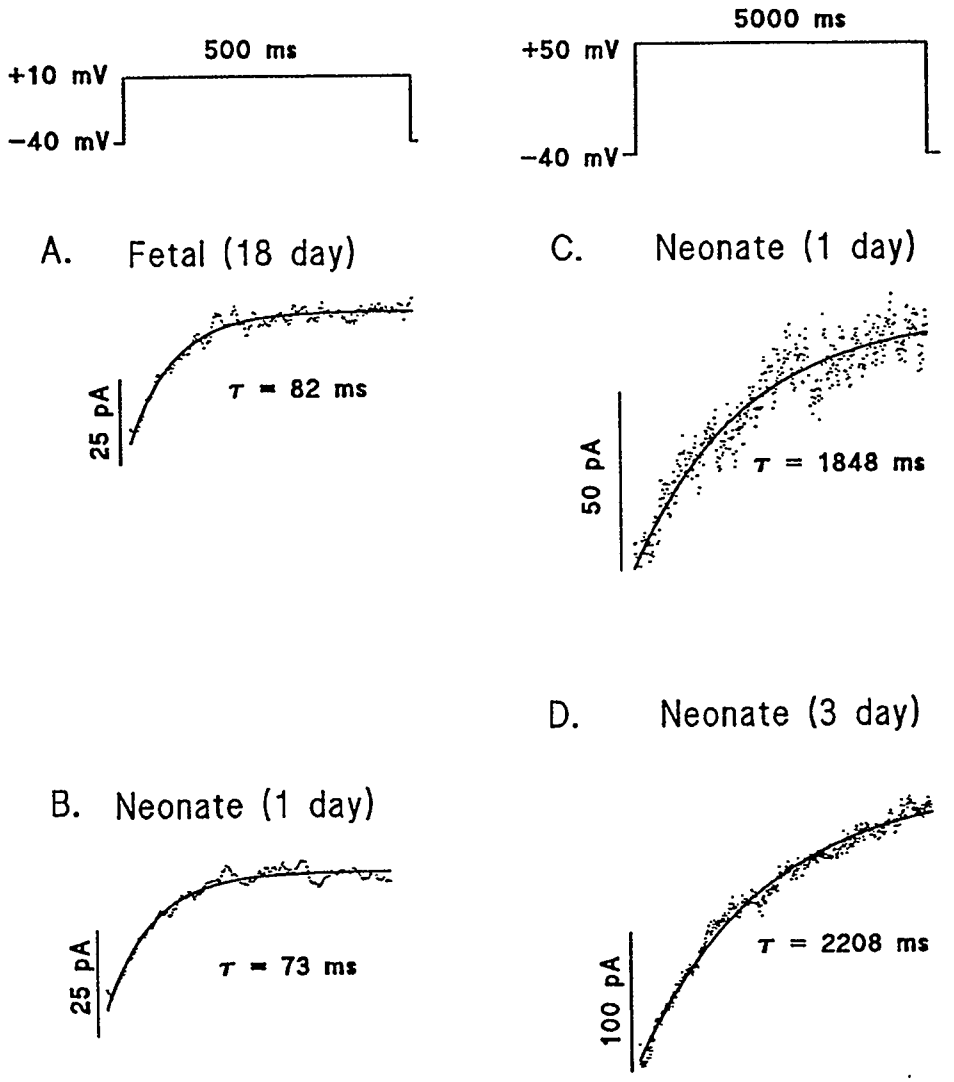


**Figure 14** **Representative mono-exponential fittings for $I_K$ activation in fetal, day 1 and day 3 neonatal mouse ventricular myocytes.** Panel A shows that $I_{Kr}$ elicited from fetal mouse ventricular myocytes activates rapidly, as judged by activation time constant. Panel B and C show that both rapidly activating current, $I_{Kr}$ and slowly activating current, $I_{Ks}$ are present in day 1 neonatal ventricular myocytes. Panel D shows that the current in day 3 neonatal ventricular myocytes activates slowly, which is consistent with $I_{Ks}$.

Results shown in Figure 15 compares the effects of dofetilide (1 $\mu$M) on $I_K$ activated during depolarization from -40 mV to +10 mV for 5000 ms in fetal (Panel A), day 3 neonatal (Panel B) and adult (Panel C) mouse ventricular myocytes. The tail current was completely abolished by dofetilide in fetal mouse ventricular myocyte (n=5), suggesting that only $I_{Kr}$ contributes to this tail current. However, in day 3 neonate, dofetilide only partially blocked the tail current (n=4). This finding suggests that both the dofetilide-sensitive current, $I_{Kr}$ and the dofetilide-insensitive current, $I_{Ks}$ contribute to the tail current. In adult mouse ventricular myocytes, the current evoked by the same protocol displayed very rapid activation and inactivation (n=8). These properties fundamentally differ from the properties of $I_{Kr}$ and $I_{Ks}$. Dofetilide at 1 $\mu$M did not have any effect on this transient outward current in adult mouse ventricular myocytes (n=4).

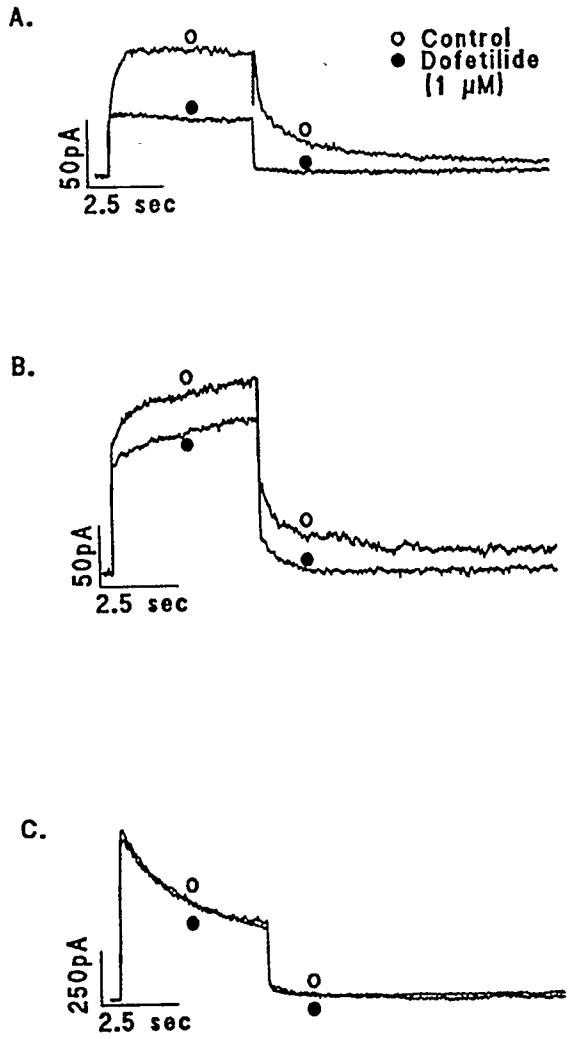


**Figure 15** **Effects of dofetilide on $I_K$ in mouse ventricular myocytes recorded at different developmental stages.** Dofetilide (1$\mu$M) completely abolished the $I_K$ tail current in fetal mouse ventricular myocytes (Panel A) but only partially blocked the $I_K$ tail current in day 3 neonatal mouse ventricular myocytes (Panel B). Dofetilide had no effects on the current recorded in adult mouse ventricular myocytes (Panel C).

***Relations between developmental changes in $I_K$ and the action potential configuration in mouse ventricle assessed by conventional microelectrode technique***

This dissertation has shown that the expression of $I_K$ in mouse ventricular myocytes changes remarkably during development. Can these changes in $I_K$ expression in mouse ventricular myocytes result in a corresponding alteration in the action potential configuration? Figure 16 shows the representative action potential recordings obtained from fetal, neonatal and adult mouse ventricular endocardium under drug-free conditions. The action potential in fetal mouse ventricular endocardium has a distinct plateau with long duration. The action potential duration in mouse ventricle dramatically decreased within 1 day after birth, then further shortened by the third day of postnatal life. The action potential configuration became spike-like in the adults. Action potentials with large and rapid phase 1 repolarization followed by a prolonged plateau (130 to 150 ms) at more negative potentials ($\approx$ -40 mV) were observed in 3 of 60 records from 12 adult mice. Since these distinct and uncommon action potentials may have been recorded from a distinct cell type, such as Purkinje fibers, this type of action potential was not included in the data analysis in the present study. The action potential characteristics in each age group are summarized in Table 3.

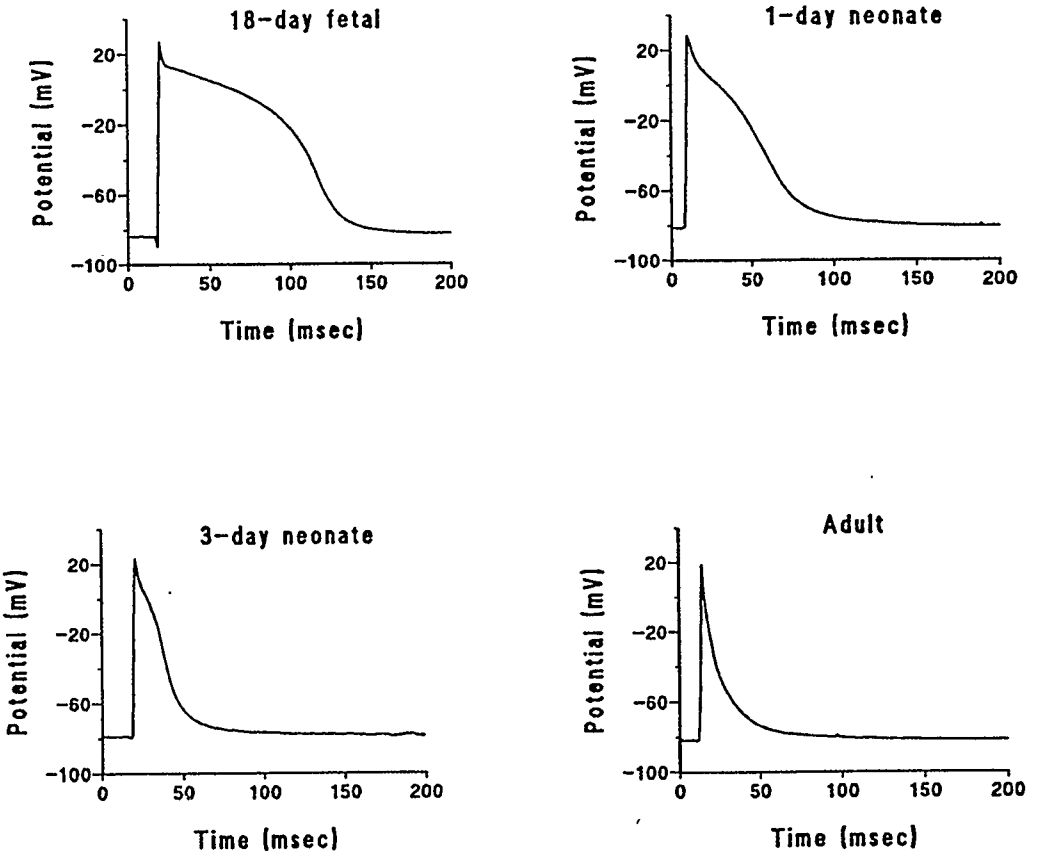


**Figure 16** **Examples of the representative action potentials in fetal, day 1, day 3 neonatal and adult mouse ventricular endocardium.** The preparations were perfused with normal Tyrode solution at 37°C and were paced at 2 Hz. The profound decreases in action potential duration with age may result from developmental changes in $K^+$ currents underlying the action potential repolarization in mouse heart (see Table 3).

**Table 3** **The Characteristics of Action Potentials in Mouse Ventricular Endocardium During Development**

| Age | RMP (mV) | $APD_{50}$ (ms) | $APD_{95}$ (ms) | $V_{max}$ (V/sec) |
|---|---|---|---|---|
| **Fetal (18 days)** | -81±2 | 74±11 | 133±20 | 210±54 |
| **Neonate (1 day)** | -80±2 | 43±14* | 94±16* | 207±66 |
| **Neonate (3 days)** | -80±3 | 18±6*† | 51±9*† | 182±49 |
| **Adult** | -81±2 | 10±3*†‡ | 67±20*† | 221±45 |

Values represent mean ± S.D ($n \geq 8$ for each groups); * denotes significantly different from fetal, $p<0.01$; † denotes significantly different from the day 1 neonate, $p<0.01$; ‡ denotes significantly different from the day 3 neonate; RMP represents resting membrane potential; $APD_{50}$ and $APD_{95}$ represent the action potential duration at 50% and 95% repolarization, respectively; $\dot{V}_{max}$ denotes the maximum upstroke velocity of the phase 0 of the action potentials.

To examine whether age-dependent changes in the action potential configuration in mouse ventricular endocardium were related to the developmental changes in cardiac $I_K$, the extent of the action potential prolongation by selective $I_K$ channel blockers was assessed in fetal, neonatal and adult mouse ventricular endocardium. Since both $I_{Kr}$ and $I_{Ks}$ are present in mouse ventricular myocytes during development, the responses of the action potential to a selective $I_{Kr}$ blocker, dofetilide (21,84) and a selective $I_{Ks}$ blocker, indapamide (167) were assessed. Figure  illustrates the representative examples of the effects of dofetilide (1 $\mu$M) on the action potential duration in mouse ventricle at each developmental age groups. The mean data are summarized in Figure 18. The action potential duration in fetal mouse ventricular endocardium was dramatically prolonged by dofetilide ($APD_{95}$ 137% $\pm$ 18%, n=7). The extent of the action potential prolongation by dofetilide profoundly decreased during the first day of life ($APD_{95}$ 75% $\pm$ 29%, n=5) and further decreased by the 3rd day for neonates ($APD_{95}$ 20% $\pm$ 15%, n=5). In adult ventricular endocardium, dofetilide did not prolong the action potential duration (n=4). Dofetilide at 1 $\mu$M had no significant effects on resting membrane potential and $\dot{V}_{max}$ for all age groups.

In contrast to the effects of dofetilide on the action potential duration, at the same pacing cycle length, $I_{Ks}$ channel blocker, indapamide (100 $\mu$M) did not significantly prolong the action potential duration at any age groups. This finding suggests that $I_{Ks}$ is not likely to play an important role in the action potential repolarization in mouse heart.

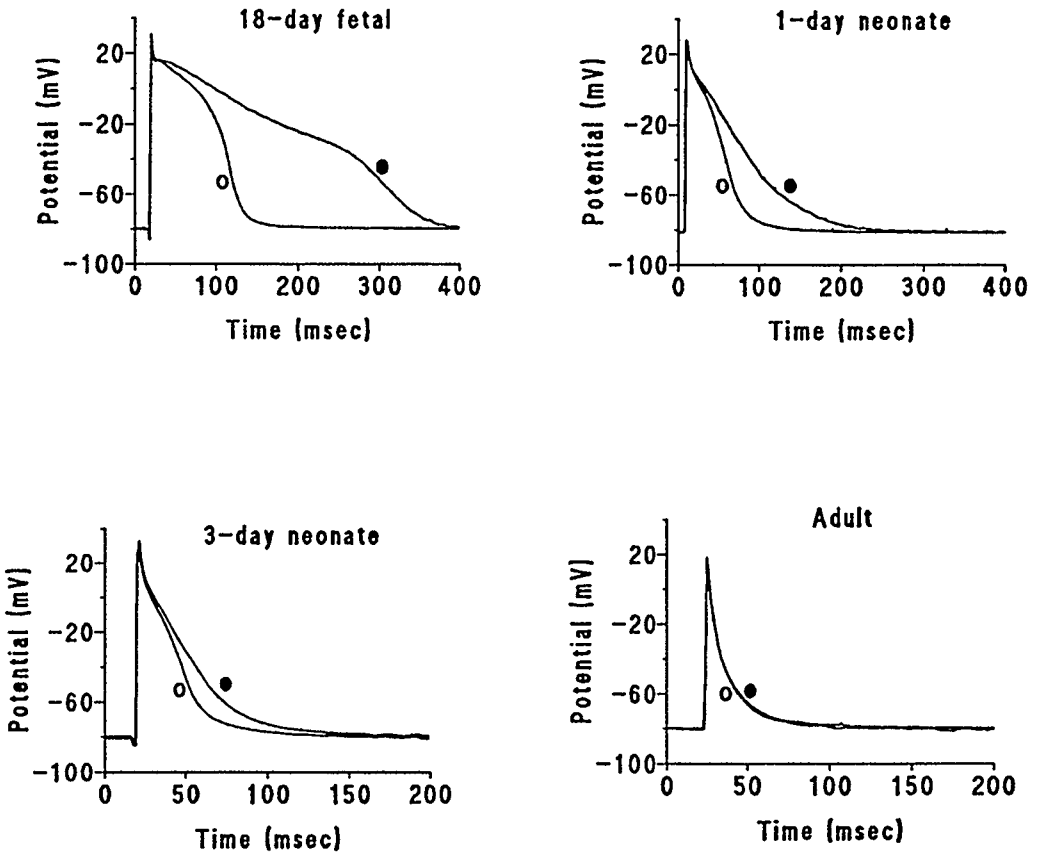


**Figure 17** **Representative examples of the effects of dofetilide on action potential duration in fetal, day 1, day 3 neonatal and adult mouse ventricular endocardium.** Dofetilide (1 $\mu$M) produced a remarkable prolongation of the action potential duration in fetal mouse heart. However, the effects of dofetilide dramatically decreased during early postnatal period. In adult mice, dofetilide did not lengthen the action potential duration.

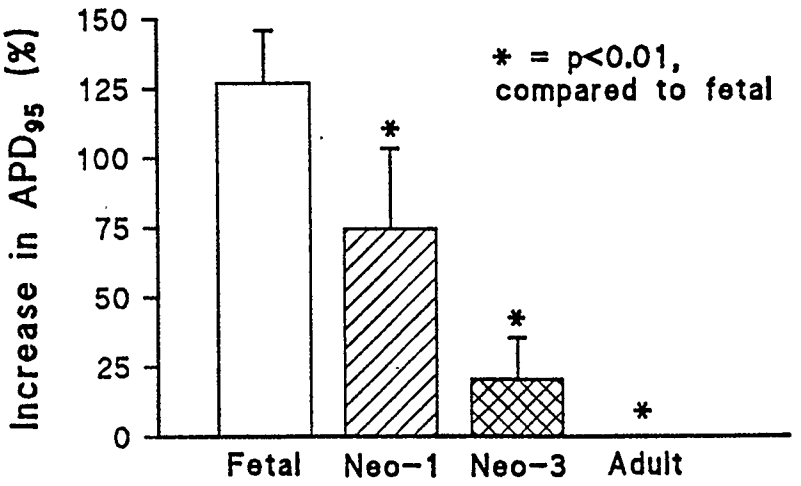


**Figure 18** **Effects of dofetilide on the action potential prolongation in mouse heart during development.** The data in each age group were obtained from at least 4 different recordings and presented as mean ± S.D. Neo-1 and Neo-3 denote day 1 and day 3 neonates. The mean data show that effects of dofetilide on the action potential prolongation in mouse heart progressively and significantly decreased during development.

***Age-related changes in $I_{Kr}$ channels in mouse ventricle assessed by [$^3$H]-dofetilide binding assay***

It has been reported that [$^3$H]-dofetilide is a specific radioligand for $I_{Kr}$ channels in guinea pig ventricular myocytes (25,41). Therefore, an [$^3$H]-dofetilide binding assay was employed to study the developmental changes in $I_{Kr}$ channels in mouse heart. Under our experimental conditions, the specific binding of [$^3$H]-dofetilide was 50-63% in the crude ventricular membrane homogenate from fetal and day 1 and day 3 neonatal mice. The specific binding of [$^3$H]-dofetilide was not detected in adult mouse ventricular homogenate.

A representative Scatchard plot of the [$^3$H]-dofetilide binding isotherm in fetal mouse ventricular homogenate is shown in Figure 19. Scatchard analysis of this fitting indicates a single [$^3$H]-dofetilide binding site with a high binding affinity. The averaged $K_d$ of [$^3$H]-dofetilide binding in fetal tissues was 13 $\pm$ 2 nM (n=4). During early postnatal development, the Scatchard analysis showed that the $K_d$ of the [$^3$H]-dofetilide binding site significantly increased to 37 $\pm$ 7 nM in day 3 neonatal ventricular homogenate ($p<0.05$, n=8) without a change in $B_{max}$. Although the $B_{max}$ values were not significantly changed during early postnatal development, the declined affinity during development suggests that the properties of [$^3$H]-dofetilide binding protein may be altered at 3 days after birth. In adult mouse ventricular homogenate, no specific [$^3$H]-dofetilide binding was detected. Presence of the high affinity [$^3$H]-dofetilide binding sites in fetal mouse ventricular homogenate and absence in adult mouse ventricles support the parallel electrophysiological findings. Mean data of $K_d$ and $B_{max}$ of [$^3$H]-dofetilide binding in the

preparations of mouse ventricular homogenate from different age groups are summarized in Table 4.

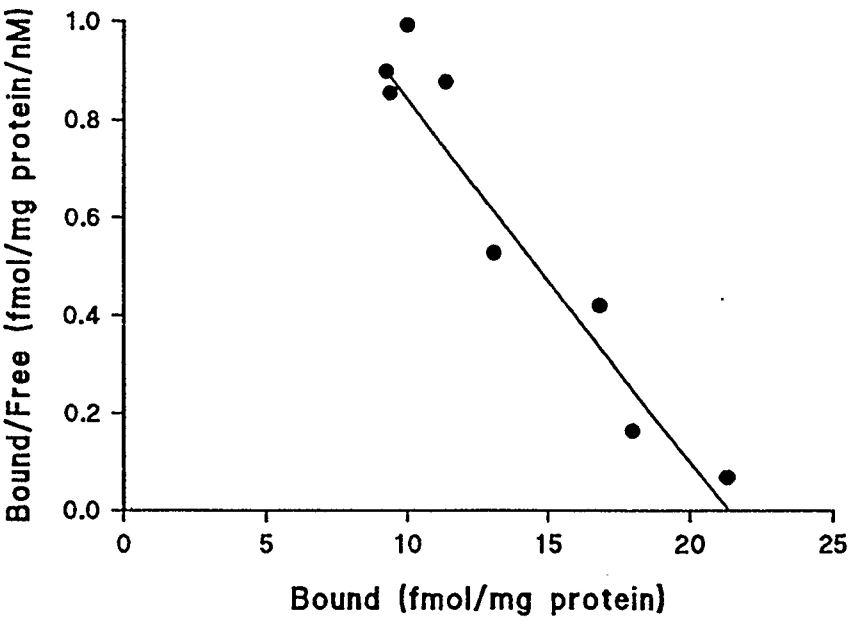


**Figure 19** **An example of Scatchard analysis of dofetilide binding to fetal mouse ventricular homogenate.** The data were best fit to a single binding site model. The slope of the curve represents the affinity of [$^3$H]-dofetilide binding to its binding site expressed as $K_d$. The X intercept of the curve represents the maximal binding density as $B_{max}$ (for $K_d$ and $B_{max}$ values see Table 4).

**Table 4** **Comparison of $K_d$ and $B_{max}$ of [$^3$H]-Dofetilide Binding to Mouse Ventricular Membrane Homogenate During Development**

| Age | $K_d$ (nM) | $B_{max}$ (fmol/mg protein) | n |
|---|---|---|---|
| **Fetal (18 days)** | 13±2 | 26±5 | 4 |
| **Neonate (1 day)** | 17±3 | 33±6 | 6 |
| **Neonate (3 days)** | 37±7* | 21±2 | 8 |
| **Adult** | NSB | NSB | 7 |

* denotes significant difference from the results of fetal mouse group, $P<0.05$. NSB represents no specific [$^3$H]-dofetilide binding in adult mouse ventricle.

## 4.2 Developmental Changes in the Transient Outward Currents, $I_{to}$ in Mouse Ventricle

Developmental changes in cardiac $I_{to}$ have been documented in many species, however they have not been investigated in mouse heart. Thus, this dissertation aimed to evaluate whether $I_{to}$ in mouse heart also changes during development. First, $I_{to}$ was measured using whole-cell patch-clamp technique. The following properties of $I_{to}$ in single ventricular myocytes during development were assessed: the current-voltage relations; the density of $I_{to}$; the inactivation kinetics; the steady-state inactivation of $I_{to}$ and responses to 4-aminopyridine (4-AP, an $I_{to}$ blocker). Percentage of the cells that expressed $I_{to}$ in fetal mouse ventricular myocytes was very low, therefore, the measurements of $I_{to}$ in fetal mouse ventricular myocytes are not presented in this dissertation. Secondly, the physiological significance of $I_{to}$ in the action potential repolarization was also determined by assessment of the extent of the action potential prolongation by 4-AP in the mouse ventricular tissue from day 1, day 3 neonatal and adult mice at physiological temperature (37°C).

### 4.2a Age-related changes in $I_{to}$ in mouse ventricular myocytes assessed by whole-cell patch-clamp technique

***Current-voltage relations and the density of $I_{to}$ in mouse ventricular myocytes during development***

To record $I_{to}$, the outward currents were routinely measured during depolarization to membrane potentials between -60 mV and +50 mV in 10 mV increments from a

holding potential of -70 mV unless indicated otherwise. Figure 20 shows the representative recordings of the superimposed transient outward currents elicited by this protocol from a day 1 neonatal mouse ventricular cell (Panel A), a day 3 neonatal mouse ventricular cell (Panel B) and a adult mouse ventricular cell (Panel C). The transient outward currents shown in Figure 20 progressively increased during depolarization to more positive test potentials and the largest amplitudes of the outward currents were evoked at +50 mV in all three age groups. The currents activated rapidly in response to the cell membrane depolarization and exhibited a incomplete inactivation during the depolarizing pulses. The rates of the inactivation of the transient outward currents were obviously different between neonates and adult. The currents in day 1 and day 3 neonatal mouse ventricular myocytes inactivated faster than those seen in adult mouse ventricular myocytes and reached a steady-state within 250 ms. In contrast, the transient outward current in adult mouse ventricular myocytes inactivated slowly and did not reach the steady state even at the end of 1000 ms depolarization pulse.

Because the transient outward currents in adult mouse ventricular myocytes inactivated slowly, a longer depolarization protocol was used to allow more time for the inactivation process. Figure 21 displays the transient outward currents in adult mouse ventricular myocytes elicited by three different depolarization pulses. The inactivation of the transient outward current was close to a steady state level at the end of a 3500 ms depolarization pulse.

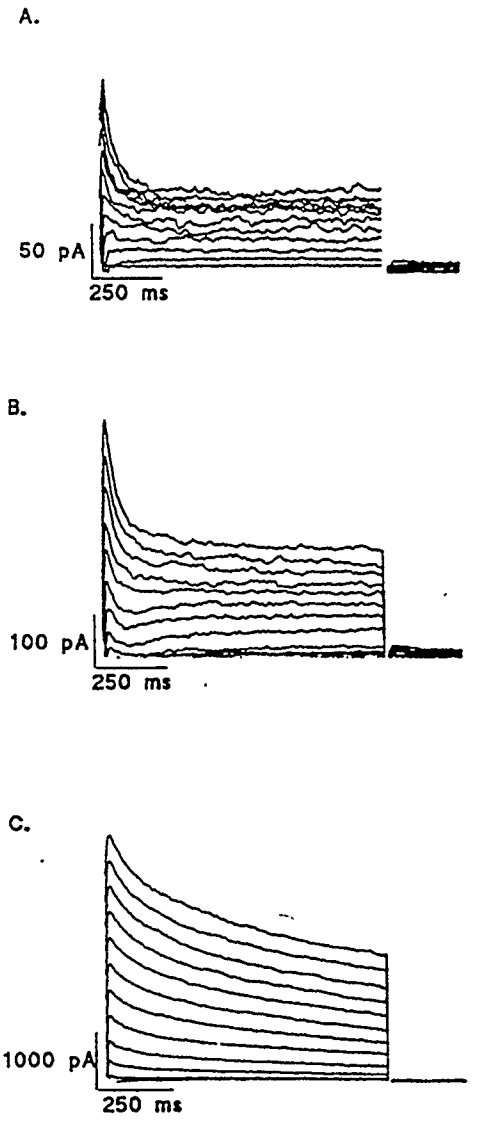


**Figure 20** **Transient outward currents in mouse ventricular myocytes during development.** The currents were evoked by depolarizing the cells from a holding potential of -70 mV to a maximum of +50 mV, in 10 mV increments. The inactivation kinetics of the transient outward currents in day 1 (Panel A) and day 3 (Panel B) neonatal mouse ventricular myocytes were different from those observed in adult mouse ventricular myocytes (Panel C). The amplitude of the transient outward current significantly increased in mouse ventricular myocytes during development.

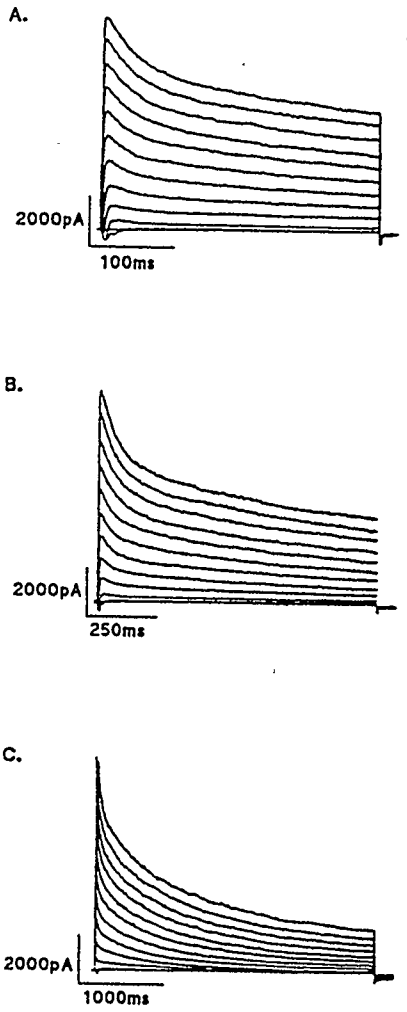


**Figure 21** **Effects of the depolarizing pulse duration on the transient outward currents in adult mouse ventricular myocytes.** The cell was held at -70 mV and then depolarized to one of 12 levels, separated by 10 mV increments, up to a maximum of +50 mV. The currents shown in this Figure were recorded from the same cell at different depolarization pulse duration: 350 ms (Panel A), 1000 ms (Panel B) and 3500 ms (Panel C).

For plots of current-voltage relations, the amplitudes of peak outward current in response to each depolarizing step were measured in day 1 and day 3 neonatal and adult mouse ventricular myocytes. The density of peak outward current was examined by normalizing the individual current amplitudes to cell capacitance. These values were then averaged (n=16) and plotted as a function of test potential (Figure 22A). Unlike $I_{Kr}$, $I_{to}$ channel appears to have relatively linear ion transfer characteristics in physiological $K^+$ concentrations. In all age groups, activation of the currents was voltage-dependent, and no apparent saturation in current was observed over the test potentials ranging from -30 mV to +50 mV. The activation threshold of the outward current was approximately -20 mV in both day 1 and day 3 neonatal ventricular myocytes. However, the current was activated at more negative threshold (-50 mV) in adult mouse ventricular myocytes. As shown in Figure 22A, the mean densities of the peak outward current significantly and progressively increased in the mouse ventricular myocytes during development. At +50 mV, the density of the peak currents increased from 6.7 $\pm$ 0.4 pA/pF in day 1 neonatal mouse ventricular myocytes to 12.9 $\pm$ 1.1 pA/pF in day 3 neonatal mouse ventricular myocytes ($p<0.01$). The density of the total peak currents further significantly increased to 27.2 $\pm$ 5.7 pA/pF in adult mouse ventricular myocytes ($p<0.01$).

If the total peak current consists of a transient outward component ($I_{to}$) and a non-inactivating component (the sustained current, $I_{sus}$), the increase in the density of the total peak currents may be due to either an increase in $I_{to}$, or an increase in $I_{sus}$ or both. To examine the contributions from each of these components to the developmental changes

in the total outward peak current in mouse ventricular myocytes, $I_{sus}$ was measured and subtracted from the total outward peak current. The residual current after $I_{sus}$ subtraction was considered as the transient outward current, $I_{to}$. The current-voltage relationship of $I_{to}$ and $I_{sus}$ in each age group were illustrated in Figures 22B and 22C. During development, the density of $I_{to}$ in mouse ventricular myocytes profoundly increased. At +50 mV the density of $I_{to}$ increased from 3.0 $\pm$ 0.3 pA/pF in day 1 to 7.0 $\pm$ 0.5 pA/pF in day 3 neonatal mouse ventricular myocytes. In adult mouse ventricular myocytes, $I_{to}$ further significantly increased to 19.1 $\pm$ 4.7 pA/pF ($p<0.01$). The increase in the density of $I_{sus}$ was also significant but less dramatic compared with these substantial increases in the density of $I_{to}$ in mouse heart during development. Therefore, the developmental increase in the total outward peak currents are mainly due to increases in $I_{to}$.

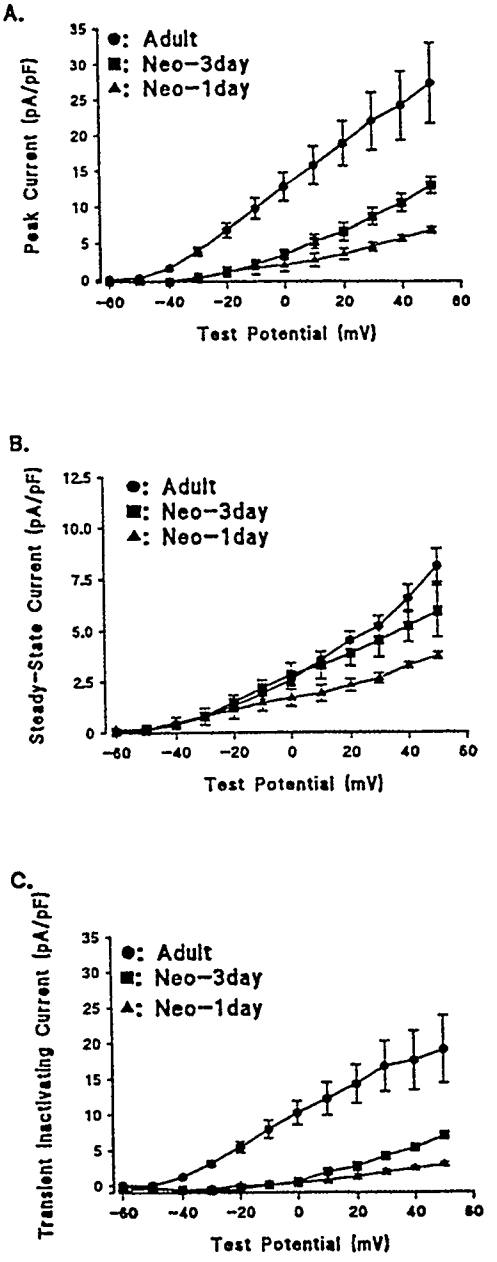


**Figure 22** **Current-voltage relationships of the transient outward currents in mouse ventricular myocytes in different age groups.** The current-voltage relationships of the peak outward current (Panel A), the non-inactivating sustained current ($I_{sus}$) (Panel B) and the inactivating outward current ($I_{to}$) (Panel C) in day 1, day 3 and adult mouse ventricular myocytes are compared. In neonatal mouse ventricular myocytes, $I_{sus}$ was measured at the end of a 1000 ms depolarization pulse. In adult mouse ventricular myocytes, $I_{sus}$ was measured at the end of a 3500 ms depolarization pulse. $I_{to}$ was obtained by subtracting $I_{sus}$ from the peak outward current. The results shown in this Figure indicate that $I_{to}$ is the main contributor to the developmental increases in the density of the total peak currents.

***The inactivation kinetics of the transient outward currents in mouse heart during development.***

The inactivation time constants of the transient outward currents in mouse ventricular myocytes from day 1 and day 3 neonates and adults were determined by the exponential fitting program in CLAMPFIT software. At test potentials between +10 mV and +50 mV, the decay phases of the transient outward currents in day 1 and day 3 neonatal mouse ventricular myocytes were well described by a single exponential function. The inactivation time course in adult mouse ventricular myocytes was well fit with a double but not a single exponential function. These results indicate that the transient outward currents in adult mouse ventricular myocytes may consist of two inactivation components. A comparison of fits to inactivating currents with mono-exponential and bi-exponential functions in day-1 and adult mouse ventricular myocytes are shown in Figure 23 (Panel A and B) and Figure 24 (Panel A and B).

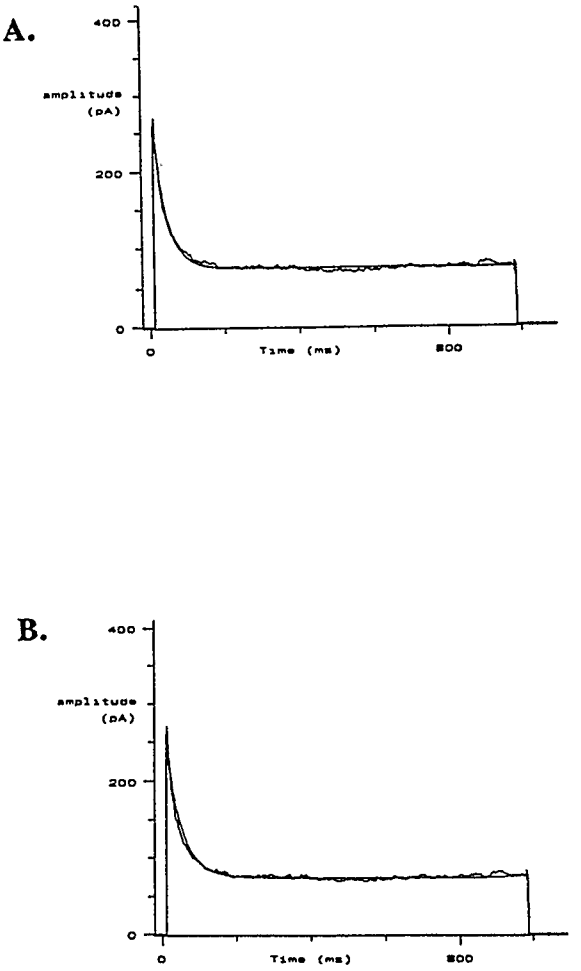


**Figure 23** **Examples of exponential fits to transient outward currents in day 1 neonatal mouse ventricular myocytes.** The transient outward current was evoked from a holding potential of -70 V to a test potential of +50 mV. The smooth curves in Panel A and Panel B represent the mono-exponential fitting and the bi-exponential fitting for the inactivation process in neonatal mouse ventricular myocytes. Since there were no significant differences between these two fittings, it is suggested that only one inactivation component contributes to the transient outward current in neonatal mouse ventricular myocytes.

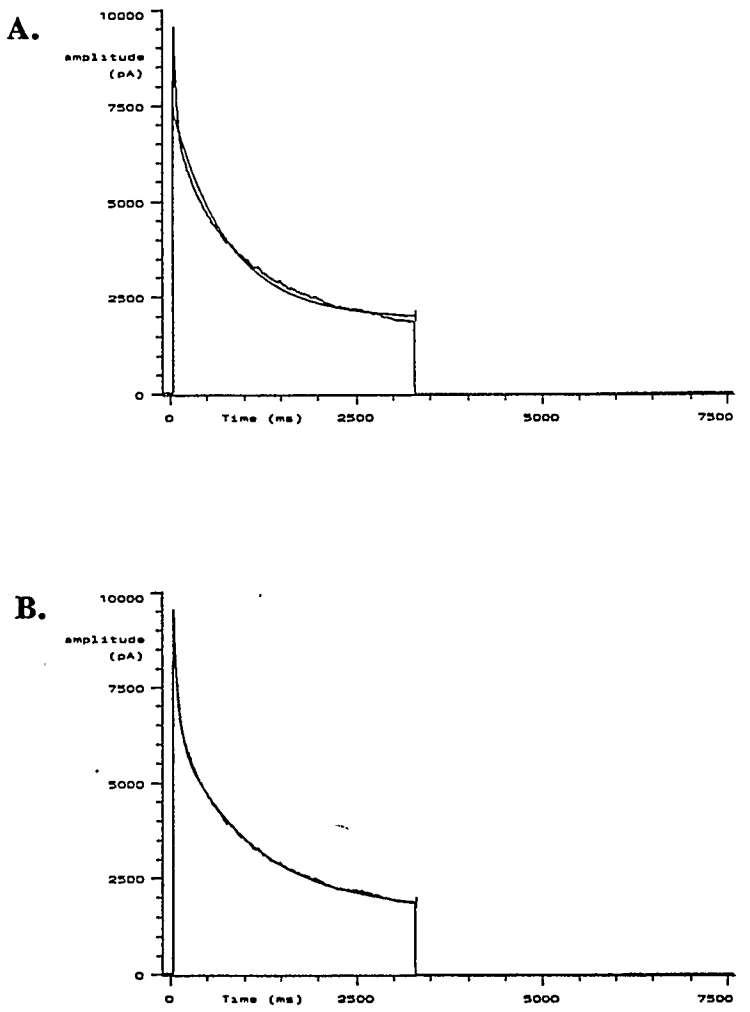


**Figure 24** **Examples of exponential fits to transient outward currents in adult mouse ventricular myocytes.** The current was evoked from a holding potential of -70 mV to a test potential of +50 mV. The smooth curves represent the mono-exponential fitting (Panel A) and the bi-exponential fitting (Panel B) for the inactivation process in adult mouse ventricular myocytes. Since the bi-exponential better fits the data, it is suggested that two components with different inactivation kinetics, or two distinct currents may contribute to the transient outward current in adult mouse ventricular myocytes.

The inactivation time constants of the transient outward currents obtained by the exponential analyses from each age groups were averaged and displayed in Figure 25. These data reveal that the inactivation time constants were voltage-independent over the potentials from +10 mV to +50 mV in all age groups. In addition, the inactivation time constants were in a similar range at all test potentials between day-1 and days-3 neonates. For example, as shown in Panel A, the inactivation time constants during depolarization steps between +10 mV and +50 mV were 66 ± 16 ms to 61 ± 10 ms in day 1 neonates, which were not significantly different from 99 ± 27 ms at +10 mV and 82 ± 20 ms at 50 mV in day 3 neonates. In contrast, the exponential fitting analyses revealed that the inactivation time constants of the transient outward currents in adult mouse ventricular myocytes consisted of two components with distinct kinetics. The decay of the fast inactivation component of the transient outward current in adult was similar to those results obtained from neonates ranging from 58 ± 5 ms at +10 mV to 69 ± 7 ms +50 mV (Panel B). However, the decay of the slow inactivation component of the transient outward current in adult was more than 10 fold slower than those in neonates (Panel B). These data suggest that the total depolarization activated outward current in adult mouse cells may contain three currents with different inactivation properties: the rapid inactivation, the slow inactivation and non-inactivation. The decay of the total outward current in adult mouse ventricular myocytes was considerably slower than that in neonatal mouse ventricular myocytes.

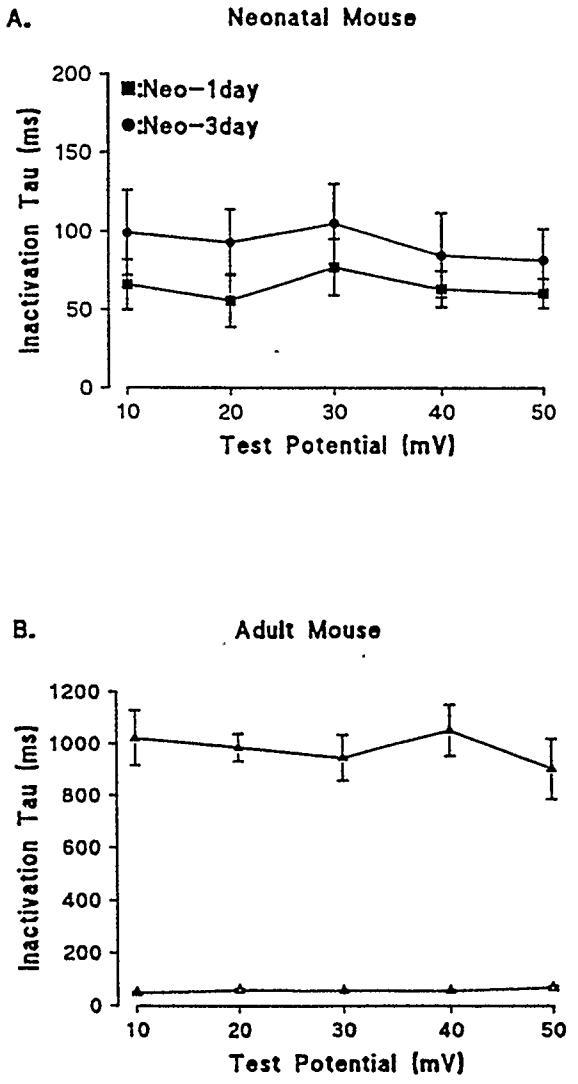


**Figure 25** **The inactivation time constants of the transient outward currents in mouse ventricular myocytes during development.** Panel A shows that the inactivation time constants in day 1 and day 3 neonatal mouse ventricular myocytes are in the similar ranges over the test potentials. The data were averaged from four individual cells of each age group. Panel B displays that there are two inactivation components with distinct time constants in adult mouse ventricular myocytes (n=5).

***Steady-state inactivation of the transient outward currents in mouse ventricular myocytes during development***

A two-pulse protocol was used to assess the voltage dependence of steady-state inactivation of $I_{to}$. The pre-pulses depolarized the cell to different membrane voltages ranging from -100 mV to 0 mV. Each pre-pulse was followed by a single test depolarization to +50 mV. Representative current traces elicited by this double pulse protocol from day 1 neonatal mouse ventricular myocytes (Panel A) and adult mouse ventricular myocytes (Panel B) are shown in Figure 26. The amplitude of the peak currents was reduced substantially when a pre-pulse progressively depolarized the cell membrane from -100 mV to 0 mV, suggesting that the numbers of channels that can be activated by the second test pulse were decreased. The amplitude of peak currents evoked during depolarization to +50 mV from a pre-pulse of -100 mV was considered as maximum activation. The peak current preceded by each pre-pulse was then measured and normalized to the maximum amplitude. Figures 26C and 26D are plots of the normalized current amplitudes obtained from day 1 neonatal and adult mouse ventricular myocytes as a function of pre-pulse potential, respectively. The curves through each data point represent the best fit by the Boltzmann equation. The mean values of $V_h$ and slope factors obtained by Boltzmann equation for day 1 neonate were -67 $\pm$ 4 mV and 13 $\pm$ 2 mV (n=6). These results indicate that the currents undergo substantially steady-state inactivation at the potentials close to the resting membrane potentials. At -67 mV, approximately 50% of the available channels have been inactivated in neonatal mouse ventricular myocytes. In contrast to the neonates, the channels in adult mouse ventricular

myocytes undergo steady-state inactivation at much more positive potentials with a value of $V_h$ -46 $\pm$ 3 mV and slope factor 12 $\pm$ 1 mV (n=7).

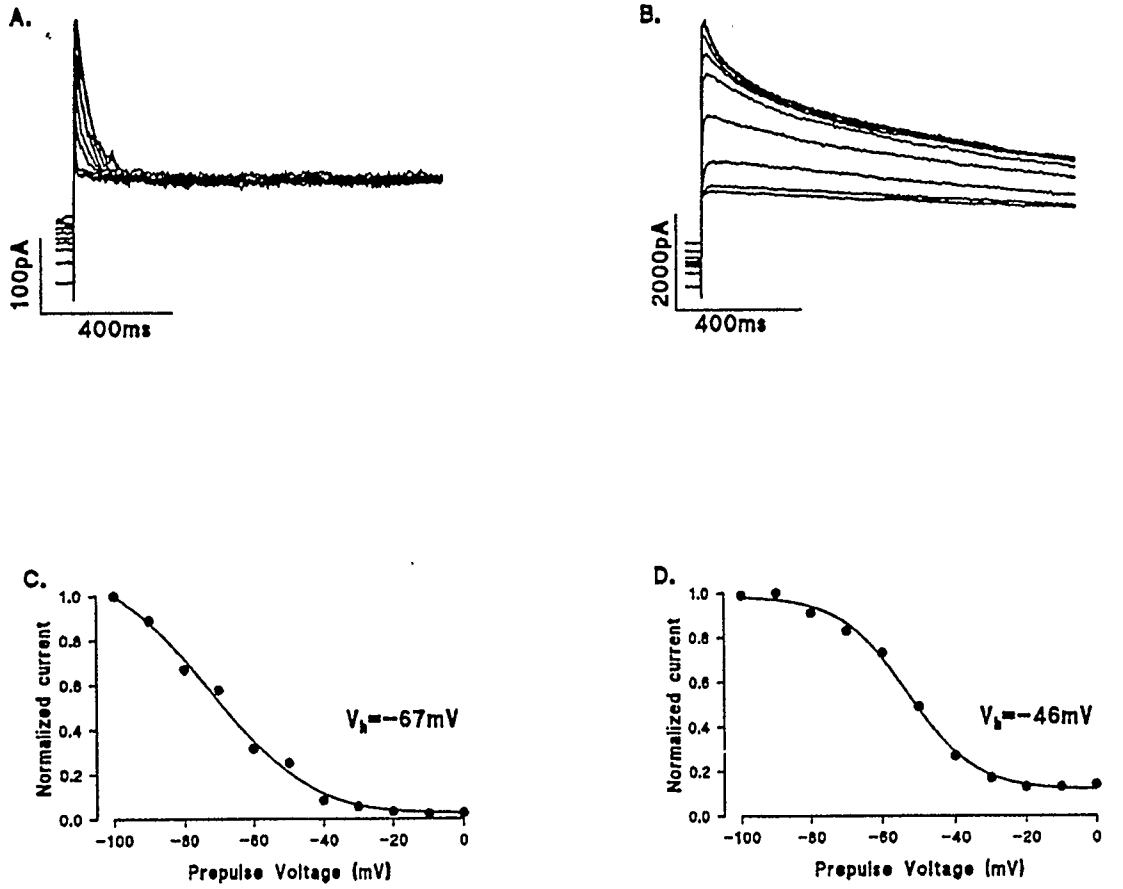


**Figure 26** **Examples of the steady-state inactivation in day 1 neonatal and adult mouse ventricular myocytes.** Panel A and Panel B show the examples of the currents evoked in neonatal and adult mouse ventricular myocytes. The plots shown in Panel C and Panel D were best described by the Boltzmann equation. The amplitude of the currents in Panel D varied by $\leq$ 20% at pre-pulse potentials between -100 mV and -70 mV, indicating that the currents undergo little steady-state inactivation over these potentials in adult mouse ventricular myocytes; In contract, the amplitudes of the currents in day 1 neonatal mouse ventricular myocytes decreased remarkably from the pre-pulses potentials between -100 mV and -70 mV. At -70 mV, almost half of the peak currents inactivated.

*Effects of 4-aminopyridine on $I_{to}$ in mouse ventricular myocytes*

4-aminopyridine (4-AP) is widely used as a blocker of the voltage-dependent, $Ca^{2+}$ independent transient outward current, $I_{to}$ (89). The effects of 4-AP on the transient outward currents were examined in day 1 neonatal and adult mouse ventricular myocytes. A single depolarization pulse was applied to depolarize the ventricular myocytes from -80 mV to +50 mV for 1000 ms. The transient outward currents elicited by this protocol were recorded under drug-free and after application of 4-AP (1 mM). As shown in Figure 27, after application of 1 mM 4-AP, the transient outward currents were profoundly decreased in both day-1 neonatal (Panel A) and adult (Panel B) mouse ventricular myocytes. Similar results were observed in 5 neonatal cells and 8 adult cells. Subtraction of the 4-AP sensitive currents from the total outward current revealed that 4-AP blocked both components of the transient outward currents in adult mouse ventricular myocytes. The inhibition by 4-AP of the transient outward currents could be completely reversed after 15 min washout with normal Tyrode's solution.

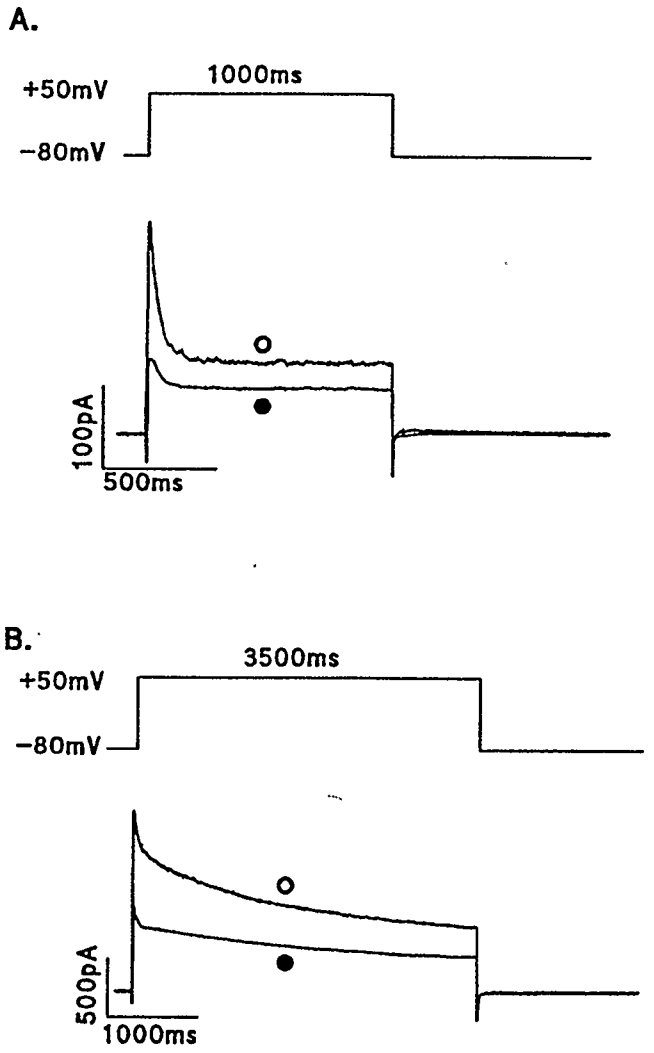


**Figure 27** **Effects of 4-AP on the transient outward currents in day 1 neonatal and adult mouse ventricular myocytes.** The transient outward currents in both neonatal (Panel A) and adult cells (Panel B) were first recorded under drug-free conditions (○), then measured after application of 4-AP (1 mM) (●). Similar results were obtained in 5 cells in day 1 neonates and 8 cells in adult.

### 4.2b The relations between developmental changes in $I_{to}$ and the action potential configuration in mouse ventricle

The greater density of the peak transient outward current and the slower inactivation time constants in adult mouse ventricular myocytes lead to a reasonable hypothesis that the action potential repolarization will be more rapid in adult than neonatal mouse ventricles.

To test this hypothesis, the effects of 4-AP on action potential duration were further assessed in mouse ventricular endocardium using conventional microelectrode technique. The myocardial preparations from day 1, day 3 neonatal and adult mice were continuously paced at 2 Hz. The action potentials in each age group were recorded before (○) and after application of 1 mM 4-AP (●) and are shown in Figure 28. In the absence of the drug, the action potential recorded from day 1 neonatal preparation displayed a small amplitude of phase 1 repolarization, followed by a clear plateau, the phase 2 repolarization. In contrast, the initial repolarization of the action potential was considerably more rapid in day 3 neonatal and adult mouse ventricular preparations. The mean data of the characteristics of the action potentials are summarized in Table 3 (page 73). The developmental increase in the rate of the repolarization in the mouse ventricular tissues supports the above hypothesis which is based on the findings of the macroscopic $K^+$ current changes in neonatal and adult mouse ventricular cells. These data suggest that developmental changes in $I_{to}$ density are physiologically relevant and contribute to developmental changes in action potential configuration of mouse heart.

Since the density of the transient outward $K^+$ currents in adult mouse ventricular

myocytes was higher than those in the neonates, one would expect that 4-AP produces a more significant prolongation of the action potential duration in the adult. As shown in Figure 28, 4-AP indeed produced a greater prolongation of action potential duration in adult than in neonatal mouse ventricular preparations.

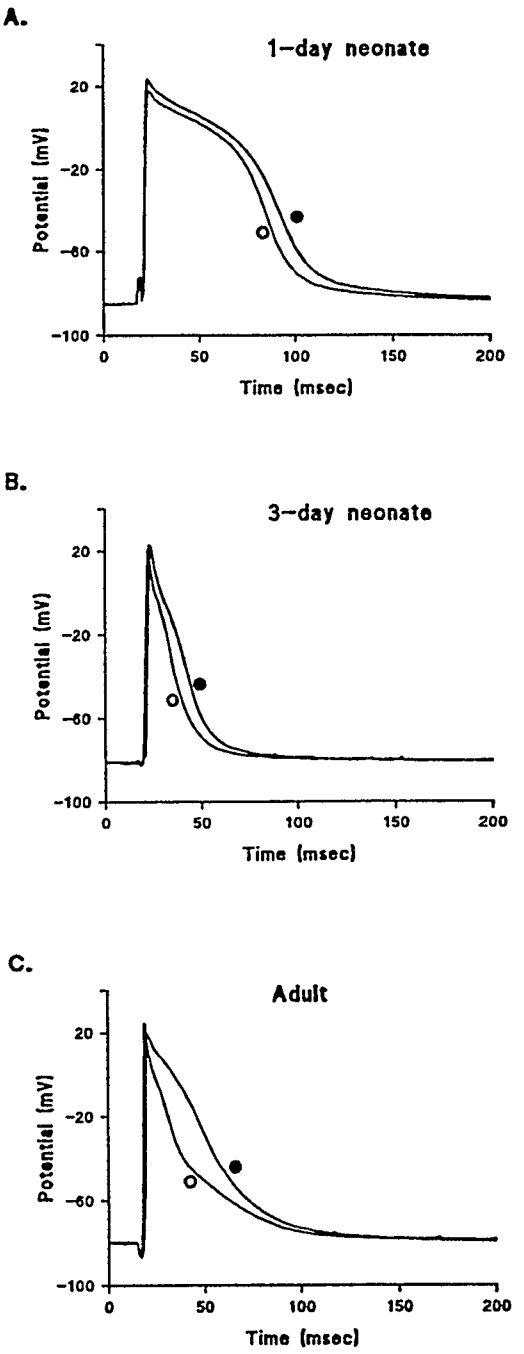


**Figure 28** **Effects of 4-AP on action potential duration in mouse ventricular myocardium during development.** The myocardial preparations were perfused with normal Tyrode solution at 37°C and the tissues were constantly paced at 2 Hz. The action potentials were recorded under drug-free (○) and after application of 1 mM 4-AP (●). The effects of 4-AP in all age groups were more profound in the initial phase of the repolarization, but with a significantly greater prolongation of action potential duration in the adult as compared to the neonates.

## 4.3 Developmental Changes in $I_{K1}$ in Mouse Ventricle

Developmental changes in cardiac $I_{K1}$ have been documented in many species, but it has not been previously investigated in mouse heart. To determine whether $I_{K1}$ is also altered during development, whole-cell $I_{K1}$ was measured in fetal, neonatal and adult mouse ventricular myocytes. Since $I_{K1}$ is mainly responsible for maintaining the resting membrane potential, the changes in $I_{K1}$ may result in alteration of the resting membrane potential in mouse heart during development. Therefore, the cellular resting membrane potentials in ventricular tissue from fetal, day 1 and day 3 neonatal and adult mice were also measured using conventional microelectrode methods.

### 4.3a Age-related changes of $I_{K1}$ in mouse ventricular myocytes assessed by whole-cell voltage-clamp technique

In order to record $I_{K1}$, a typical hyperpolarization voltage pulse protocol was used. The cells from fetal, day 1 and day 3 neonatal, and adult mouse hearts were clamped at -50 mV (to diminish the contaminations of $I_{Na}$ and $I_{to}$). Then the cells were pulsed to test potentials of -110 mV to -20 mV for 1000 ms applied in 10 mV increments. In all age groups, the currents evoked by this protocol exhibited pronounced inward rectification. When hyperpolarizing pulses were applied, large inward currents were observed. However, there was little outward current when test potentials were more positive than -70 mV. Figure 29 shows the representative examples of the whole-cell $I_{K1}$ traces in the ventricular myocytes isolated from day 1 neonatal (Panel A) and adult mice (Panel B).

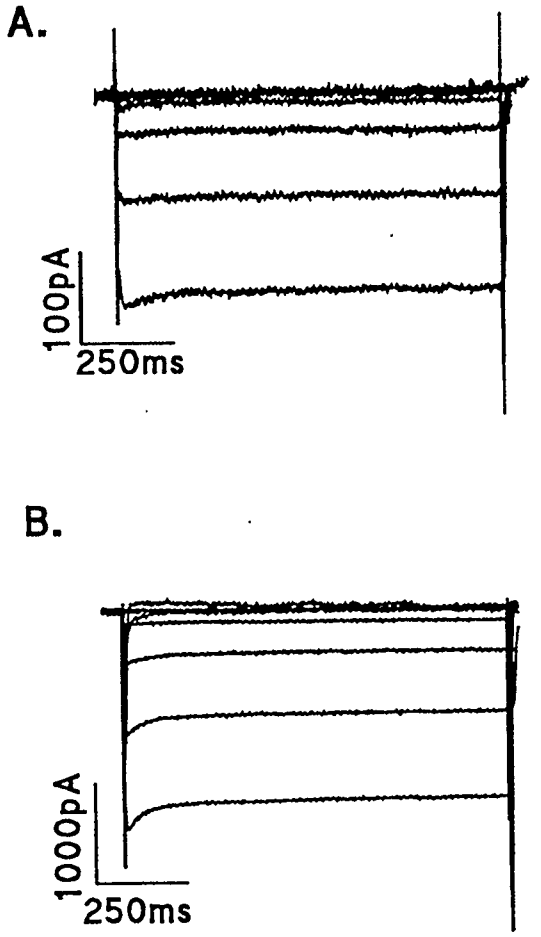


**Figure 29** **Representative recordings of $I_{K1}$ in mouse ventricular myocytes isolated from day 1 neonatal and adult mice.** The cells were held at -50 mV. The current traces were elicited by the test potentials ranged from -110 mV to -40 mV, spaced at 10 mV intervals. $I_{K1}$ recorded from day 1 neonatal (Panel A) and adult mouse ventricular myocytes displays similar biophysical properties.

The density of $I_{K1}$ in each age group was obtained by measuring the amplitudes of the currents at the end of 1000 ms pulses at each test potential and then the measured amplitudes in each age group were normalized by their cell capacitance. Figure 30 displays the current-voltage relationships of $I_{K1}$ in mouse ventricular myocytes during development. The prominent negative slope conductance between -60 mV to -20 mV found in many other species, i.e. in rabbit ventricular myocytes, was not obvious in mouse ventricular myocytes in any age group. In addition, the density of both inward and outward $I_{K1}$ did not significantly change in mouse ventricular myocytes during development.

$I_{K1}$ in mouse ventricular myocytes in all age groups was sensitive to the $I_{K1}$ channel blocker, $BaCl_2$. Figure 31 illustrates representative examples of $I_{K1}$ in day 1 neonatal mouse ventricular myocytes before (Panel A), and after application of 0.1 mM $BaCl_2$ (Panel B). $BaCl_2$ significantly blocked $I_{K1}$ in neonatal mouse ventricular myocytes. This effect was reversible after washout with drug-free Tyrode's solution. Figure 32 shows a similar effect of $BaCl_2$ on $I_{K1}$ in adult mouse ventricular myocytes.

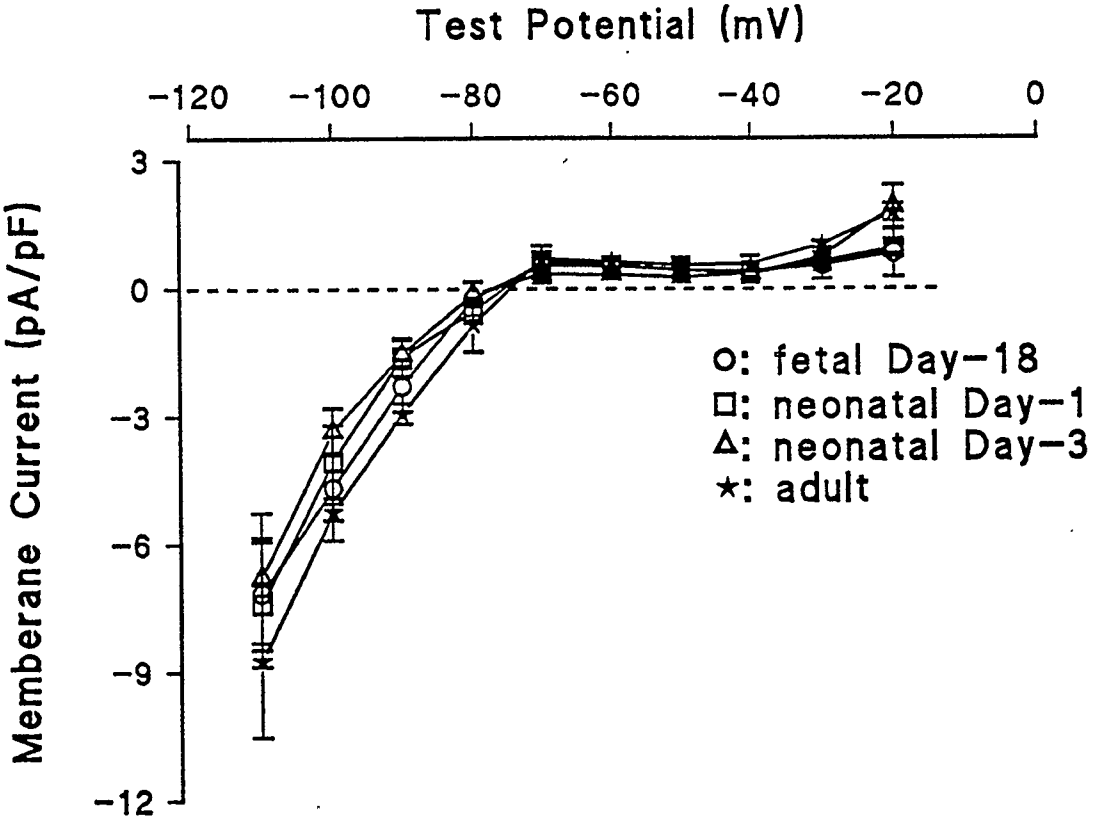


**Figure 30** **Current-voltage relationships of $I_{K1}$ in mouse ventricular myocytes during development.** The mean data were obtained from at least 4 individual cells at each age groups. No significant differences in the density (pA/pF) of $I_{K1}$ current were observed in mouse ventricular myocytes isolated from fetal, day 1 neonatal, day 3 neonatal and adult mice.

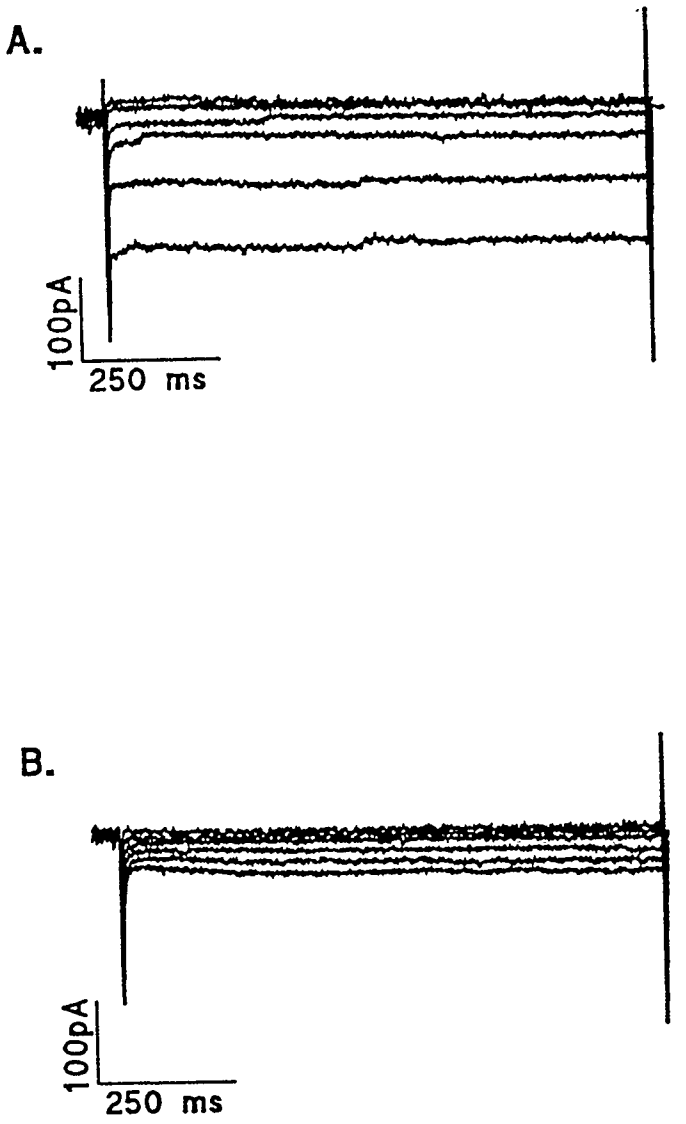


**Figure 31** **Effects of $BaCl_2$ on $I_{Ki}$ in day 1 neonatal mouse ventricular myocytes.** Panels A and B show the currents recorded before and after $BaCl_2$ (0.1 mM) perfusion. $BaCl_2$ significantly blocks the current. Similar results were obtained in 4 neonatal cells.

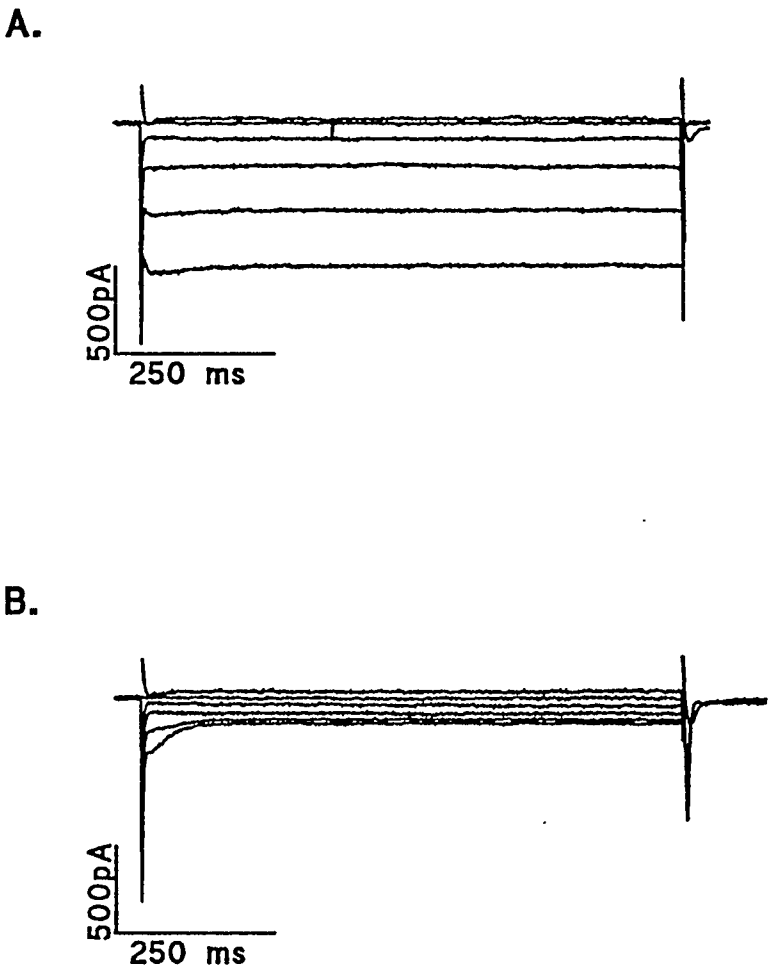


**Figure 32** **Effects of $BaCl_2$ on $I_{K1}$ in adult mouse ventricular myocytes.** Panels A and B show the currents recorded before and after $BaCl_2$ (0.1 mM) superfusion. $I_{K1}$ in adult mouse ventricular myocytes is very sensitive to $BaCl_2$. Similar results were obtained in 4 adult ventricular cells.

### 4.3b Assessment of the relations between $I_{K1}$ and the resting membrane potential in mouse heart during development

The major function of $I_{K1}$ is to maintain the cell resting membrane potential. Age-related increase in cardiac $I_{K1}$ in rat ventricular myocytes has been found to be related to the changes in the resting membrane potential during development. Therefore, the developmental changes in cardiac $I_{K1}$ can be indirectly assessed by measurement of resting membrane potentials. The resting membrane potentials in mouse ventricular endocardium from fetal, day 1 and day 3 neonatal and adult mice were measured by conventional microelectrode techniques. The values of resting membrane potentials were found to be not significantly different in mouse ventricle during development. The mean data are summarized in Table 3 (page 73). These findings are consistent with the data of whole-cell $I_{K1}$ recordings in mouse ventricular myocytes. However, these data are different from previous studies that reported developmental changes in cardiac $I_{K1}$ of other species such as rat and rabbit (75,108,173,145).

# CHAPTER 5: DISCUSSION

Developing heart has been a subject of investigation for many decades. The electrophysiology of developing heart was investigated first by visual means, i.e., by observing the rate of heart contraction and later by recording transmembrane potentials (microelectrode recordings). Numerous studies have been published on the development of normal cardiac action potentials in a variety of species. The pattern of developmental changes in the action potential configuration differs depending on species. For example, the plateau of the action potential with initial notch in adult canine ventricle is not found in neonate (81). The action potential in neonatal rat ventricle displays a prolonged plateau. The plateau disappears during development leaving a spike-like action potential in adult rat. The different patterns of developmental changes in the action potentials indicate that age-related expression of ionic channels in the heart varies among species.

With technological advances in single-cell and single-channel electrophysiological techniques, the study of ionic currents that underlie cardiac action potentials was made possible. It is well known that cardiac $K^+$ currents are mainly responsible for repolarization of the action potential. As a result, the age-related changes in the action potential configuration and the age-related expression of cardiac $K^+$ currents have been investigated in many species including rat, rabbit, canine and human (26,78, 81,90,108,157). However, these previous studies have mainly focused on developmental changes in cardiac $I_{to}$ and $I_{K1}$ and there are few investigations of developmental changes in cardiac $I_K$. In addition, there is no published study regarding to developmental changes in $K^+$ currents in mouse heart from fetal to adult. As discussed before, the

pattern of expression of $K^+$ currents in the heart is species-dependent. Thus, it is important to study $K^+$ currents expressed in mouse heart during normal development. This information is essential prior to defining which $K^+$ channels should be targeted for creating transgenic mouse models.

This dissertation, for the first time identifies the $K^+$ currents in fetal mouse ventricular myocytes as well as the developmental changes in cardiac $K^+$ currents in mouse ventricle from late fetal to adult. The main novel findings of this dissertation are: 1). $I_{Kr}$, the dominant repolarizing $K^+$ current in fetal mouse ventricular myocytes is developmentally down-regulated during the first few days of neonatal life. $I_{Ks}$ is transiently expressed in mouse heart during the early postnatal period; 2) In contrast, $I_{to}$ is developmentally up-regulated in mouse ventricular myocytes and increases six-fold in adult mouse ventricular myocytes as compared to day 1 neonates; 3) Unlike $I_K$ and $I_{to}$, the expression of $I_{K1}$ in mouse ventricle is relatively constant during the development period ranging from late fetal life to adult stages. The detailed results will be discussed separately in the following order: the developmental changes in $I_K$ in mouse ventricle; the developmental changes in $I_{to}$ in mouse ventricle; the developmental changes in $I_{K1}$ in mouse ventricle; future mechanistic studies.

## 5.1 Developmental Changes of $I_K$ in Mouse Ventricle

### 5.1a Summary of results

Expression of $I_{Kr}$ and $I_{Ks}$ in mouse heart is developmentally regulated. $I_{Kr}$ is the dominant repolarizing $K^+$ current in fetal mouse ventricles, but its expression is altered during early postnatal development and it disappears in adult mouse ventricular myocytes. Expression of $I_{Ks}$ is transient in mouse heart. $I_{Ks}$ is absent in fetal, co-exists with $I_{Kr}$ in the early neonatal stages, and disappears in adult mouse heart. The results of microelectrode studies support the findings of voltage-clamp data. Dofetilide (a selective $I_{Kr}$ channel blocker) produces a profound prolongation of the action potential duration in fetus; less prolongation of action potential duration in neonate as compared to that in fetus; but has no effect on action potential duration in adult. Finally, in keeping with these electrophysiological findings, the bindings of [$^3$H]-dofetilide to mouse ventricular preparation are also altered during development. High affinity [$^3$H]-dofetilide binding sites are present in fetal mouse ventricles, but absent in adult mouse ventricle. In addition, the binding affinity of [$^3$H]-dofetilide in day 3 neonatal mouse ventricle significantly decreases as compared to fetal mouse ventricle. These data suggest that conformational changes in the dofetilide binding site on $I_{Kr}$ channels in mouse ventricle may occur during perinatal development.

### 5.1b Comparison with previous studies of $I_K$ in mammalian heart

The cardiac $I_K$ has been identified in many species and is one of the major outward $K^+$ currents in cardiac myocytes responsible for the repolarization of the action potential (59,148). It is well known that $I_K$ in many species consists of two components, $I_{Kr}$ and $I_{Ks}$, which can be distinguished by their activation kinetics, rectification properties and drug sensitivity (60,122,146,147). The single channel conductances of $I_{Kr}$ and $I_{Ks}$ are also different. In general, single channel conductance of $I_{Kr}$ is larger (8-13 pS) than $I_{Ks}$ (<1-5 pS) in symmetrical $K^+$ (72,79,151,171,172,175).

However, there are not always two components of $I_K$ in the heart. Depending on species and region of the heart, the delayed rectifier $K^+$ current may appear to be only one component, such as $I_{Ks}$ in guinea pig nodal cells (2) and only $I_{Kr}$ in rabbit atrial and ventricular myocytes and rabbit nodal cells (79,116,171). In addition, $I_{Kr}$ and $I_{Ks}$ densities vary in different myocardial cell types and in different regions of the ventricle. For example, $I_{Kr}$ and $I_{Ks}$ densities in guinea pig atrial myocytes are approximately two-fold higher than those in guinea pig ventricular myocytes, contributing to a shorter action potential duration in atrium than ventricle (147).

$I_K$ in mouse heart was first reported by Honore *et al* (71). They found that $I_K$ in cultured newborn mouse ventricular myocytes had biophysical properties similar to the characteristics of $I_{Ks}$ and cloned minK current i.e.: slow kinetics of activation; outward rectification; sensitivity to clofilium and regulation by protein kinase C activators (71). These results suggest that $I_{Ks}$ exists in newborn mouse heart. However, these studies did not determine whether $I_{Kr}$ was also present in neonatal mouse ventricle. Recently, Nuss

and Marban reported that $I_K$ in a mixed population of 1 and 3 day old neonatal mouse ventricular myocytes consisted of both components: $I_{Kr}$ and $I_{Ks}$, but largely $I_{Ks}$ (125). In addition, it has been reported that AT-1 cells derived from transgenic mice express only $I_{Kr}$ (186). In contrast to findings in neonatal mouse ventricular myocytes and similar to those findings in AT-1 cells, the results obtained from this dissertation indicate that mouse ventricular myocytes isolated from a late stage of fetus displays a delayed rectifier $K^+$ current with biophysical properties similar to $I_{Kr}$ described in guinea pig ventricular myocytes, but not $I_{Ks}$ (146). First, $I_{Kr}$ in fetal mouse ventricular myocytes and guinea pig ventricular myocytes was fully activated at 0 mV in less than 500 ms, whereas full activation of $I_{Ks}$ took a few seconds. Secondly, $I_{Kr}$ in fetal mouse ventricular myocytes and in guinea pig ventricular myocytes showed a negative slope conductance at membrane potentials > 0 mV. In contrast, $I_{Ks}$ in guinea pig ventricular myocytes displays outward rectification (146). Thirdly, the half activation potentials and slope factors of $I_{Kr}$ were similar in fetal mouse ventricular myocytes (-16.3 mV and 6.3 mV), and in guinea pig ventricular cells (-21.5 mV and 7.5 mV). On the other hand, the half activation potential for $I_{Ks}$ in guinea pig ventricular cells was more positive (+15.7 mV) and the slope factor was less steep (12.7 mV). Fourthly, dofetilide at a concentration of 1 $\mu$M completely abolished the $I_K$ tail current in fetal mouse ventricular myocytes. In contrast, using the same concentration of dofetilide, the tail current was partially inhibited and the dofetilide-resistant current ($I_{Ks}$) was still observed in guinea pig ventricular cells (84).

A recently published paper (Davies et al, Circ Res. 1996) showed that $I_{Kr}$ was the

dominant delayed rectifier $K^+$ current in mouse ventricular myocytes of fetal day 11 to day 20, but $I_{Ks}$ was not observed until day 20, just before birth (37). These findings are very similar to the results in fetal mouse ventricles shown in the present study. The paper of Davies et al complements our study in that Davies et al only focused on intra-utero-development, whereas the present study systematically examined the age-developmental changes in $I_K$ in mouse ventricle from late fetal to adult. In this dissertation, $I_K$ was characterized in mouse ventricular myocytes isolated from different ages ranging from late fetal, day 1 and day 3 neonates and adult, and therefore, dramatic developmental changes in $I_K$ in mouse heart were revealed. $I_K$ in mouse heart changes substantially during the perinatal period: from $I_{Kr}$ as the solely expressed $I_K$ in fetal mouse ventricular myocytes; to $I_{Kr}$ solely expressed and/or $I_{Kr}$ and $I_{Ks}$ co-expressed in day 1 neonates; and further to $I_{Kr}$ and $I_{Ks}$ co-expressed, but largely $I_{Ks}$ in day 3 neonates. Finally, neither $I_{Kr}$ nor $I_{Ks}$ was observed in adult mouse ventricular myocytes. These findings indicate that expression of $I_{Kr}$ and $I_{Ks}$ channels in mouse ventricle are not static, but are profoundly altered during development.

In addition, the data regarding developmental changes in cardiac $I_K$ in other species are also quite limited. A previous study by Abrahamsson *et al* compared the sensitivity of fetal and adult rat heart to Class III antiarrhythmic drugs (1). There are both similarities and differences between their findings and the present study. Similar to the present study, almokalant (an $I_K$ channel blocker) significantly prolonged the action potential duration in fetal rat heart, but did not prolong the action potential duration in adult rat heart. However, Abrahamsson *et al* did not systematically assess $I_K$ in each

developmental stage. They only examined the $I_K$ in fetal and adult rat ventricular myocytes. They found that both fetal and adult rat ventricular myocytes displayed an almokalant-sensitive current, which was not consistent with the results observed in mouse ventricular myocytes. In addition, $I_{Kr}$ and $I_{Ks}$ were not distinguished in their study. In this dissertation, developmental changes in $I_K$ have been investigated in fetal, neonatal and adult mouse heart using three different techniques. Both $I_{Kr}$ and $I_{Ks}$ were found to be developmentally regulated in mouse heart, but with different pattern. $I_{Kr}$ is down-regulated in mouse heart during development. $I_{Ks}$ is only transiently expressed in mouse ventricle during early postnatal development.

### 5.1c Functional role of $I_{Kr}$ in mouse ventricular myocytes

This dissertation has demonstrated that the action potential configuration in mouse ventricle significantly changes during development. Most action potential recordings in mouse ventricle were performed with conventional microelectrode techniques since it method allowed stable recording of the action potentials for a few hours under physiological conditions (at 37°C and without dialysis of the cells). Using this method also avoids exposure of tissues to collagenase. However, the microelectrode recordings could not directly assess the properties of individual currents and their functional role in cardiac action potential repolarization. Alternatively, the action potentials were also recorded in single cells using current-clamp technique. The results obtained by these two methods are very similar.

Functional roles of $I_{Kr}$ and $I_{Ks}$ in the action potential repolarization and their possible role in the evolution of action potentials in mouse ventricle during development were assessed using selective $I_{Kr}$ and $I_{Ks}$ channel blockers: dofetilide and indapamide. As expected, dofetilide significantly prolonged the action potential duration in fetal mouse ventricular myocytes (current clamp) and ventricular tissues (conventional microelectrode). During dofetilide perfusion, some of the fetal mouse ventricular myocytes failed to repolarize the action potential and ADs occurred, which was associated with a complete block of $I_{Kr}$. The effects of dofetilide on action potentials dramatically diminished immediately after birth and progressively decreased during early postnatal development. Dofetilide did not prolong action potentials in adult mouse ventricle. These results suggest that $I_{Kr}$ is an essential repolarizing $K^+$ current in fetal,

but not in adult mouse ventricles. In addition, these results imply that the developmental shortening of the action potential duration is not due to decreases in $I_{Kr}$. A decrease in $I_{Kr}$ alone would result in prolongation of action potential duration.

On the other hand, although $I_{Ks}$ was present in neonatal mouse heart, $I_{Ks}$ channel blocker, indapamide (167) did not significantly prolong action potential duration in neonates under the conditions used in the present study. Since $APD_{50}$ and $APD_{95}$ in ventricles of day 3 neonates were only 18 $\pm$ 6 ms and 51 $\pm$ 9 ms at pacing frequency of 2 Hz (37°C, Table 3, page 73), such a short duration of the action potentials is expected to activate little $I_{Ks}$. This may explain the lack of effects of indapamide on action potential prolongation in neonatal mouse heart. The additional factors may also contribute to the lack of effects of indapamide on action potential prolongation. They are: 1). $I_{Kr}$ and $I_{to}$ were also observed in neonatal mouse ventricular myocytes and their activation kinetics are much faster than $I_{Ks}$; 2). At day 3 neonate, the density of $I_{to}$ in mouse ventricular myocytes dramatically increased. The large magnitude and rapid activation rate of $I_{to}$ in mouse ventricular cells may dominate repolarization in day 3 neonates, and thereafter, until adult; 3). The pacing frequency used in this study was not fast enough to observe the effects of $I_{Ks}$ on action potential repolarization.

### 5.1d [$^3$H]-dofetilide binding study

The findings of developmental changes in $I_{Kr}$ in mouse ventricle were further supported by the results obtained from [$^3$H]-dofetilide binding assay. A high affinity [$^3$H]-dofetilide binding site was found in fetal mouse ventricles, but was absent in adult mouse ventricle. However, the biology of $I_K$ channel expression in the early postnatal period is complicated in mouse heart. The extent of action potential prolongation by dofetilide decreased profoundly in neonatal mouse ventricle as compared to that in fetal mouse ventricle, suggesting that the number of functional $I_{Kr}$ channels involved in action potential repolarization was reduced. However, the results from radioligand binding assays showed that the density of [$^3$H]-dofetilide binding sites ($B_{max}$) was unchanged from fetal to day 3 neonatal mouse ventricle, indicating that the number of the $I_{Kr}$ channels expressed in the mouse ventricle may remain relatively constant over this early neonatal period. However, the $K_d$ of [$^3$H]-dofetilide binding in day 3 neonatal mouse ventricle was significantly increased as compared with that in fetal mouse ventricle, indicating a developmental decrease in the [$^3$H]-dofetilide binding affinity in neonatal mouse ventricle. Although the perinatal change in $K_d$, instead of $B_{max}$ of [$^3$H]-dofetilide binding in mouse heart are not common, similar findings were also reported in another receptor-ligand interaction system (136). Richards *et al* found that the $B_{max}$ of [$^3$H]5-hydroxytryptamine binding in ovine cerebral cortex was constant from 120 days gestation through the early neonatal period (3 weeks after birth). However, there was a significant increase in the $K_d$ of [$^3$H]5-hydroxytryptamine binding at 1-5 days after birth compared to all other age groups (136).

Two potential mechanisms are proposed to explain the results of [$^3$H]-dofetilide binding obtained in neonatal mouse ventricle. First, the [$^3$H]-dofetilide binding site (protein) may undergo conformational changes and these conformational changes appear to precede the complete loss of the [$^3$H]-dofetilide binding sites. As a result, the affinity of [$^3$H]-dofetilide binding in mouse heart decreased, but the total density of [$^3$H]-dofetilide binding in mouse heart was not changed in the early neonates. Secondly, in addition to the conformational changes in the dofetilide binding protein itself, protein-protein interactions may allosterically modulate the affinity of a ligand for its binding site, such as has been reported for interactions of adenylate cyclase with the $\beta$-receptor (24,38,68,150). Recently Yang *et al* have reported that expression of minK gene can regulate $I_{Kr}$ channels in AT-1 cells (187). Since the levels of the minK mRNA transiently increase in mouse heart just before birth and reach a peak at neonatal day 7 (49), the sharp increase in the expression of minK during perinatal period may modulate $I_{Kr}$ channels. As a result, the interaction between minK protein and $I_{Kr}$ channel protein may alter the affinity of [$^3$H]-dofetilide binding in day 3 neonatal mouse heart.

The estimated density of [$^3$H]-dofetilide binding sites may be higher than the estimated number of $I_{Kr}$ channels per ventricular myocyte in mouse heart. However, several unknown factors and assumptions may account for this discrepancy. For example, the single channel conductance and open probability of $I_{Kr}$ in mouse heart may differ from the values previously reported in other species (72,151,171); Most single channel recordings were carried out under symmetric [$K^+$] condition. Under this condition, the single channel conductance was larger than the conductance obtained from

physiological condition. In addition, Sanguinetti et al reported that the kinetics of $I_{Kr}$ inactivation were much more rapid than activation. Therefore, $I_{Kr}$ evoked by the conventional activation protocols does not manifest the total current. All these factors may result in under-estimate $I_{Kr}$ channel number in mouse heart. In addition, it is unknown how many dofetilide binding sites exist on each $I_{Kr}$ channel. Thus, it is impossible to accurately convert the density of [$^3$H]-dofetilide binding sites into $I_{Kr}$ channel numbers per cell.

In the present study, both electrophysiological measurements and [$^3$H]-dofetilide binding results show concordant developmental changes in $I_{Kr}$. Both $I_{Kr}$ current and the high affinity [$^3$H]-dofetilide binding sites are present in fetal mouse ventricle but are absent in adult mouse ventricle.

### 5.1e Relationships between cardiac $I_K$ channels and cloned $K^+$ channels

The biophysical differences between $I_{Kr}$ and $I_{Ks}$ indicate the expression of two distinct molecular entities. This idea is supported by the recent findings that two candidate genes may encode $I_{Kr}$ and $I_{Ks}$ channel proteins (52,65,149,162). Sanguinetti *et al* have shown that *HERG* encodes a delayed rectifier $K^+$ channel with biophysical characteristics nearly identical to $I_{Kr}$ in native cardiac myocytes. The mouse homolog of *HERG* has been identified and named *MERG*. It is abundant in mouse heart (101). However, it is unknown whether expression of *MERG* mRNA and the protein coded by *MERG* is developmentally regulated. It will be very interesting if expression of *MERG* is also developmentally regulated in a manner similar to $I_{Kr}$ in mouse heart.

Of all channels cloned to date, minK is the most likely candidate to underlie $I_{Ks}$ since the minK current shares many biophysical properties with $I_{Ks}$ in native cardiac myocytes (52,65,149,162). Both $I_{Ks}$ in native cardiac myocytes and the minK current display slow activation kinetics, a current-voltage relationship with a positive slope conductance, and similar responses to intracellular regulators (71). However, some studies suggest that minK itself does not form a functional $K^+$ channel but encodes a regulator protein, which may regulate the expression of other ionic channels (9,187). For example, Yang *et al* recently reported that expression of the minK gene in AT-1 cells upregulates $I_{Kr}$ amplitude, but there is no sign of $I_{Ks}$ expression in AT-1 cells (187). Thus, the functional and physiological roles of minK are still uncertain.

This dissertation has shown that $I_{Ks}$ was absent in fetal and adult mouse ventricular myocytes, but was observed in day 1 neonatal mouse ventricular myocytes.

An increase in $I_{Ks}$ was observed in day 3 neonatal mouse ventricular myocytes. Therefore, it appears that $I_{Ks}$ is only transiently expressed in mouse ventricular myocytes during the early postnatal development. If minK indeed encodes $I_{Ks}$ channels, the levels of minK mRNA would also be expected to change during a similar developmental period. Recently, Felipe *et al* showed that minK mRNA in mouse heart was dramatically altered during development (47). The expression of minK mRNA peaked in day 2 neonate and was found at extremely low levels in fetal and adult mouse heart. These results are in accordance with the pattern of developmental changes in $I_{Ks}$ in mouse heart observed in the present study.

## 5.2 Developmental Changes of $I_{to}$ in Mouse Ventricle

### 5.2a Summary of results

The action potential in fetal mouse ventricle exhibits a long duration with prominent plateau phase, which shortens immediately after birth and progressively decreases thereafter. In keeping with these changes in the action potential duration, the density of $I_{to}$ in mouse ventricle also changes substantially during the same developmental period. $I_{to}$ is generally absent in fetal mouse ventricular myocytes. However, it was observed in approximately 30% of day 1 neonatal mouse ventricular myocytes. The density of $I_{to}$ in mouse ventricular myocytes increased approximately six fold from day 1 neonate to adult. In addition, the inactivation kinetics of $I_{to}$ were fundamentally different between neonatal and adult mouse ventricular myocytes. The inactivation time course of $I_{to}$ in neonatal mouse ventricular myocytes was faster than that in adult. Exponential analyses reveal that the inactivation process of $I_{to}$ was well described by a single exponential equation in the neonatal mouse ventricular myocytes, whereas it was best described by a two exponential function in adult mouse ventricular myocytes. The developmental increases in the density of $I_{to}$ in mouse ventricular myocytes along with the alteration in its inactivation kinetics may be closely related to the developmental shortening of the action potential duration in mouse heart.

### 5.2b Comparison with previous findings

The characteristics of $I_{to}$ in adult mouse ventricular myocytes were first examined by Benndorf and Nilius (13). Using whole-cell voltage clamp technique, they observed a large voltage-dependent, 4-AP sensitive transient outward current in adult mouse ventricular myocytes. This dissertation reports similar results in adult mouse ventricular myocytes. However, the inactivation kinetics of the whole-cell transient outward current characterized in this dissertation were very different from the previous report by Benndorf and Nilius (13). The differences may be due to different experimental conditions used between these two studies. First, the currents were evoked from different holding potentials: -50 mV (Benndorf and Nilius) vs -70 mV (this dissertation). Secondly, the duration of the depolarization pulses in Benndorf and Nilius was only 50 ms. In such a short time course, the inactivation of $I_{to}$ was far from complete. Therefore the inactivation time constants of $I_{to}$ based on measuring such a short time course may result in inaccurate values. Thirdly, the temperatures used were different: 36°C (Benndorf and Nilius) vs 22°C (the present study). All these factors may result in the different inactivation kinetics of $I_{to}$.

The features of the transient outward current in adult mouse ventricular myocytes characterized in the present study are not identical to the properties of $I_{to}$ in adult ventricular myocytes of other species. Typically, $I_{to}$ activates and inactivates rapidly in adult ventricular myocytes such as in rat, rabbit and canine. Also the inactivation time course of $I_{to}$ has been shown to be best fit by a single exponential function in the ventricular cells isolated from the heart of these species. In contrast, the inactivation

kinetics of the transient outward current in adult mouse ventricular myocytes (n=36) shown in this dissertation were much slower than those recorded in rat, rabbit and canine ventricular myocytes. In addition, in the present study the inactivation time course of the transient outward current in adult mouse ventricular myocytes was best described by a two exponential equation, suggesting that the transient outward current consists of two inactivation components: a fast inactivation component and slow inactivation component. Although these findings are not in agreement with $I_{to}$ in adult ventricular myocytes from other species, they are similar to the transient outward $K^+$ currents recorded in rat **atrial** myocytes (17). Boyle and Nerbonne distinguished two components of the transient outward current in rat atrial myocytes and showed that the inactivation time constant for the fast inactivating component was 181 $\pm$ 124 ms and the inactivation time constant for the slowly inactivating component was 3006 $\pm$ 1016 ms (17).

In addition to the fast and slow inactivation components of the transient outward currents, a rapidly activating, non-inactivating component ($I_{sus}$) was also recorded in adult mouse ventricular myocytes. Thus, the total outward current recorded in adult mouse ventricular myocytes appears to be the sum of three current components.

The finding of developmental increases in the density of $I_{to}$ in mouse ventricular myocytes are similar to the previous reports of the age-related increases in $I_{to}$ in rat, rabbit, canine and human heart. In addition, a developmental increase in $I_{sus}$ was also noted in the present study. The magnitude of an increase in $I_{sus}$ was not as large as that of $I_{to}$ in mouse heart during development. Gross *et al* recently found that $I_{sus}$ in human atrial myocytes also increased significantly with age, but the density of $I_{to}$ in human atrial

myocytes was not changed during development (62).

Developmental changes in the inactivation kinetics of $I_{to}$ observed in mouse ventricular myocytes display a different pattern from previous studies in other species. Generally, the inactivation time course in neonatal heart is much slower than in mature heart. For example, Jeck and Boyden have shown a rapidly activating, slowly inactivating outward current in about 23% of all neonatal canine epicardial cells (81). They claimed that this slow inactivating current was never observed in adult myocytes. In contrast, the transient outward current in mouse ventricular myocytes inactivated more rapidly in neonates than in adult. The rapid inactivation of $I_{to}$ in neonatal mouse ventricular myocytes was also shown by Nuss and Marban (125). These data indicate that expression of $I_{to}$ channels in mouse ventricular myocytes occurs earlier than in other species.

To my knowledge, there is no study addressing the age-related changes in expression of the *Shaker*-related $K^+$ channel mRNAs in mouse heart. Also there is no clear clue about the relationships between the cloned $K^+$ channels and cardiac $K^+$ currents in mouse ventricle. Therefore, assessment of the developmental changes in $K^+$ channel expression at the molecular level may provide useful information about the relationship between the cloned $K^+$ channels and wild-type $K^+$ currents in mouse heart.

### 5.2c Functional role of $I_{to}$ in action potential repolarization in mouse heart during development

Although the transient outward current is present in neonatal mouse ventricular myocytes, at a membrane potential of -67 mV, approximately half of the available $I_{to}$ channels are closed due to steady-state inactivation. In addition, the activation threshold in neonate was more positive than that in adult. Moreover, the inactivation kinetics were faster in the neonate than in adult. As a result, $I_{to}$ is expected to be less important for action potential repolarization in neonatal mouse ventricle than in adult mouse ventricle. In contrast, $I_{to}$ in adult mouse ventricular myocytes displays a large magnitude, relatively negative activation threshold and slow inactivation kinetics. Therefore, $I_{to}$ is believed to be an important factor in repolarization of the action potential in adult mouse ventricle. Also developmental increases in $I_{to}$ may be the major contributor to the developmental shortening of action potential duration in mouse heart. These predictions regarding the functional roles of $I_{to}$ in action potential repolarization during development were supported by studies with the $I_{to}$ channel blocker, 4-AP. The extent of action potential prolongation by 4-AP was significantly greater in adult than in neonatal mouse ventricular myocardium at pacing cycle length of 2 Hz.

## 5.3 Developmental Changes of $I_{K1}$ in Mouse Ventricle

### 5.3a Summary of results

This dissertation demonstrates that the whole-cell current density of $I_{K1}$ does not significantly alter in mouse ventricular myocytes during development (from late fetal to adult). In parallel microelectrode studies, it was shown that the resting membrane potential in mouse ventricular endocardium does not developmentally change, but remains relatively constant.

### 5.3b Comparison with previous findings

Developmental changes in $I_{K1}$ in cardiomyocytes have been investigated in rat (90,108,173) and rabbit (75,145). Controversial results were observed in the rat ventricular myocytes. Kilborn and Fedida reported that $I_{K1}$ significantly decreased between day 1 and day 10 neonatal rat ventricular myocytes (90). In contrast, Wahler found that $I_{K1}$ significantly increased between day 3 and day 10 neonatal rat ventricular myocytes and remained relatively constant until adult (173). Wahler found that $I_{K1}$ decreased dramatically in culture, depending on the age of the rat from which the cells were obtained. For example, day 1 neonatal cells in culture for 3 days did not cause significant differences in the magnitude of $I_{K1}$ as compared to $I_{K1}$ recorded in freshly isolated cells. However, day 9 to day 13 neonatal cells in culture for 3 days showed a significant decrease in the amplitude of $I_{K1}$ (173). Therefore it is possible that a developmental decrease in $I_{K1}$ reported by Kilborn and Fedida may be due to a modification of $I_{K1}$ channels induced by cell culture (173). Moreover, using both whole-

cell configuration and single channel analysis, Masuda and Sperelakis also demonstrated that $I_{K1}$ in rat ventricular myocytes increased from fetal until neonatal day 5-10 and remained constant thereafter (108). In addition, the study in rabbit ventricular myocytes also showed that $I_{K1}$ markedly increased between fetal day 21 and 28 (full term, 31 days), and it remained constant until the neonatal period, following which it further increased slightly until adult (75). Another study by Sanchez-Chapula *et al* also showed that the density of $I_{K1}$ in rabbit ventricular myocytes increased from day 1 and day 3 neonates to adult (145).

Developmental changes in $I_{K1}$ in mouse heart have not been systematically examined from fetal to adult. Recently, Davies et al examined $I_{K1}$ in fetal mouse myocytes (37). They found that $I_{K1}$ density did not significantly change in fetal mouse ventricular myocytes (from day 11 to day 20 fetus), but percentage of the cells that expressed $I_{K1}$ increased fourfold in late fetal developmental stage (day 17 to day 20) as compared to early fetal stage (day 11 to day 13). In the present study, $I_{K1}$ has been measured in mouse ventricular myocytes from late fetus (day 18), neonates (day 1 and day 3) and adult. In contrast to those previous observations, neither the density nor the expression frequency of $I_{K1}$ in mouse ventricular myocytes significantly change from late fetal development to adult in the present study. In addition, it has been noticed that $I_{K1}$ in mouse ventricular myocytes exhibited pronounced inward rectification, with little current at potentials positive to -60 mV in all age groups. The negative slope conductance of the outward portion of $I_{K1}$ was not as obvious as those in rabbit ventricular myocytes (154).

Kojima *et al* reported that the resting membrane potential in rat ventricular tissue increased from -55 mV at fetal day 12 to -80 mV at fetal day 18, and at day 1 neonates, it reached the adult level. However, no evidence of significant changes in the resting membrane potential was observed in mouse ventricular endocardium from late fetal to adult. These results indicate that at the late fetal developmental stage, both the density of $I_{K1}$ and the resting membrane potential in mouse ventricle have already reached the adult level.

Although several inward rectifier $K^+$ channel genes have been cloned, age-related expression of the cloned $K^+$ channels in the heart has not been investigated. The knowledge of developmental expression of these $K^+$ channels will aid in defining their function and the relation to the wild-type $I_{K1}$ in cardiac myocytes. Therefore, it will be very interesting to explore the molecular mechanisms that modify the expression of cardiac $K^+$ channels at a given age.

## 5.4 Future Studies

### 5.4a Potential mechanisms

It is known that the levels of circulating hormones, autonomic innervation and intracellular regulators substantially alter during perinatal development and parallel electrophysiological changes in the heart (93). Therefore, it is possible that changes in one or more of these extracellular and intracellular signals in combination may be responsible for the regulation of $K^+$ channel expression in the developing heart via direct or indirect pathways as diagrammed below.

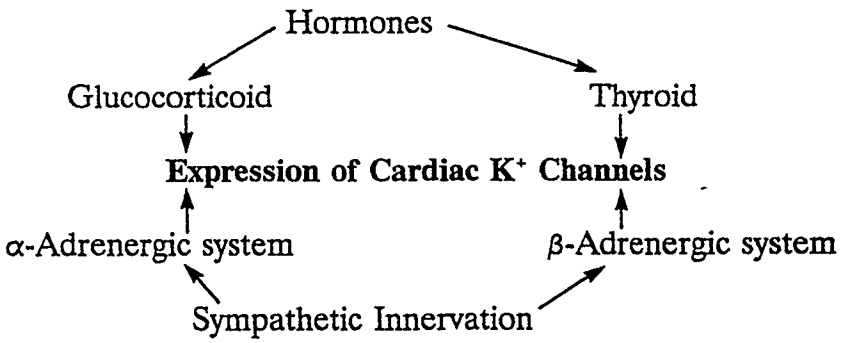


***Hormones and $K^+$ channel expression in the developing heart***

Several studies have demonstrated that hormones, such as glucocorticoid and thyroid hormones change dramatically during late gestation and immediately after birth, leading to speculation that such changes may affect the morphology of cardiac action potentials and expression of different cardiac $K^+$ channels over the same period.

<u>Glucocorticoid</u> The maternal levels of glucocorticoid (corticosterone) sharply decline on day 19 of gestation in rat. After birth, the circulating hormone levels in the

newborn decline continuously until the adrenals synthesize and release the hormone during the third postnatal week (32). The relation between action potential shortening and a concomitant decline in circulating glucocorticoid levels in the newborn rat has been examined by Penefsky and McCann (130). They found that treatment of newborn rats with only one injection of dexamethasone (a synthetic glucocorticoid) largely inhibited the initial rapid repolarization, thereby, prevented the disappearance of the plateau phase and the shortening of the action potentials. If the effects of dexamethasone on the action potential duration are through regulation of $K^+$ channel expression, it is likely that existence of glucocorticoid in the circulation may inhibit certain types of $K^+$ channel expression during development. In other words, the normal decline of glucocorticoid in the perinatal period may induce the expression of a $K^+$ channel or change the existing channel numbers.

Recently, it has been reported that dexamethasone specifically upregulated Kv1.5 channel gene expression in rat ventricle, but had no effects on Kv1.4 and Kv2.1 mRNA levels (161). Although this study was not designed to assess the mechanisms by which dexamethasone altered $K^+$ channel expression during development, these data suggest that dexamethasone may regulate the developmental expression of $K^+$ channels. Kv1.5 is not likely to underlie developmental changes in action potentials in mouse heart since dexamethasone was found to prevent the normal shortening of the action potential during development (130).

**Thyroid Hormone** It has been reported that thyroid hormones gradually increase in the

last few days of gestation (39,53,126), with an abrupt increase during the first few hours of extrauterine life (39). Thyroid hormones can influence rat fetal development even before the thyroid gland becomes fully active (2-3 days before birth) (114). According to the studies of $T_3$ receptor ontogenesis by Perez-Castillo, the rat heart gradually develops the capacity to respond to thyroid hormone from the 13th day of gestation onwards, with maximum responsiveness at 20-30 days of postnatal life (131). These data indicate that before establishment of fetal thyroid function, thyroid hormones from the mother may influence fetal development. It is known that thyroid hormone is important for developmental processes occurring in the last days of fetal life and during the postnatal period. However, little is known about the specific events, such as expression of cardiac $K^+$ channels triggered by thyroid hormones. Thyroid hormone may modify cardiac $K^+$ currents in adult heart. For example, $I_K$ in guinea pig ventricular myocytes and $I_{to}$ in rabbit ventricular myocytes were significantly enhanced, resulting in a shortening of action potential in hyperthyroidism (143,153). However, Shimoni *et al* found that under hyperthyroid conditions $I_{to}$ was not significantly altered in rat ventricular myocytes (155), which contrasts with the finding of a distinct increase in $I_{to}$ in the ventricular myocytes isolated from hyperthyroid rabbit. These data, therefore indicate that thyroid hormone does regulate the $K^+$ channel gene expression in heart, but its effects are cell type-specific or species-dependent. These results also lead to the hypothesis that alteration in the circulating concentrations of thyroid hormones during the perinatal period may be an important factor for regulating the expression of certain types of $K^+$ channels in mouse heart during development. This hypothesis will be tested in

future studies.

***Sympathetic innervation and $K^+$ channel expression in the developing heart***

**Nerve growth factor (NGF)** During normal development, complete maturation of the sympathetic nervous system takes place after birth. The density of intramural innervation increases gradually in the rat heart during the first 2-3 weeks of life, by which time the degree of innervation of the adult is attained (61). In the rabbit heart, innervation develops fully over the first 5 weeks after birth (128).

To evaluate whether the postnatal evolution of sympathetic innervation occurs concurrently with changes in cardiac repolarization, Malfatto *et al* treated rats with either NGF to accelerate innervation, or antiserum to NGF to retard innervation at 10 days of age (106). They found that antiserum-treated rats exhibited a longer QT interval on ECG than the NGF- or placebo-treated rats, indicating that sympathetic innervation indeed modifies the process of cardiac repolarization. In addition, they also suggested that the modulation of sympathetic innervation by NGF was associated with an increase in $\alpha_1$ receptor-effector coupling with no significant effect on $\beta$-adrenergic system (159). However the relationships between innervation and specific ion channels which underlie the action potential repolarization were not determined in that study.

Recently, Liu *et al* continued to explore the effects of NGF on cardiac repolarization by measuring whole-cell $K^+$ currents (99). They demonstrate that sympathetic innervation regulates $K^+$ currents in rat ventricular myocytes during early postnatal development. The densities of $I_{to}$ and $I_{K1}$ in neonatal rat ventricular myocytes

treated with antiserum were significantly lower than those treated with NGF. In parallel to these $K^+$ current changes, the action potential duration and QT interval were also significantly longer in the antiserum-treated neonatal rats than in NGF-treated neonatal rats. Therefore, it is likely that sympathetic innervation provides a "signal" that results in the shortening of action potential duration by regulating the expression of $K^+$ channels in the developing heart. However, a direct relationship between expression of $K^+$ channels and $\alpha$ and $\beta$-adrenergic stimulation during development was not determined.

### *$\alpha$- and $\beta$-Adrenergic stimulation and cardiac $K^+$ channel expression*

To my knowledge, there is no report about the direct relationship of the $K^+$ channel expression, and $\alpha$- and $\beta$-adrenergic activities in the developing heart. However, modulation of $K^+$ channels by $\alpha$- and $\beta$-adrenergic agonists have been demonstrated in the adult heart from different species. Generally, both $\alpha_1$- and $\beta$-adrenergic stimulation enhances $I_{Ks}$ in guinea pig ventricular myocytes (54,165,174,176). In contrast, $\alpha_1$- and $\beta$-adrenergic stimulation decreases $I_{to}$ in rabbit cardiac myocytes (46,47), in rat ventricular myocytes (4,134) and in canine Purkinje fibers (120). $\alpha_1$- and $\beta$-adrenergic stimulations also reduce the amplitude of $I_{K1}$ in rabbit cardiac myocytes (48).

$\alpha_1$- and $\beta$-Adrenergic stimulation in cardiac myocytes is associated with activation of protein kinase C (PKC) and protein kinase A (PKA) pathways. Recently, Murray *et al* showed that phorbol esters resulted in a significant reduction in Kv1.4 current (118). In contrast, Matsubara *et al* reported that treatment of primary cultured rat neonatal cardiac myocytes with phorbol ester substantially increased Kv1.4 mRNA expression

(109). These data suggest that regulation of $K^+$ channel expression by PKC is species- and age-dependent. Although the physiological correlate of Kv1.4 current in native cardiac myocytes is not well understood, these results suggest that direct $K^+$ channel phosphorylation by PKC may be one of the molecular mechanisms of regulating functional $K^+$ channels in the developing heart. On the other hand, intracellular cAMP levels and PKA activation are associated with upregulation of Kv1.5 gene transcription (113). These data suggest that expressions of Kv1.4 and Kv1.5 are regulated through different intracellular pathway. In addition, dramatic alterations of intracellular PKC and PKA activities occur during perinatal period (93), which may modify the expression of cardiac $K^+$ channel expression during development.

***Is there a common pathway of $K^+$ channel regulation between developing heart and diseased heart?***

It has been shown that certain heart diseases such as cardiac hypertrophy induce a re-expression of a fetal gene program (168). This implies that there may be some common regulatory pathways between the diseased heart and fetal developing heart. These regulatory pathways may involve several intracellular and extracellular signalling systems. It has been reported that myocardial hypertrophy in both human and animal models, such as the spontaneously hypertensive rat (SHR) is associated with changes in intracellular signals, including increased intracellular concentrations of $Ca^{2+}$, inositol phosphates, and diacylglycerol. The increased concentrations of these intracellular factors result in PKC activation (112). Interestingly, these intracellular factors are also

altered in the heart during development.

In addition, electrophysiological studies have demonstrated that transmembrane action potentials were significantly prolonged in hypertrophied ventricles of renal hypertensive rat (RHR), SHR and hypertrophied ventricles in other species, including human (7,66). Similarly, in fetal or early postnatal rat heart, the action potential duration is prolonged as compared with that in adult rat heart. The prolonged action potential duration in hypertrophied heart is thought to be due to a decrease in the amplitudes of $I_{to}$ (184). Interestingly, an absence of $I_{to}$ in fetal rat heart and a lower density of $I_{to}$ in neonatal rat ventricular myocytes is also considered to contribute to the prolonged action potential duration observed in fetal and neonatal rat heart. These similarities between the diseased heart and the developing heart indicate that understanding of the regulation of $K^+$ channel expression in the normal developing heart may provide insights into the mechanisms underlying modification of $K^+$ channel expression in the diseased heart.

### 5.4b Future studies to address potential mechanisms

The following aspects will be assessed in future studies to explore the mechanisms of the regulation of cardiac $K^+$ channels during development.

1. The effects of thyroid hormones on cardiac $K^+$ channel expression during development.
2. The effects of glucocorticoid hormone on cardiac $K^+$ channel expression during development.
3. The effects of $\alpha$- and $\beta$-adrenergic activities on cardiac $K^+$ channel expression during development.
4. The effects of intracellular messengers, such as cAMP, PKA, $[Ca^{2+}]_i$ and PKC on cardiac $K^+$ channel expression during development.

Regulation of $K^+$ channel protein expression by these extracellular and intracellular signals may occur at any level including transcription, translation and post-translation. In addition, these factors may directly modified cardiac $K^+$ channel function without effects on channel protein synthesis. Thus, the future studies may involve several techniques such as Northern blot (mRNA), Western blot (protein) analysis and patch clamp. The measurements of mRNA for the $K^+$ channels such as *HERG* (or *MERG*), minK, Kv4.2, Kv1.4, Kv1.5, Kv2.1 and IRK1 may provide valuable information on the developmental changes in $K^+$ channel expression and the relationships between native cardiac $K^+$ channels and cloned $K^+$ channels.

## 5.5 Limitations

All patch clamp experiments were carried out at room temperature in this dissertation. Since activation and inactivation kinetics of the ionic currents including the $K^+$ currents are very sensitive to temperature, the results obtained at room temperature may not accurately describe the properties of the cardiac $K^+$ currents at physiological temperature. However, the microelectrode results of this dissertation, which were performed at 37°C support the patch-clamp findings of the developmental changes in the $K^+$ currents in mouse heart.

Since developmental change in sarcoplasmic reticulum occurs in the heart, this change may result in developmental changes in $Ca^{2+}$-dependent transient outward current. Although in the present study, developmental changes in $I_{to}$ (voltage-dependent, $Ca^{2+}$-independent transient outward current) were examined in the presence of a $Ca^{2+}$ channel blocker, nisoldipine (0.4 $\mu$M) in the external solution and EGTA (5 mM) in the internal solution, the effect of $Ca^{2+}$-dependent transient outward current on the results of developmental changes in $I_{to}$ could not be completely excluded.

Ion currents were distinguished on the basis of biophysical characteristics and response to selective pharmacologic blockers. No attempt was made to assess if developmental changes altered the concentration -response relationships to these blocker. We recognize that all blockers are selective, not perfectly. However, pharmacologic responses are linked to a biophysical assessment of currents in this dissertation.

In addition, as discussed, the $B_{max}$ of [$^3$H]-dofetilide binding sites may not quantitatively reflect the actual number of $I_{Kr}$ channels in mouse ventricles. However,

the data obtained from [$^3$H]-dofetilide binding assay may qualitatively reflect the pattern of developmental changes in $I_{Kr}$ channels in mouse ventricles.

# CHAPTER 6: CONCLUSIONS

1) Developmental changes in $I_{Kr}$, $I_{Ks}$ and $I_{to}$ occur in mouse heart

2) These developmental changes result both from alteration in the density of these $K^+$ currents and from expression of different $K^+$ currents at different times during development.

3) Developmental changes in action potential configuration are related to developmental changes in expression of $K^+$ currents in mouse heart.

## 6.1 Significance of Findings

The findings of age-related alterations in $K^+$ currents and action potential configuration in mouse heart have made a contribution to our knowledge about the electrophysiological changes in cardiac cells during normal development. Since expression of $K^+$ currents changes dramatically in perinatal mouse heart, the heart at each developmental stage may exhibit different responses to $K^+$ channel blockers. For example, fetal mouse heart is much more sensitive to $I_{Kr}$ channel blocker, dofetilide, than adults. If this result has applicability to humans, the human fetus may have extreme sensitivity to $I_{Kr}$ channel blockers and this class of drug should be avoided or used with extreme caution in this situation. In addition, the diseased heart at any age may mimic the events occurring in embryonic or fetal life. Thus, an understanding of the developmental biology of the cardiovascular system may be a prerequisite for prevention and optimal management of heart disease at any age. The modulators that trigger alteration of $K^+$ channel expression may be similar for both the developing heart and the diseased heart. Future studies to address the potential mechanisms by which cardiac $K^+$ channel expression is regulated during development may provide important insights for understanding the modulation of the cardiac $K^+$ channel expression in the diseased heart. Furthermore, with the advances in molecular techniques, transgenic mouse models will facilitate the mechanistic studies of the certain heart diseases. From this point of the view, the results obtained from this dissertation not only illustrate the characteristics of $K^+$ currents in mouse ventricular myocytes during normal development, but also provide a basic knowledge for future studies of ionic currents in transgenic mouse.

## REFERENCES

1. Abrahamsson C, Palmer M, Ljung B, Duker G, Baarnhielm C, Carlsson L, Danielsson B. Induction of rhythm abnormalities in the fetal rat heart. A tentative mechanism for the embryotoxic effect of the class III antiarrhythmic agent almokalant. *Cardiovasc Res.* 1994; 28:337-344.

2. Anumonwo JMB, Freeman LC, Kwok WM, Kass RS. Delayed rectification in single cells isolated from guinea pig sinoatrial node. *Am J Physiol.* 1992; 262:H921-H925.

3. Antzelevitch C, Sicouri S, Lukas A, Nesterenko VV, Liu DW, Di Diego JM. Regional differences in the electrophysiology of ventricular cells: Physiological and clinical implications. *In* Zipes DP, Jalife J. (eds): Cardiac Electrophysiology: From Cell to Bedside. 2nd edition, W.B. Saunders Company, 1995; pp 228-245.

4. Apkon M, Nerbonne JM. $\alpha_1$-Adrenergic agonists selectively suppress voltage dependent $K^+$ currents in rat ventricular myocytes. *PNAS.* 1988; 85:8756-8760.

5. Apkon M, Berbonne JM. Characterization of two distinct depolarization-activated $K^+$ currents in isolated rat ventricular myocytes. *J Gen Physiol.* 1991; 97:973-1011.

6. Arena JP, Walsh KB, Kass RS: Measurement, block, and modulation of potassium channel currents in the heart. *In* Colatsky TJ (ed): Potassium Channels: Basic Function and Therapeutic Aspects. New York, Alan R. Liss, 1990; pp 43-63.

7. Aronson RS. Characteristics of action potentials of hypertrophied myocardium from rats with renal hypertension. *Circ Res.* 1980;47:443-454.

8. Ashford MLJ, Bond CT, Blair TA, Adelman JP. Cloning and functional expression of a rat heart $K_{ATP}$ channel. *Nature* 1994; 370:456-459.

9. Attali B, Guillemare E, Lesage F, Honore E, Romey G, Lazdunski M, Barhanin J. The protein IsK is a dual activator of $K^+$ and $Cl^-$ channels. *Nature.* 1993; 365:850-852.

10. Backx PH, Marban E. Background potassium current active during the plateau of the action potential in guinea pig ventricular myocytes. *Circ Res.* 1993; 72:890-900.

11. Barry DM, Trimmer JS, Merlie JP, Nerbonne JM. Differential expression of voltage-gated $K^+$ channel subunits in adult rat heart: Relation to functional $K^+$ channels? *Circ Res.* 1995; 77:361-369.

12. Benndorf K, Boldt W, Nilius B. Sodium current in single myocardial mouse cells. *Pflugers Arch.* 1985; 404:190-196.

13. Benndorf K, Nilius B. Properties of an early outward current in single cells of the mouse ventricle. *Gen Physiol Biophys.* 1988; 7:449-466.

14. Bennett PB, McKinney LC, Kass RS, Begenisich T. Delayed rectification in the calf cardiac Purkinje fibre. *Biophys J.* 1985; 248:553-567.

15. Beuckelmann DJ, Nabauer M, Erdmann E. Alterations of $K^+$ currents in isolated human ventricular myocytes from patients with terminal heart failure. *Circ Res.* 1993; 73:379-385.

16. Bond CT, Pessia M, Xia XM, Lagrutta A, Kavanaugh MP, Adelman JP. Cloning and Expression of a family of inward rectifier potassium channels. *Receptors and Channels.* 1994; 2:183-191.

17. Boyle WA, Nerbonne JM. Two functionally distinct 4-aminopyridine-sensitive outward $K^+$ currents in rat atrial myocytes. *J Gen Physiol.* 1992; 100:1041-1067.

18. Brown AM. Functional bases for interpreting amino acid sequences of voltage-

dependent $K^+$ channels. *Annu Rev Biophys Biomol Struct.* 1993; 22:173-198.

19. Campbell DL, Rasmusson RL, Qu Y, Strauss HC. The calcium-independent transient outward potassium current in isolated ferret right ventricular myocytes. I. Basic characterization and kinetic analysis. *J Gen Physiol.* 1993;101:571-601.

20. Campbell DL, Rasmusson RL, Comer MB, Strauss HC. The cardiac calcium-independent transient outward potassium current: Kinetics, molecular properties, and role in ventricular repolarization. *In* Zipes DP, Jalife J (eds): Cardiac Electrophysiology: From Cell to Bedside. 2nd Edition, W.B. Saunders Company, 1995; pp83-95.

21. Carmeliet E. Voltage- and time-dependent block of the delayed $K^+$ current in cardiac myocytes by dofetilide. *J Pharmacol Exp Ther.* 1992; 262:809-817.

22. Carmeliet E, Mubagwa K. Changes by acetylcholoine of membrane currents in rabbit cardiac Purkinje fibers. *J Physiol (Lond).* 1986;371:201-217.

23. Castellino RC, Morales MJ, Strauss HC, Rasmusson RL. Time- and voltage-dependent modulation of a Kv1.4 channel by a $\beta$-subunit (Kv$\beta$3) cloned from ferret ventricle. *Am J Physiol.* 1995; 269:H385-H391.

24. Catterall WA. Inhibition of voltage-sensitive sodium channels in neuroblastoma cells by antiarrhythmic drugs. *Mol Pharmacol.* 1981; 20:356-362.

25. Chadwick CC, Erin AM, O'Connor B, Volberg WA, Smith DI, Wedge KJ, Hill RJ, Briggs GM, Pagani ED, Silver PJ, Krafte DS. Identification of a specific radioligand for the cardiac rapidly activating delayed rectifier $K^+$ channel. *Circ Res.* 1993;72:707-714.

26. Chen FH, Wetzel GT, Friedman WF, Klitzner TS. Single-channel recording of Inwardly rectifying potassium currents in developing myocardium. *J Mol Cell Cardiol.* 1991; 23: 259-267.

27. Chiamvimonvat N, Kargacin ME, Clark RB, Duff HJ. Effects of intracellular calcium on sodium current density in culture neonatal rat cardiac myocytes. *J Physiol(Lond).* 1995; 483:307-318.

28. Chien KR. Molecular advances in cardiovascular biology. *Science.* 1993; 269:916-917.

29. Clark RB, Giles WR, Imaizumi Y: Properties of the transient outward current in rabbit atrial cells. *J Physiol (Lond).* 1988; 405:147-168.

30. Clarkson CW, Crumb Jr. WJ, Pigott JD, Brown AM. Developmental changes in potassium currents recorded from human atrial myocytes. *Biophys. J.* 1994; 86: A326 (Abstract).

31. Clay JR, Ogbaghebriel A, Paquette T, Sasyniuk BI and Shrier A. A quantitative description of the E-4031-sensitive repolarization current in rabbit ventricular myocytes. *Biophysical J.* 1995; 69:1830-1837.

32. Cohen A. Adrenal and plasma corticosterone levels in the pregnant fetal and neonatal rat, in the perinatal period. *Hormone and Metabolism Research.* 1976; 8:474-478.

33. Colastsky J, Follmer CH, Starmer CF. Channel specificity in antiarrhythmic drug action. Mechanism of potassium channel block and its role in suppressing and aggravating cardiac arrhythmias. *Circulation.* 1990; 82:2235-2242.

34. Coraboeuf E, Carmeliet E. Existence of two transient outward currents in sheep cardiac Purkinje fibres. *Pflugers Arch.* 1982; 392:352-359.

35. Curran ME, Splawski I, Timothy KW, Vincent GM, Green ED, Keeting MK. A molecular basis for Cardiac arrhythmia: *HERG* mutations cause long QT syndrome. *Cell* 1995; 80:795-803.

36. Dascal N, Lim NF, Schriebmayor W, Wang W, Davison N, Lester HA. Expression of an atrial G-protein channel in *Xenopus* oocytes. *Proc Natl Acad Sci.* 1993; 90:10235-10239.

37. Davies MP, An RH, Doevendans P, Kubalak S, Chien KR, Kass RS. Development changes in ionic channel activity in the embryonic murine heart. *Circ Res.* 1996;78:15-25.

38. DeLean A, Stadel JM, Lefkowitz RJ. A ternary complex model explains the agonist-specific binding properties of the adenylate cyclase-coupled beta-adrenergic receptor. *J Biol Chem.* 255:7108-7117, 1980

39. Devaskar UP, Devaskar SU, Sadiq HF, Chechani V. Ontogeny of plasma free thyroid and maternofetal transfer of thyroid hormones in rabbit. *Dev Pharmacol Ther.* 1986; 9:115-123.

40. Dixon JE, McKinnon D. Quantitative analysis of potassium channel mRNA expression in atrial and ventricular muscle of rats. *Circ Res.* 1994; 75:252-262.

41. Duff HJ, Feng ZP, Sheldon RS. High and low affinity site for [$^3$H]-dofetilide binding to guinea pig myocytes *Circ Res.* 1995; 77:718-725.

42. Dyson E, Kubalak SW, Schmid-Schonbein GW, Delano F, Sucov H, Evans RM, Ross JR, Chien KR. Atrial-like phenotype leads to embryonic ventricular failure in RXRa -/- mice. *Proc Natl Acad Sci USA.* 1995; 92:7386-7390.

43. Escande D, Loisance D, Planche C, Coraboeuf E. Age-related changes of action potential plateau shape in isolated human atrial fibers. *Am J Physiol.* 1985; 249:H843-H850.

44. Escande D, Coulombe A, Faivre JF, Deroubaix E, Coraboeuf E. Two types of transient outward currents in adult human atrial cells. *Am J Physiol.* 1987; 252:H142-H148.

45. Fakler B, Brandle U, Glowatzki E, Weidemann S, Zenner HP, Ruppersberg JP. Strong voltage-dependent inward rectification of inward rectifier $K^+$ channels is caused by intracellular spermine. *Cell.* 1995; 80:149-154.

46. Fedida D, Shimoni Y, Giles WR. A novel effect of norepinephrine on cardiac cells is mediated by $alpha_1$-adrenoceptor. *Am J Physiol.* 1989; 256:H1500-H1504.

47. Fedida D, Shimoni Y, Giles WR. Alpha-adrenergic modulation of the transient outward current in rabbit atrial myocytes. *J Physiol (Lond).* 1990;423:257-277.

48. Fedida D, Braun AP, Giles WR. $\alpha$-Adrenoceptor reduce background $K^+$ current in rabbit ventricular myocytes. *J Physiol (Lond).* 1991; 441: 673-684.

49. Felipe A, Knittle T, Doyle K, Snyders DJ, Tamkun MM. Differential expression of $I_{sk}$ mRNAs in mouse tissue during development and pregnancy. *Am J Physiol.* 1994; 267:C700-C705.

50. Ficker E, Taglialatela M, Wible BA, Henley CM, Brown AM. Spermine and spermidine as gating molecules for inward rectifier $K^+$ channels. *Science.* 1994; 266:1068-1072.

51. Field LJ. Transgenic mice in cardiovascular research. *Annu Rev Physiol.* 1993; 55:97-114.

52. Folander K, Smith JS, Antanavage J, Bennett C, Stein RB, Swanson R. Cloning and expression of the delayed-rectifier $I_{sK}$ channel from neonatal rat heart and diethylstilbestrol-primed rat uterus. *Proc Natl Acad Sci USA.* 1990; 87:2975-2979.

53. Fraser M, Liggins CG. Thyroid hormone kinetics during late pregnancy in the ovine fetus. *J Dev Physiol.* 1988; 10:461-471.

54. Freeman LC, Kwok WM, Kass RS. Phosphorylation-independent regulation of cardiac $I_K$ by guanine nucleotides and isoproterenol. *Am J Physiol.* 1992; 262: H1298-H1302.

55. Freeman LC, Kass RS. Expression of a minimal $K^+$ channel protein in mammalian cells and immunolocalization in guinea pig heart. *Circ Res.* 1993; 73:968-973.

56. Furukawa T, Kimura S, Furukawa N, Bassett AL, Myerburg RJ. Potassium rectifier currents differ in myocytes of endocardial and epicardial origin. *Circ Res.* 1992; 70:91-103.

57. Giles WR, van Ginneken A. A transient outward current in isolated cells from the crista terminalis of rabbit heart. *J Physiol (Lond).* 1985;368:243-264.

58. Giles WR, Imaizumi Y. Comparison of potassium currents in rabbit atrial and ventricular cells. *J. Physiol (Lond).* 1988; 405:123-145.

59. Gintant GA, Cohen IS, Datyner NB, Klein RP. Time-dependent outward currents in the heart. *In* Fozzard HA, Haber E, Jennings RB, Katz AM, Morgan AE (eds): The Heart and Cardiovascular System: Scientific Foundations. New York, Raven Press, 1992; pp.1121-1169.

60. Gintant GA. Two components of delayed rectifier current in canine atrium and ventricle: Dose $I_{Ks}$ play a role in the reverse rate dependence of class II agents?. *Circ Res.* 1996;78:26-37.

61. Goldstein MA, Traeger L: Ultrastructural changes in postnatal development of the cardiac myocyte. *In* Legato M (ed): The Developing Heart. Boston, MA, Martimus Nijhoff Publishing, 1985, pp.1-20.

62. Gross GJ, Burke RP, Castle NA. Characterization of transient outward current in young human atrial myocytes. *Cardiovas Res.* 1995; 29:112-117.

63. Hall AE, Hutter OF, Noble D. Current-voltage relations of Purkinje fibres in sodium deficient solutions. *J Physiol (Lond).* 1963; 166:225-240.

64. Hamill OP, Marty A, Neher E, Sakmann B, Sigworth FG. Improved patch clamp techniques for high-resolution current recording from cells and cell-free membrane patches. *Pfluegers Arch.* 1981; 391:85-100.

65. Hausdorff SF, Goldstein SAN, Rushin EE, MIller C. Functional characterization of a minimal $K^+$ channel expressed from a synthetic gene. *Biochemistry.* 1991; 30:3341-3346.

66. Hayashi H, Shibaba S. Electrical property of cardiac cell membrane of spontaneously hypertensive rat. *Eur J Pharmacol.* 1974;27:355-359.

67. Heidbuchel H, Vereecke J, Carmeliet E. The electrophysiological effects of acetylcholine in single human atrial cells. *J Mol Cell Cardiol.* 1987; 19:1207-1219.

68. Hill RJ, Duff HJ, Sheldon RS. Class I antiarrhythmic drug receptor: biochemical evidence for state-dependent interaction with quinidine and lidocaine. *Mol Pharmacol.* 1989; 36:150-159.

69. Hille B. Ionic Channels of Excitable Membranes. Sinauer Associates. Sunderlan, MA. 1992.

70. Ho K, Nichols CG, Lederer WJ, Lytton J, Vassilev PM, Kanazirska MV, and Herbert SC. Cloning and expression of an inwardly rectifying ATP-regulated potassium channel. *Nature.* 1993; 362:31-38.

71. Honore E, Attali B, Romey G, Heurteaux C, Ricard P, Lesage F, Lazdunski M, Barhanin J. Cloning, expression, pharmacology and regulation of a delayed rectifier $K^+$ channel in mouse heart. *EMBO J.* 1991;10:2805-2811.

72. Horie M, Hayaski S, Kawai C. Two types of delayed rectifying $K^+$ channels in atrial cells of guinea pig heart. *Jpn J Physiol.* 1990;40:479-490.

73. Hoshi, T., Zagotta, W. N., Aldrich, R. W.: Biophysical and molecular mechanisms of *Shaker* potassium channel inactivation. *Science.* 1990; 250:533-538.

74. Hoshi T, Zagotta WN, Aldrich RW. Two types of inactivation in shaker K channels: effects of alterations in the carboxy terminal region. *Neuron.* 1991; 7:547-556.

75. Huynh TV, Chen F, Wetzel GT, Friedman WF, Klitzner TS. Developmental changes in membrane $Ca^{2+}$ and $K^+$ currents in fetal, neonatal and adult rabbit ventricular myocytes. *Circ Res.* 1992; 70:508-515.

76. Isacoff EY, Jan YN, Jan LY. Identification of a putative receptor for the cytoplasmic inactivation gate in the *Shaker* $K^+$ channel. *Nature.* 1991; 353: 86-90.

77. Ishii K, Yamagashi T, Taira N. Cloning and functional expression of a cardiac inward rectifier $K^+$ channel. *FEBS lett.* 1994; 338:107-111.

78. Iverson L, Rudy B. The role of the divergent amino caid carboxyl terminals domains on the inactivation properies of potassium channels derived from the *Shaker* gene of *Drosophila. J Neurocsi.* 1990; 10:2903-2916.

79. Ito H, Ono K. A rapidly activating delayed rectifier $K^+$ channel in rabbit sinoatrial node cells. *Am J Physiol.* 1995; 269:H443-H452.

80. Jan LY, Jan YN. Structural elements involved in specific $K^+$ channel functions. *Annu Rev Physiol.* 1992; 54:537-555.

81. Jeck CD, Boyden PA. Age-related appearance of outward currents may contribute to developmental differences in ventricular repolarization. *Circ Res.* 1992; 71:1390-1403.

82. Joho RH. Toward a molecular understanding of voltage-gated potassium channels. *J Cardiovasc Electrophysiol.* 1992; 3:589-601.

83. Josephson IR, Sperelakis N. Developmental increases in the inwardly-rectifying $K^+$ current of embryonic chick ventricular myocytes. *Biochim Biophys Acta.* 1990; 1052:123-127.

84. Jurkiewicz NK, Sanguinetti MC. Rate-dependent prolongation of cardiac action

potentials by a methanesulfonanilide class III antiarrhythmic agent. *Circ. Res.* 1993; 72:75-83.

85. Kaczmarek LK. Voltage-dependent potassium channels: minK and Shaker families. *New Biol.* 1991; 3:315-323.

86. Kameyama M, Kakei M, Sato R, Shibasaki T, Matsuda H, Irisawa H. Intracellular $Na^+$ activates a $K^+$ channel in mammalian cardiac cells. *Nature* 1984; 309:354-356.

87. Kass RS. Nisoldipine: a new, more selective calcium current blocker in cardiac Purkinje fibers. *J Phar Exp Ther.* 1982; 223:446-456.

88. Kass RS, Freeman LC. Potassium channels in the heart: cellular, molecular and clinical implications. *Trends Cardiovascular Med.* 1993; 3:149-159.

89. Kenyon JL, Gibbons WR. 4-Aminopyridine and the early outward current of sheep cardiac Purkinje fibers. *J Gen Physiol* 1979; 73:139-157.

90. Kilborn MJ, Fedida DA. A study of the developmental changes in outward currents of rat ventricular myocytes. *J Physiol (Lond).* 1990; 430:37-60.

91. Kleiman RB, Houser SK. Outward current in normal and hypertrophied feline ventricular myocytes. *Am J Physiol.* 1989; 256:H1450-H1461.

92. Kojima M, Sada H, Sperelakis N. Developmental changes in $\beta$-adrenergic and cholinergic interactions on $Ca^{2+}$-dependent slow action potentials in rat ventricular muscles. *Br J Pharmacol.* 1990a; 99:327-333.

93. Kojima M, Sperelakis N, Sada H. Ontogenesis of transmembrane signaling systems for control of cardiac $Ca^{2+}$ channels. *J Devel Physiol.* 1990b; 14:181-219.

94. Konarzewska H, Peeters GA, Sanguinetti MC. Repolarizing $K^+$ currents in nonfailing human hearts: similarities between right septal subendocardial and left subepicardial ventricular myocytes. *Circulation.* 1995; 92:1179-1187.

95. Krapivinsky G, Gordon EA, Wickman K, Velimirovic B, Krapivinsky L, Clapham DE. The G-protein-gated atrial $K^+$ channel $I_k$ Ach is a heteromultimer of two inwardly rectifying $K^+$-channel proteins. *Nature.* 1995; 374:135-141.

96. Kubo Y, Baldwin TJ, Jan YN, Jan LY. Primary structure and functional expression of a mouse inward rectifier potassium channel. *Nature.* 1993a;

362:127-132.

97. Kubo Y, Reuveny E, Slesinger PA, Jan YN and Jan LY. Primary structure and functional expression of a rat G-protein-coupled muscarinic potassium channel. *Nature.* 1993b; 364:802-806.

98. Liu DW, Gintant GA, Antzelevitch C. Ionic basis for electrophysiological distinctions among epicardial, midmyocardial, and endocardial myocytes from the free wall of the canine left ventricle. *Circ Res.* 1993;72:671-687.

99. Liu QY, Rosen MR, Robinson RB. Sympathetic innervation modulates repolarizing $K^+$ currents in neonatal rat ventricular epicardial myocytes. *Circulation.* 1995; 92:I-639 (Abstract).

100. Litovsky SH, Antzelevitch C. Transient outward current prominent in canine ventricular epicardium but not endocardium. *Circ. Res.* 1988; 62:116-126.

101. London B, Newton KP, Vesely MR, Wong JCL, Ginsburg GS, Satler CA. Cloning the mouse homolog of the long QT syndrom gene *HERG. Circulation.* 1995; 92:I-233 (Abstract).

102. Lopatin AN, Makhina EN, Nichols CG. Potassium channel block by cytoplasmic

polyamines as the mechanism of intrinsic rectification. *Nature*. 1994; 372:366-369.

103. Lopez GA, Jan YN, Jan LY. Hydrophobic substitution mutations in the S4 sequence alter voltage-dependent gating in *Shaker* $K^+$ channels. *Neuron* 1991; 7:327-336.

104. Lopez-Barneo J, Hoshi T, Heinemann SH, Aldrich RW. Effects of external cations and mutations in the pore region on C-type inactivation of shaker potassium channel inactivation. *Science*. 1993; 262:757-759.

105. Lynch JJ, Sanguinetti MC, Kimura S, Bassett AL. Therapeutic potential of modulating potassium currents in the diseased myocardium. *FASEB J*. 1992; 6:2952-2960.

106. Malfatto G, Rosen TS, Steinberg SF, Ursell PC, Sun LS, Daniel S, Danilo Jr P, Rosen MR. Sympathetic neural modulation of cardiac impulse initiation and repolarization in the newborn rat. *Circ Res*. 1990; 66:427-437

107. Maltsev VA, Wobus AM, Rohwedel J, Bader M, Hescheler J. Cardiomyocytes differentiated in vitro from embryonic stem cells developmentally express cardiac-specific genes and ionic currents. *Circ Res*. 1994; 75:233-244.

108. Masuda H, Sperelakis N. Inwardly rectifying potassium current in rat fetal and neonatal ventricular cardiomyocytes. *Am J Physiol.* 1993; 265:H1107-H1111.

109. Matsubara H, Uzuki J, Inada M. *Shaker*-related potassium channel, Kv1.4, mRNA regulation in cultured rat heart myocytes and differential expression of Kv1.4 and Kv1.5 genes in myocardial development and hypertrophy. *J Clin Invest.* 1993; 92:1659-1666.

110. Matsuda H, Saigusa A, Irisawa H. Ohmic conductance through the inwardly rectifying K channel and blocking by internal $Mg^{2+}$. *Nature* 1987; 325:156-159.

111. McDonald TF, Trautwein W. The potassium current underlying delayed rectification in cat ventricular muscle. *J Physiol (Lond).* 1978; 274:217-245.

112. Morgan HE and Baker KM. Cardiac hypertrophy, mechanical, neural and endocrine dependence. *Circulation.* 1991; 83:13-25.

113. Mori Y, Matsubara H, Koren G. cAMP modulates the expression of a rat delayed rectifier $K^+$ channel at the pretranslational level. *J Mol Cell Cardiol.* 1992; 24:S227 (Abstract).

114. Morreale de Escobar G, Pastor R, Obregon MJ, Escobar del Rey F. Effects of

maternal hypothyroidism on the weight and thyroid hormone content of rat embryonic tissue: Before and after onset of fetal thyroid function. *Endocrinology*. 1985; 117:1890-1900.

115. Murai T, Kakizuka A, Takumi T, Ohkubo H, NAkanishi S. Molecular cloning and sequence analysis of human genomic DNA encoding a novel membrane protein which exhibits a slowly activating potassium channel activity. *Biochem Biophys Res Commun.* 1989; 161:176-181.

116. Muraki K, Imaizumi Y, Watanabe M, Habuchi Y, Giles WK. Delayed rectifier $K^+$ current in rabbit atrial myocytes. *Am J Physiol.* 1995; 269:H524-532.

117. Murphy E, Freudenrich CC, Lieberman M. Cellular magnesium and Na/Mg exchange in heart cells. *Annu Rev Physiol.* 1991; 53:273-287.

118. Murray KT, Fahrig SA, Deal KK, Po SS, Hu NN, Synders DJ, Tamkun MM, Bennett PB. Modulation of an inactivating human cardiac $K^+$ channel by protein kinase C. *Circ Res*. 1994; 75:999-1005.

119. Nabauer M, Beuckelmann DJ, Uberfuhr P, Steinbeck G. Regional differences in current density and rate-dependent properties of the transient outward current in subepicardial and subendocardial myocytes of human left ventrice.

*Circulation.* 1996; 93:168-177.

120. Nakayama, T., Fozzard, H.A.: Adrenergic modulation of the transient outward current in isolated canine Purkinje cells. *Circ. Res.* 1988; 62: 162-172.

121. Noble D, Tsien RW. Outward membrane currents activated in the plateau range of potentials in cardiac Purkinje fibres. *J Physiol (Lond).* 1969; 200: 205-231.

122. Noma A, Irisawa H. A time and voltage-dependent potassium current in the rabbit sinoatrial node cell. *Pflugers Arch.* 1976; 366:251-258.

123. Noma A. ATP-regulated $K^+$ channels in cardiac muscle. *Nature.* 1983; 305:147-148.

124. Noma A, Shibasaki T. Membrane current through adenosine-triphosphate-regulated potassium channels in guinea-pig ventricular cells. *J Physiol.* 1985; 363:463-480.

125. Nuss HB, Marban E. Electrophysiological properties of neonatal mouse cardiac myocytes in primary culture. *J Physiol (Lond).* 1994; 479:265-279.

126. Nwosu UC, Kaplan MM, Utiger RD, Delivoria-Papadopoulos M. Surge of

plasma triiodothyronine before birth in sheep. *Am J Obstet Gynecol.* 1978; 132:489-494.

127. Pacioretty LM, Gilmour RF, JR. Developmental changes of action potential configuration and $I_{to}$ in canine epicardium. *Am J Physiol.* 1995; 268:H2513-H2521.

128. Papka RE. Development of innervation to the ventricular myocardium of the rabbit. *J Mol Cell Cardiol* 1981; 13:217-228.

129. Paulmichl M, Nasmith P, Hellmiss R, Reed K, Boyle WA, Nerbonne JM, Peralta EG, Clapham DE. Cloning and expression of a rat cardiac delayed rectifier potassium channel. *Proc Natl Acad Sci.* 1991; 88:7892-7895.

130. Penefsky ZJ, McCann FV. Electrical properties of developing rat heart: Effects of dexamethasone. *J Develop Physiol.* 1989; 12:27-33.

131. Perez-Castillo A, Bernal J, Ferreiro B, Pans T. The early ontogenesis of thyroid hormone receptor in the rat fetus. *Endocrinology.* 1985; 117:2457-2461.

132. Pongs O. Molecular biology of voltage-dependent potassium channels. *Physiol Rev.* 1992; 72:S69-S88.

133. Pragnell M, Snay KJ, Trimmer JS, MacLusky NJ, Naftolin F, Kaczmarek LK, Boyle MB. Estrogen induction of a small, putative $K^+$ channel mRNA in rat uterus. *Neuron* 1990; 4:807-812.

134. Ravens U, Wang XL, Wettwer E. $\alpha$-Adrenoceptor stimulation reduces outward currents in rat ventricular myocytes. *J Pharmacol Exp Ther.* 1989; 250:264-370.

135. Rettig J, Heinemann SH, Wunder F, Lorra C, Parcej DN, Dolly JO, Pongs O. Inactivation properties of voltage-gated $K^+$ channels altered by presence of $\beta$-subunit. *Nature.* 1994; 369:289-294.

136. Richards GE, Lakoski JM, Black EW, Halpern RE, Ball K, Gluckman PD. The ontogeny of [$^3$H]5-hydroxytryptamine binding in the lamb: effects of in vivo thyroidectomy. *International J Develop Neorosci.* 1990; 8:541-547.

137. Robbins J. Genes targeting: the precise manipulation of the mammalian genome. *Circ Res.* 1993; 73:3-9.

138. Roberds SL, Tamkun MM. Cloning and tissue-specific expression of five voltage-gated potassium channel cDNAs expressed in rat heart. *Proc Natl Acad Sci.* 1991a; 88:1798-1802.

139. Roberds S L, Tamkun MM. Developmental expression of cloned cardiac potassium channels. *FEBS* 1991b; 284:152-154.

140. Roberds SL, Knoth KM, Po S, Blair TA, Bennett PB, Hartshorne RP, Synders DJ, Tamkun MM. Molecular biology of the voltage-gated potassium channels of the cardiovascular system. *J Cardiovasc Electrophysiol.* 1993; 4:68-80.

141. Rosen MR. The Sicilian Gambit - a new approach to the classification of antiarrhythmic drugs based on their action on arrhythmogenic mechanisms. *Circulation* 1991; 84:1831-1851.

142. Rosen MR, Jeck CD, Steinberg SF. Autonomic modulation of cellular repolarization and of the electrocardiographic QT interval. *J Cardiovasc Electrophysiol.* 1992; 3:487-499.

143. Rubinstein I, Binah O. Thyroid hormone modulates membrane currents in guinea-pig ventricular myocytes. *Naunyn-Schmiedeberg's Arch Pharmacol.* 1989; 340:705-711.

144. Sakmann B, Noma A, Trautwein W. Acetylcholine activation of single muscarinic potassium channels in isolated pacemaker cells of the mammalian heart. *Nature*. 1983; 303:250-253.

145. Sanchez-Chapula J, Elizalde A, Navarro-Polanco R, Barajas H. Differences in outward currents between neonatal and adult rabbit ventricular cells. *Am J Physiol.* 1994; 266:H1184-H1194.

146. Sanguinetti MC, Jurkiewicz NK. Two components of cardiac delayed rectifier $K^+$ current: differential sensitivity to block by class III antiarrhythmic agents. *J Gen Physiol.* 1990; 96:195-215.

147. Sanguinetti MC, Jurkiewicz NK. Delayed rectifier outward $K^+$ current is composed of two currents in guinea pig atrial cells. *Am J Physiol.* 1991; 260: H393-H399.

148. Sanguinetti MC, Jurkiewicz NK. Delayed rectifier potassium channels of cardiac muscle. *In* Spooner PM, Brow. AM, Catterall WA, Kaczorowski GJ, Strauss HC. (eds): Ionic Channels in the Cardiovascular System: Function and Dysfunction. Futura Publishing Company Inc. Armonk, NY, 1994; pp121-143.

149. Sanguinetti MC, Jiang C, Curran ME, Keating MT. A mechanistic link between an inherited and an acquired cardiac arrhythmia: *HERG* encodes the $I_{Kr}$ potassium channel. *Cell.* 1995; 81:299-307.

150. Sheldon RS, Duff HJ, Thakore E, Hill RJ. Class I antiarrhythmic drugs: allosteric inhibitors of [$^3$H]-batrachotoxinin binding to rat cardiac sodium channels. *J Phar Exp Ther.* 1994; 268:187-194.

151. Shibasaki T. Conductance and kinetics of delayed rectifier potassium channels in nodal cells of the rabbit heart. *J Physiol (Lond).* 1987; 387:227-250.

152. Shibata EF, Drury T, Refsum H, Aldrete V, Giles WR. Contributions of a transient outward current to repolarization in human atrium. *Am J Physiol.* 1989; 257: H1773-1781.

153. Shimoni Y, Banno H, Clark R. Hyperthyroidism selectively modified a transient potassium current in rabbit ventricular and atrial myocytes. *J Physiol (Lond).* 1992a; 457:369-389.

154. Shimoni Y, Clark RB, Giles WR. Role of an inwardly rectifying potassium current in rabbit ventricular action potential. *J Physiol (Lond).* 1992b; 448:709-727.

155. Shimoni Y, Severson DL. Thyroid status and potassium currents in rat ventricular myocytes. *Am J Physiol.* 1995; 268:H576-H583.

156. Siegelbaum SA, Tsien RW. Calcium-activated transient outward current in calf Purkinje fibres. *J Physiol (Lond).* 1980; 299:485-506.

157. Sperelakis N, Haddad GE. Developmental changes in membrane electrical properties of the heart. *In* Sperelakis N. (eds): Physiology and Pathophysiology of the Heart. Norwell, Mass Kluwer Academic Publishers, 1995; pp669-700.

158. Steinberg SF, Rosen TS, Malfatto G and Rosen MR. β-Adrenergic modulation of cardiac rhythm in rat model of altered sympathetic neural development *J Mol Cell Cardiol.* 1991; 23 (Suppl) I:47-52.

159. Stuhmer W, Ruppersberg JP, Schroter KH, Sakmann B, Stocker M, Giese KP, Perschke A, Baumann A, Pongs O. Molecular basis of functional diversity of voltage-gated potassium channels in mammalian brain. *EMBO J.* 1989; 8:3235-3244.

160. Swanson R, Marshall J, Smith JS, Williams JB, Boyle MB, Folander K, Luneau CJ, Antanavage J, Oliva C, Buhrow SA, Bennett C, Stein RB, Kaczmarek LK. Cloning and expression of cDNA and genomic clones encoding three delayed rectifier potassium channels in rat brain. *Neuron.* 1990; 4:929-939.

161. Takimoto K, Levitan ES. Glucocorticoid induction of Kv1.5 $K^+$ channel gene

expression in ventricle of rat heart. *Circ Res*. 1994; 75:1006-1013.

162. Takumi T, Ohkubo H, Nakanishi S. Cloning of a membrane protein that induces a slow voltage-gated potassium current. *Science*. 1988; 242:1042-1045.

163. Tamkun MM, Knoth KM, Walbridge JA, Kroemer H, Roden DM, Glover DM. Molecular cloning and characterization of two voltage-gated $K^+$ channel cDNAs from human ventricle. *FASEB J*. 1991; 5:331-337.

164. Timpe LC, Schwarz TL, Tempel BL, Paparian DM, Jan YN, Jan JL. Expression of functional potassium channels from shaker cDNA in *Xenopus* oocytes. *Nature*. 1988; 331:143-145.

165. Tohse N, Kameyama M, Irisama H. Intracellular $Ca^{2+}$ and protein kinase C modulate $K^+$ current in guinea pig heart cells. *Am J Physiol*. 1987; 253:H1321-H1324.

166. Trube G, Hescheler J. Inward-rectifying channels in isolated patches of the heart cell membrane: ATP-dependent and comparison with cell-attached patches. *Pflugers Arch*. 1984; 401:178-184.

167. Turgeon J, Daleau P, Bennett PB, Wiggins SS, Selby L, Roden DM. Block of

$I_{Ks}$, the slow component of the delayed rectifier $K^+$ current, by the diuretic agent indapamide in guinea pig myocytes. *Circ Res.* 1994; 75:879-886.

168. van Bilsen M, Chien KR. Growth and hypertrophy of the heart: towards an understanding of cardiac specific and inducible gene expression. *Cardiovasc Res.* 1993; 27:1140-1149.

169. Vandenberg CA. Inward rectification of a potassium channel in cardiac ventricular cells depends on internal magnesium ions. *Proc Natl Acad Sci.* 1987; 84:2560-2564.

170. Vandenberg CA. Cardiac inward rectifier potassium channel. *In* Spooner PM, Brown AM, Catterall WA, Kaczoroski GJ, Strauss HC (eds): Ion Channels in the Cardiovascular System: Function and Dysfunction. Futura Publishing Company, Inc. Armonk, NY. 1994; pp145-167.

171. Veldkamp MW, van Ginnéken ACG, Bouman LN. Single delayed rectifier channels in the membrane of rabbit ventricular myocytes. *Circ Res.* 1993; 72:865-878.

172. Veldkamp MW, van Ginneken ACG, Opthof T, Bouman LN. Delayed rectifier channels in human ventricular myocytes. *Circulation.* 1995; 92:3497-3504.

173. Wahler GM. Developmental increases in the inwardly rectifying potassium current of rat ventricular myocytes. *Am J Physiol.* 1992; 262:C1266-C1272.

174. Walsh KB, Begenisich TB, Kass RS. ß-Adrenergic modulation in the heart - independent regulation of K and Ca channels. *Pflugers Arch.* 1988; 411:232-234.

175. Walsh KB, Arena PA, Kwok WM, Freeman L, Kass RS. Delayed rectifier potassium channel activity in isolated membrane patches of guinea pig ventricular myocytes. *Am J Physiol.* 1991; 260:H1390-H1393.

176. Walsh KB, Kass RS. Distinct voltage-dependent regulation of a heart-delayed $I_K$ by protein kinases A and C. *Am J Physiol.* 1991; 261:C1081-C1090.

177. Wang L, Chiamvimonvat N, Duff HJ. Interaction between selected sodium and potassium channel blockers in guinea pig papillary muscle. *J Pharmacol Exp Ther.* 1993; 264:1056-1062.

178. Wang Z, Fermini B, Nattel S: Delayed outward current and repolarization in human atrial myocytes. *Circ Res.* 1993a; 73:276-285.

179. Wang Z, Fermini B, Nattel S: Sustained depolarization-induced outward current in human atrial myocytes: Evidence for a novel delayed rectifier $K^+$ current

similar to Kv1.5 cloned channel currents. *Circ Res.* 1993b; 73:1061-1076.

180. Warmke J, Drysdale R, Ganetzky B. A distinct potassium channel polypeptide encoded by the drosophila eag locus. *Science.* 1991; 252:1560-1562.

181. Warmke JE, Ganetzky B. A family of potassium channel genes related to *eag* in *Drosophila* and mammals. *Proc Natl Acad Sci.* USA 1994; 91:3438-3442.

182. Wible BA, De Biasi M, Majumder K, Taglialatela M, Brown AM. Cloning and functional expression of an inwardly rectifying $K^+$ channel from human atrium. *Circ Res.* 1995; 76:343-350.

183. Wei A, Covarrubas M, Butter A, Baker A, Pak M, Salkoff L. $K^+$ current diversity is produced by an extended gene family conserved in *Drosophila* and mouse. *Science.* 1990; 248:599-602.

184. Xu XP, Best PM. Decreased transient outward $K^+$ current in ventricular myocytes from acromegalic rats. *Am J Physiol.* 1991; 260:H935-H942.

185. Xu HD, Barry DM, Trimmer JS, Merlie JP, Nerbonne JM. Differential expression of voltage-gated $K^+$ channel $\alpha$ subunits and functional $K^+$ channels during postnatal development. *Circulation.* 1995; 92:I372 (Abstract).

186. Yang T, Wathen MS, Felipe A, Tamkun MM, Snyders DJ, Roden DM. $K^+$ currents and $K^+$ channel mRNA in cultured atrial cardiac myocytes (AT-1 cells). *Circ Res.* 1994; 75:870-878.

187. Yang T, Kupershmidt S, Roden DM. Anti-minK antisense decreases the amplitude of the rapidly activating cardiac delayed rectifier $K^+$ current. *Circ Res.* 1995; 77:1246-1253.

188. Yue DT, Marban E. A novel cardiac potassium channel that is active and conductive at depolarized potentials. *Pflugers Arch.* 1988;413:127-133.